Université de Montréal

Le rôle de la protéine interagissant avec hedgehog (Hhip) dans la formation rénale modulée par le diabète maternel et dans la néphropathie diabétique

par

Xinping Zhao

Programme de sciences biomédicales

Faculté de médecine

Thèse présentée à la faculté des études supérieures

en vue de l'obtention du grade de docteurès sciences (Ph.D.)

en sciences biomédicales

September 2018

Université de Montréal

Le rôle de la protéine interagissant avec hedgehog (Hhip) dans la formation rénale modulée par le diabète maternel et dans la néphropathie diabétique

par

Xinping Zhao

Sera évaluée par un jury composé des personnes suivantes :

Dre Jolanta Gutkowska
Présidente rapporteuse

Dre Shao-Ling Zhang
Directeur de recherche

Dr John S.D. Chan
Codirectrice de recherche

Dr Casimiro Gerarduzzi
Membre du jury

Dr Jun-Li Liu
Examinateur externe

Dr Marek Jankowski
Représentant de la doyenne

Résumé

Nous avons précédemment rapporté que le diabète maternel altère la néphrogenèse chez la progéniture diabétique de notre modèle murin de diabète maternel. Notre analyse par puce à ADN réalisée sur les reins néonatals de ces descendants de grossesse diabétique a révélé que l'expression de la protéine interagissant avec hedgehog (Hhip) était significativement surexprimée par rapport au groupe contrôle. En tant qu'antagoniste de Sonic hedgehog (Shh) qui joue un rôle essentiel dans la différenciation cellulaire, la croissance et le modelage tissulaire pendant le développement des reins et la fibrose rénale, Hhip se lie à Shh et atténue sa bioactivité. Il a été rapporté que la protéine Hhip est principalement exprimée dans les cellules endothéliales vasculaires et les cellules adjacentes à celles exprimant Shh. Cependant, le rôle fonctionnel de l'expression de Hhip dans les reins en développement et matures est à peine connu.

Nous avons tout d'abord établi le profil d'expression de Hhip dans les reins embryonnaires. Dans notre modèle murin de diabète maternel, nous avons observé que l'expression du gène *Hhip* est différemment surexprimée dans le mésenchyme métanéphrique différencié et l'épithélium du bourgeon urétérique de la progéniture. En utilisant des cellules mésenchymateuses métanéphriques en culture (cellules MK4), nous avons démontré que le D-glucose élevé (25 mM D-glucose) stimulait spécifiquement l'expression de Hhip de façon dépendante du temps, puis ciblait la signalisation TGFβ1. De plus, la surexpression de Hhip augmentait l'expression des gènes pro-apoptotiques [NF-kB (P50/p65) et p53] et inhibait l'expression des gènes prolifératifs (i.e. Shh, Pax2, N-myc et p27Kip1). Finalement, nous avons démontré que le diabète maternel qui altère le développement des reins pourrait jouer un rôle dans les interactions de la voie Hhip et TGFβ1-SMAD (Diabetologia 2014).

Après la naissance, dans le rein normal non-diabétique, l'expression de Hhip est quiescente; une expression basale et limitée de Hhip (ARNm et protéine) est détectable dans les cellules endothéliales glomérulaires matures, les podocytes et les cellules épithéliales tubulaires rénales. Alors que les lésions des cellules épithéliales glomérulaires (GECs) et des podocytes sont la caractéristique de la lésion rénale précoce de la néphropathie diabétique (DN), nous avons examiné plus en détail le rôle de l'expression rénale de Hhip dans certains modèles de

diabète murin—e.g. souris Akita, souris db/db et souris Hhip hétérozygote (Hhip +/−) rendus diabétiques avec de faibles doses de streptozotocine (LDSTZ). Nos données révèlent que l'hyperglycémie (ou un taux élevé de glucose *in vitro*) active l'expression du gène Hhip dans les cellules endothéliales glomérulaires et les podocytes. En particulier, l'hétérozygosité de Hhip protège l'intégrité glomérulaire avec moins de pertes de podocytes et améliore les paramètres rénaux [c.-à-d., une diminution du ratio albumine/créatinine urinaire (ACR, une caractéristique de l'apparition de la maladie rénale) et les caractéristiques de la DN (hypertrophie rénale, augmentation du taux de filtration glomérulaire, glomérulosclérose et fibrose)]. Prises dans leur ensemble, nos données suggèrent que l'augmentation de l'expression rénale de Hhip due aux concentrations élevées de glucose peut déclencher directement le processus d'apoptose et de fibrose des cellules endothéliales glomérulaires observé dans le diabète et qu'elle joue un rôle clé dans le développement et la progression de la DN (Sci. Report 2018).

Mots-clés : Expression des gènes de Hhip, diabète maternel, néphrogenèse, néphropathie diabétique, dérivé réactif de l'oxygène

Abstract

We previously reported that maternal diabetes impairs nephrogenesis in diabetic progeny in our maternal diabetes murine model. Our gene-array performed in neonatal kidneys of those affected offspring revealed that hedgehog interacting protein (Hhip) expression was significantly upregulated, as compared to the control group. As an antagonist of sonic hedgehog (Shh) which plays an essential role in cell differentiation, growth and tissue patterning during kidney development and kidney fibrosis, Hhip binds to Shh and attenuates its bioactivity. It is reported that Hhip is predominantly expressed in vascular endothelial cells and cells adjacent to those expressing Shh. However, the functional role of Hhip expression in the developing and mature kidney is barely known.

We first established the expression pattern of Hhip in embryonic kidneys. We observed in our murine model of maternal diabetes that Hhip gene expression is differentially up-regulated in differentiated metanephric mesenchyme and ureteric bud epithelium of the offspring. Using cultured metanephric mesenchymal cells (MK4 cells), we demonstrated that high D-glucose (25 mM D-Glucose) specifically stimulated Hhip expression in a time-/dose-dependent manner, and then targeted TGFβ1 signaling. In addition, overexpression of Hhip increased the expression of pro-apoptotic genes [NF-kB (p50/p65) and p53] and inhibited the expression of proliferative genes (i.e., Shh, Pax2, N-myc, and p27kip1). Finally, we demonstrated that maternal diabetes impairing kidney development might mediate the interactions of Hhip and TGFβ1-Smad pathway (*Diabetologia 2014*).

After birth, in normal non-diabetic state, Hhip expression is quiescent; a limited basal Hhip expression (mRNA and protein) is detectable in mature glomerular endothelial cells, podocytes and renal tubular epithelial cells. While glomerular epithelial cells (GECs) and podocyte injury is the hallmark of early renal injury in diabetic nephropathy (DN), we further examined the role of renal Hhip expression in murine diabetes models--e.g., Akita mice, db/db mice and heterozygous Hhip deficiency ($Hhip^{+/-}$) mice rendered diabetic with low-dose streptozotocin (LDSTZ). Our data revealed that hyperglycemia (or high glucose in vitro) activates Hhip gene expression in glomerular endothelial cells and podocytes. In particular, Hhip heterozygosity protects glomerular integrity with less podocyte loss and improved renal

outcomes [i.e., decreased urinary albumin/Creatinine (Cre) ratio (ACR, a hallmark of onset of kidney disease) and DN-features (renal hypertrophy, increased glomerular filtration rate, glomerulosclerosis and fibrosis)]. Taken together, our data suggest that high glucose-elevated renal Hhip expression may directly trigger the process of apoptosis and fibrosis in glomerular endothelial cells in diabetes and it plays a key role in the development and progression of DN (*Sci. Report 2018*).

Keywords: Hhip gene expression, maternal diabetes, nephrogenesis, diabetic nephropathy, reactive oxygen species

Table of Contents

List of Figures

Table of abbreviations

A	ACR	Albumin/creatinine ratio
	AGEs	Advanced glycation end products
	AngII	Angiotensin II
	α-SMA	α-smooth muscle actin
B	Bcl-2	B-cell lymphoma 2
	BMP4	Bone morphogenetic protein
C	COPD	Chronic obstructive pulmonary disease
	CAKUT	Congenital anomalies of the kidney and urinary tract
D	DHE	Dihydroethidium
	Dhh	Desert hedgehog
	DM	Diabetes mellitus
	DN	Diabetic Nephropathy
E	ECM	Extracellular matrix
	ECs	Endothelial cells

	EMT	Epithelial-mesenchymal transition
	EndoMT	Endothelial-mesenchymal transition
	e-NOS	Endothelial nitric oxide synthase
	ESRD	End-stage renal disease
G	GBM	Glomerular basement membrane
	GDM	Gestational diabetes mellitus
	GDNF	Glial derived neurotrophic factor
	GECs	Glomerular endothelial cells
	GFR	Glomerular filtration rate
	GLUT2	Glucose transporter 2
H	Hh	Hedgehog
	Hhip	Hedgehog-interacting protein
	HO·	Hydroxyl radical
	H_2O_2	Hydrogen peroxide
	HOCl	Hypochlorous acid

I	IDMs	Infants of diabetic mothers
	IF	Immunofluorescence
	IHC	Immunohistochemistry
	Ihh	Indian hedgehog
	IP	Intraperitoneal
	IUGR	Intrauterine growth restriction
L	LDSTZ	Low-dose streptozotocin
M	MAPK	Mitogen-activated protein kinases
	mECs	murine SVEC4-10 endothelial cells
	MM	Metanephric mesenchyme
	mPODs	mouse podocyte cells
N	NADPH	Nicotinamide adenine dinucleotide phosphate
	NF-κB	Nuclear factor kappa B
	NO	Nitric oxide
O	O_2	Oxygen

	O_2^-	Superoxide anion
	ONOO−	Peroxynitrite
P	PAS	Periodic-Acid Schiff
	Pax2	Paired box gene 2
	PGDM	Pre-gestational diabetes mellitus
	PKC	Protein kinase C
	Ptch1	Patched receptor
R	RAS	Renin–angiotensin system
	ROS	Reactive oxygen species
S	SBP	Systolic blood pressure
	Shh	Sonic hedgehog
	STZ	Streptozotocin
T	T1DM	Type 1 diabetes mellitus
	T2DM	Type 2 diabetes mellitus
	TGFβ1	Transforming growth factor beta 1

	TGFβRII	TGF-β receptor II
	TGFβRI	TGF-β receptor I
	TUNEL	Terminal deoxynucleotidyl transferase dUTP nick end labeling
U	UB	Ureteric bud
W	WB	Western blotting
	WD	Wolffian duct
	WT1	Wilms tumor protein

Acknowledgments

First and foremost, I would like to thank my supervisor Dr. Shaoling Zhang and co-supervisor Dr. John S.D. Chan for the opportunity they have given me to study in the biomedical science field and for their continuous support, patience, and guidance throughout my studies. It has been an honor to be their Ph.D. student. They have taught me, both consciously and subconsciously, how good basic research is done. I appreciate all their contributions of time, ideas, and funding to make my Ph.D. experience productive and stimulating. Dr. Zhang's enthusiasm and persistence for the research were inspirational and motivational for me, especially during tough times in my Ph.D. pursuit. I am also thankful for the excellent example she has set for me as a successful female scientist and professor.

I would like to thank my committee members, Dr. Jolanta Gutkowska, Dr Casimiro Gerarduzzi, Dr. Jun-Li Liu, and Dr. Marek Jankowski for their patient guidance, valuable suggestions, and encouragement. Thank you for spending time reading and commenting on my thesis manuscript.

I would like to especially thank Ms. Isabelle Chénier for helping me with lab techniques, experiments, suggestion, French translating and continuous encouragement. I also would like to thank my colleagues and friends, Dr. Chao-Sheng Lo, Dr. Shiao-Ying Chang, Min-Chun Liao, Yessoufou Aliou, Henry Nchienzia, Shuiling Zhao, Anindya Ghosh, Yixuan Shi, and Shaaban Abdo. My time in the lab was more enjoyable due to the many friends and groups that became a part of my life. They have given me selfless help almost in all aspects and been there for me at all the important moments. I appreciate all the generous help from them.

Finally, I would like to thank my family for all their continuous love, encouragement and support in my life. I grateful to my parents who supported me in all my pursuits, to my lovely daughter Cersei who is my source of energy and always inspires me to have new understanding of many things, and most of all to my loving, supportive, encouraging, and patient husband Renyuan whose support during the whole stages of this Ph.D. is so important to me.

Chapter1: Introduction and Objectives

1.1 Development of the mammalian kidney and renal malformations

1.1.1 The process of mammalian kidney development

The kidney development begins at embryonic day (E) 9.5 in the mouse when the Wolffian duct (WD) extends caudally to generate a ureteric bud (UB) outgrowth induced by interactions with the surrounding metanephric mesenchyme (MM) at E10.5 in the mouse and 5 weeks gestation in humans (Figure1-1A) [1, 2].

In response to signals from the MM, the UB elongates and invades the MM, undergoing the first branching event to form a T-shaped branch at E11.5 in the mouse [3]. Subsequently, the UB undergoes repeated cycles of elongation and branching to give rise to the renal collecting duct system, renal calyces, and ureter (Figure1-1B) [2]. This process is known as branching morphogenesis and it continues for 10 cycles to form 1500 collecting ducts in mice [4] and 15 cycles to form 60,000 collecting ducts in humans [1].

Upon invasion of the MM, the UB induces the mesenchyme to establish two cell fates – the stromal progenitor cells and the nephrogenic mesenchyme [1]. Signals from the UB promote survival of the nephrogenic mesenchyme and initiate in these cells a program of mesenchymal-epithelial transformation. MM cells around the tip of the growing and branching UB aggregate and undergo mesenchymal-to-epithelial transformation to form the renal vesicle (RV). RV elongates along the proximal-distal axis to form comma-shaped and then S-shaped nephron. S-shaped nephrons fuse with UB-derived collecting ducts to form glomerulus, proximal tubule, loop of Henle and distal tubule, thereby completing the formation of the nephron, a process termed nephrogenesis (Figure1-1C) [5]. This process will give rise to 10,000 nephrons [4] in the mouse and 200,000–1.8 million nephrons in humans [1, 4, 6, 7].

Shortly after the invasion of the ureteric bud into the metanephric mesenchyme, a third cell population, termed the renal stroma, is observed surrounding the condensed mesenchyme [8-10]. The renal stroma is a population of matrix-producing fibroblast cells that surround adjacent nephrogenic structures and collecting ducts [10]. It is required for kidney development by modulating branching morphogenesis and nephrogenesis [2, 10-12].

Organogenesis of the metanephric kidney is coordinated by complex interactions among numerous transcription/growth factors and intracellular signaling molecules that may be collectively referred to as renal developmental genes, which are expressed in the MM, stroma, angioblasts and UB [13]. Ectopic expression of these genes may contribute to renal malformations.

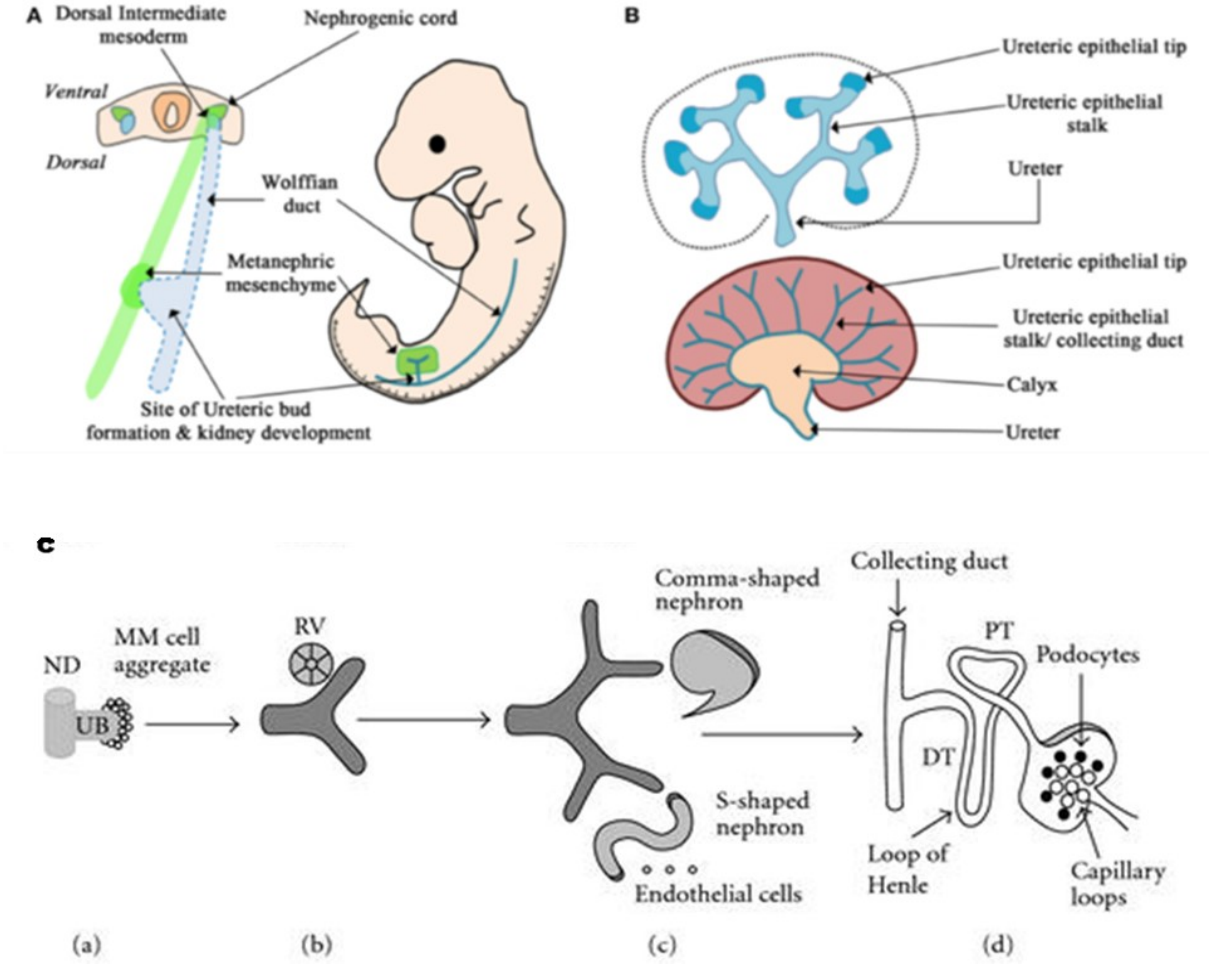

Figure1-1 Schematic representation of the normal development of the mammalian kidney. (A) The Wolffian duct originates from the dorsal intermediate mesoderm. The metanephric mesenchyme (MM) originates from the nephrogenic cord. The Wolffian duct forms an outgrowth called the ureteric bud (UB) that migrates into the surrounding mesenchyme and undergoes the first dichotomous branching morphogenesis event. (B) The ureteric epithelium is composed of the ureteric tip and stalk region. In response to signals from the mesenchyme, the tips of the ureteric epithelium undergo continued branching morphogenesis and the stalks subsequently differentiate to form the collecting duct system, renal calyx, and ureter. (C) (a) Invasion of the MM by the UB induces MM cells to aggregate around the UB tip. (b) MM cell aggregates undergo mesenchymal-to-epithelial transformation to form the renal vesicle (RV).

(c) RV elongates along the proximal-distal axis to form comma-shaped and then S-shaped nephron. Distal ends of S-shaped nephrons fuse with UB-derived collecting ducts, whereas proximal clefts form glomeruli. Endothelial cells migrate into the proximal cleft. (d) Patterning of the S-shaped nephron and UB result in formation of mature nephron which contains glomerular capillary tuft, podocytes, proximal tubule (PT), loop of Henle, distal tubule (DT), and collecting duct [2, 5].

1.1.2 Notable signaling pathways of nephrogenesis

1.1.2.1 Pax2: Earliest Marker of Nephrogenesis

Pax2 is essential in kidney formation for initiating the development of the mesonephros and metanephros from the intermediate mesoderm and is highly expressed in the UB as it undergoes branching morphogenesis [14-16]. Pax2 mutant mice exhibit complete agenesis of both kidneys and ureters, whereas heterozygous Pax2 mutations ($Pax2^{+/-}$) produce smaller kidneys [17]. There were fewer UB tips and less branching in $Pax2^{1Neu+/-}$ mutant mice (a single point mutation in the Pax2 gene) [14]. Porteous et al. demonstrated that kidney hypoplasia is associated with increased apoptosis in UB cells, with a reduced number of UB branches in the fetal kidneys of $Pax2^{1Neu+/-}$ mutant mice [15]. In humans, the loss of one Pax2 allele can result in renal hypoplasia and vesicoureteral reflux [18]. These phenotypes are consistent with the Pax2 expression pattern in the epithelial components of the mesonephros, the UB and the developing renal tubules [19].

Before induction, Pax2 protein expression demarcates the MM, activates glial cell-derived neurotrophic factor (GDNF) expression so that ureteric bud epithelial outgrowth can occur, and controls the response to inductive signals [20]. In the developing nephrons, Pax2 expression persists in the condensing cap mesenchyme around the ureteric bud tips and the comma and S-shaped bodies, being down-regulated first in the most proximal loop of the S-shaped body and then in the epithelial cells of the proximal and distal tubules. As a downstream gene of the sonic hedgehog (Shh), Pax2 could be regulated by Shh signaling [21]. Genes thought to be upregulated by Pax2 include Wilms tumor protein (WT1), GDNF, and Wnt4 in the developing Kidney [20, 22, 23].

1.1.2.2 The GDNF/c-Ret Pathway

GDNF, a gene that encodes a secreted ligand of the TGFβ1 superfamily proteins, is essential for renal development [24]. UB induction from the WD is mediated by GDNF secreted from MM, which interacts with the c-Ret receptor tyrosine kinase (RTK) expressed in the UB, to induce branching [25, 26]. After UB invasion, GDNF expression is limited to the MM, and this expression pattern is maintained throughout kidney development. The GDNF expression pattern suggests that GDNF is important not only for the initial branch induction, but also for sustaining future branch generations. Targeted mutagenesis of GDNF causes bilateral renal aplasia associated with failure of ureteric bud outgrowth [27, 28]. In humans, 5-10% of cases of renal agenesis are found to be linked with GDNF mutations [29].

In the developing kidney, Ret is initially expressed on the mesonephric duct and early UB, and later its expression is restricted to UB branch tips [30]. Mice with a c-Ret null mutation exhibit severe renal dysplasia or agenesis as a result of defective UB outgrowth [25]. In humans, 30% of cases of renal agenesis are found to be associated with Ret mutations [29]. Similarly, homozygous deletion of Ret causes the same defects in mice [25, 31], indicating a critical role played by the GDNF-cRet signaling pathway in controlling early developmental events during renal branching morphogenesis.

GDNF levels and its spatial expression are regulated by multiple transcription and growth factors, Pax2, eyes absent homolog 1 (Eya1), SIX homeobox (Six)1, 2, and 4, WT1 [32-35]. c-Ret expression and signaling activity are induced by Pax2 or retinoic acid [36-38]. Eya1 is capable of binding both Pax2 and Six1: the Eya1-Pax2 complex upregulates Six2 and GDNF, while the binding of Eya1 to Six1 turns Six1 from a repressor to an activator and upregulates Pax2, resulting in a positive feedback loop [39, 40]. Together, Six1-Eya1-Pax2 act synergistically and upregulate GDNF [41, 42]. WT1 is essential in the MM for regulation of GDNF expression and the promotion of survival of uninduced cells. In later stages, WT1 is expressed at high levels in the podocyte cells of the glomerulus, where it serves an essential function [34, 35].

1.1.2.3 Sonic hedgehog (Shh) signaling

During mammalian development, Hedgehog (Hh) signaling plays a crucial role in cell differentiation, growth and tissue patterning. Dysregulation of Hh signaling during embryogenesis results in various congenital abnormalities [21, 43-45]. There are three mammalian Hh proteins, including Sonic hedgehog (Shh), Indian hedgehog (Ihh), and Desert hedgehog (Dhh); of the three Hh genes, only Shh and Ihh expression have been described as present in the developing murine kidney. However, the absence of a renal phenotype in Ihh-deficient mice indicates that it might not play the crucial role in kidney development [46].

Shh is a paracrine protein and undergoes a series of processing steps before it is secreted from the producing cell. It is an inhibitory ligand for the Patched receptor (Ptch1), which constitutively represses Shh signaling [47, 48]. In the absence of Shh ligand, Ptch1 inhibits the ciliary localization of Smoothened (Smo), the obligatory signal transducer across the plasma membrane (Figure 1-2A). In this state, an intracellular molecular complex consisting of Kif7/Kif27, Fused (Fu) and Suppressor of Fused (Sufu) can bind full-length Gli proteins (Gli1, Gli2 and Gli3), which are glioma-associated oncogene-Kruppel family members, which then function as transcription factors of Shh, generating a C-terminally truncated Gli repressor (GliR) that localizes to the nucleus and actively represses a subset of Shh target genes. The GliR function is largely derived from Gli3 while the primary Gli activator's (GliA) activity is mostly contributed by Gli2. Gli1 is a transcriptional target of Hh signaling, acting as a transcriptional activator to reinforce GliA function. In the presence of ligand, Shh binds to Ptch1, releasing Smo (Figure 1-2B), which in turn leads to the inhibition of the molecular complex consisting of Kif7/Kif27, Fused (Fu) and Suppressor of Fused (Sufu), resulting in full length Gli processing and the production of the transcriptionally active forms of Gli (GliA). As a result, full-length GliA translocate into the nucleus and activate transcription of Shh downstream genes [49, 50].

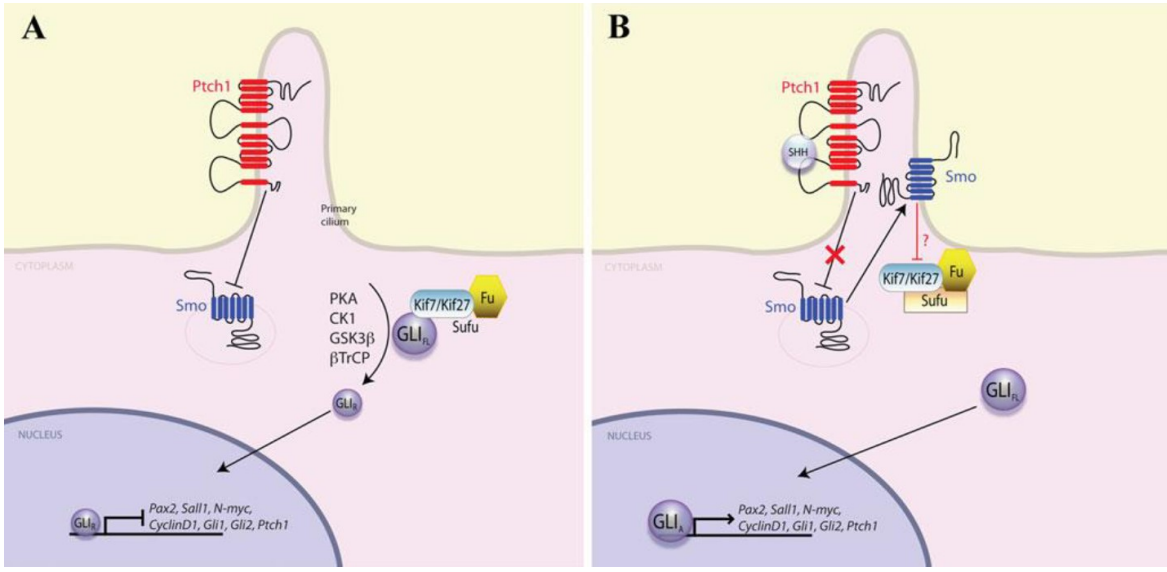

Figure 1-2 Mammalian Hedgehog (Hh) signaling pathway [50] A. In the absence of Hh ligand, Patched1 (PTCH1) blocks Smoothed' (SMO) activity, preventing its ciliary localization and its interaction with the Kif7/Kif27–Fu–Sufu complex. In turn, the recruitment of protein kinase A (PKA), casein kinase 1 (CK1), glycogen synthase kinase 3β (GSK3β), and β-transducin repeat containing protein (βTrCP) to this complex, resulting in the proteolytic cleavage of full-length GLI proteins (GLI FL), thus generating a C-terminally truncated GLI repressor (GLI R) that localizes to the nucleus and represses Hh target genes. B. Hh ligand binding to its receptor, PTCH1, relieves PTCH1-mediated inhibition of SMO and triggers the relocation of SMO to the cilium. In this state, the formation of GLI repressor is inhibited by unknown mechanisms, resulting in the translocation of full-length GLI activator proteins (GLI A) into the nucleus where they act as transcriptional activators. During renal development, Hh signaling directly promotes the expression of Pax2, Sall1, N-myc, CyclinD1, Gli1, Gli2 and Ptch1.

Shh signaling directly controls the expression of three distinct classes of genes that are required for normal renal development. They are early kidney inductive and patterning genes (Pax2, Sall1), cell cycle modulators (CyclinD1, N-myc) and the signaling pathway effectors (Gli1, Gli2) [21]. Mutations in Shh result in bilateral renal aplasia and the presence of a single, ectopic dysplastic kidney [21, 43]. Also, deletion of Gli3 in the Shh null mouse restored expression of Pax2, Sall1, CyclinD1, N-myc, Gli1, and Gli2 and rescued renal development, implicating a deleterious character of the Gli3 repressor during early stages of renal development [21].

Shh signaling activity is restricted to the presumptive ureter and medullary regions but is absent in the renal cortex. This is due to the fact that the expression of its receptor Ptch1 is

mainly expressed in the ureteric and mesenchymal cell lineage of the ureter and renal medulla [51, 52]. This indicates that the developing kidney consists of two distinct Shh signaling domains: (1) an active ureter/medullary domain representing a dominance of GliA function; (2) an inactive or repressive cortical domain representing a dominance of GliR function [50]. Shh is secreted from the distal ureter epithelium and establishes a gradient of distal (high) and proximal (low) of Shh signal. It leads to an accumulation of GliA in the ureter and medullary regions, while a high concentration of GliR is localized in the cortex of the embryonic kidney. Gli3 null ($Gli3^{-/-}$) embryos exhibit cortical developmental defects. On the other hand, Shh deficiency ($Shh^{-/-}$, $Gli2^{-/-}$, $Gli3^{\Delta 699/\Delta 699}$) leads to ureter/medullary anomalies (Figure 1-3) [51]. Interestingly, this spatial restriction of Shh signaling is evident from a very early stage of renal development, prior to cortico-medullary patterning, suggesting that Shh signaling may be critical in this patterning process. This involvement of Shh signaling is supported by the presence of renal dysplasia and severe renal patterning defects in mice and humans with mutations resulting in severe loss of Shh activity [21, 53, 54].

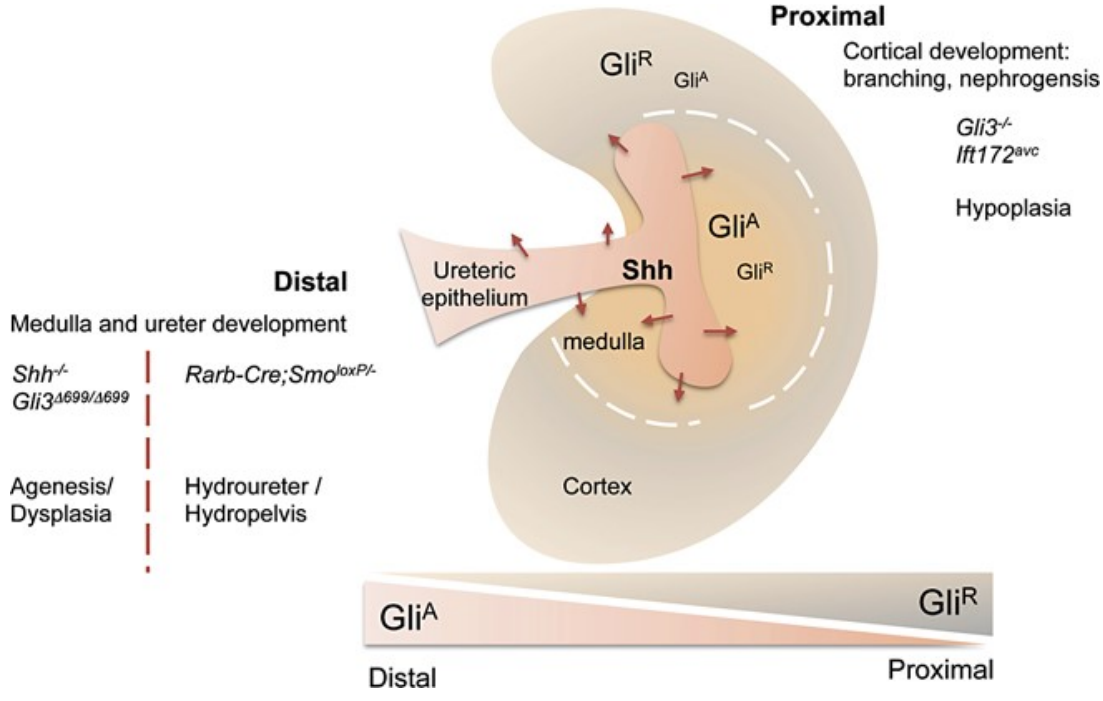

Figure 1-3 Model for Shh signaling in the developing kidney. Shh is secreted from the distal ureter epithelium and establishes a gradient of distal high and proximal low of Hh signal. It leads to an accumulation of GliA in ureter and medullary regions, while high concentration of GliR is localized in the cortex of the embryonic kidney. Mouse mutants bearing gain- or loss-

of function mutations display unique phenotypes that segregate according to the predicted balance of GliA versus GliR. Mouse bearing gain-of-function mutation ($Gli3^{-/-}$) with an absence of Gli R shows cortical developmental defects. On the other hand, Shh deficiency ($Shh^{-/-}$, $Gli2^{-/-}$, $Gli3^{\Delta 699/\Delta 699}$) leads to ureter/medullary anomalies [51, 55].

Shh causes an invasive phenotype of cultured gastric cancer cells, which is considered to be mediated by Shh-induced TGFβ ligand production [56]. TGFβ/Smad3 induces Gli2 transcription in several types of cells [57]. Several Smad proteins were shown to bind to a c-terminally of Gli3, which is produced in human diseases and may resemble the endogenously Gli3. Despite the unknown function of this Smad-Gli3 complex, TGFβ could dissociate Smads from the truncated Gli3, which may allow the GliR to antagonize Shh signaling [58]. Current knowledge about the molecular nature of the TGFβ/Shh interaction is still limited and more sophisticated cross-talk between Shh and TGFβ is expected. Hedgehog-interacting protein (Hhip) can bind Shh ligands and attenuate their bioactivities [59].

1.1.2.4 RAS

The involvement of the renin-angiotensin system (RAS) has been proposed in the regulation of the development of the UB [60-62]. According to this hypothesis, angiotensin II produced by stromal cells stimulates UB branching, upregulating Pax2 via AT2R [63]. Angiotensin II activates both angiotensin receptors type 1 and 2 on the ureteric bud to stimulate branching. It is also required for elongation of the collecting duct. RAS blockade results in renal agenesis, and mutations in the RAS have also been identified in renal tubular dysgenesis and congenital obstructive uropathy [64, 65].

1.1.2.5 Apoptosis related pathway

Apoptosis plays an important role in nephrogenesis, which requires structural formation and reformation. Apoptotic cells are characteristically found between the maturing nephrons in the mesenchyme and are frequently located next to condensed bodies of cells or at the tails of S-shaped bodies in the kidney [66, 67]. Factors controlling apoptosis have been investigated. The balance of activity between the prosurvival protein, B-cell lymphoma 2 (Bcl-2) and the proapoptotic protein, Bim, regulates subsequent apoptosis of the metanephric mesenchyme via the mitochondrial intrinsic apoptotic pathway [68]. Mice lacking Bcl-2 develop cystic

kidneys that are hypoplastic and have fewer nephrons, because Bcl-2 may block apoptosis in many kidney cell types [69]. The proapoptotic protein, the Bcl-2-interacting mediator of cell death (Bim), binds to Bcl-2, releasing Bax or Bak proteins to promote apoptosis [70].

The NF-κB transcription factors are key regulators of programmed cell death, either by apoptosis or necrosis [71]. Their activity has significant relevance for normal development in various tissues and pathogenesis of many diseases [72]. The NF-κB family has 5 proteins: RelA (p65), RelB, c-Rel, NF-κB1 (p50/p105) and NF-κB2 (p52/p100). Within most cells, under normal nonstress-related conditions, NF-κB is typically inactive and remains sequestered in the cytoplasm through its interaction with IκB proteins. Activated NF-κB is a heterodimer, which usually consists of p65 and p50 or p52 and RelB. In response to certain stresses such as hyperglycemia, elevated free fatty acids, ROS, the IκB kinase complex is activated, and IκB is phosphorylated and degraded, allowing the NF-κB heterodimers to translocate into the nucleus and subsequently regulate the expression of a large number of genes [73].

The product of tumor suppressor gene p53 is considered to regulate cell growth in two ways. It may act as a checkpoint in the cell cycle and in a separate manner to control apoptosis in response to stress [74]. In the developing mouse kidney, p53 usually is expressed in comma- and S-shaped bodies [75]. During the 8th and 9th weeks of human kidney development, p53 is detected in all structures of the developing metanephros, indicating its importance in the morphogenesis of both the collecting system and nephrons [76]. Deletion of p53 in mice does not significantly affect development [77]. However, p53 Tg mice present defective differentiation of the UB and hypoplastic kidney due to increased apoptosis in the undifferentiated mesenchyme, resulting in smaller kidneys and about half the normal number of nephrons, with compensatory hypertrophy of the glomeruli [78]. Evidence has also revealed that overexpression of p53 could cause defects in human kidney development [79].

1.1.3 Renal malformations

Renal malformations, also known as congenital anomalies of the kidney and urinary tract (CAKUT), include ureteral duplication, renal agenesis (the absence of kidneys), renal

hypoplasia (reduced kidney size), and other types of renal dysgenesis with kidneys containing abnormal structures [80, 81].

Renal agenesis is a medical condition in which one (unilateral) or both (bilateral) fetal kidneys fail to develop in newborns, with a frequency of 1/5000 and 1/30000 respectively [82]. Renal hypoplasia refers to a condition characterized by an abnormally small kidney with either a reduced number of nephrons or smaller nephrons, and there is a correlation between nephron number and the risk of developing hypertension [83]. A defect in the rate of UB branching is the most common cause of renal hypoplasia. Studies have shown that heterozygous mutations of the paired box gene 2 (Pax2) gene resulted in renal hypoplasia and diminished nephron number [84]. In rats, early in utero exposure of fetuses to hyperglycemia causes a 10-35% decrease in nephron numbers [85]. Renal dysplasia refers to the condition where a kidney does not fully develop in the womb and fails to function normally. It is typically smaller than usual, and may or may not have cysts, which are similar to sacs filled with liquid [86]. Pax2 or Wnt4 mutations may cause renal dysplasia, originating from the inhibition of mesenchymal-to-epithelial conversion or UB formation occurring at an ectopic site on the WD [87]. Polycystic kidneys are a genetic disorder that is characterized by the presence of multiple cysts. The cysts are non-functioning tubules filled with fluid, which range in size from microscopic to enormous, causing massive kidney enlargement [88].

1.2 Glucose metabolism

Intracellular glucose metabolism begins with glycolysis in the cytoplasm, which generates NADH and pyruvate (Figure 1-4A) [89]. Glycolysis consists of ten steps, split into two phases. During the first phase, it requires the breakdown of two ATP molecules. During the second phase, chemical energy from the intermediates is transferred into ATP and NADH. The breakdown of one molecule of glucose results in two molecules of pyruvate, which can be further oxidized to access more energy in later processes [90, 91]. Cytoplasmic NADH can donate reducing equivalents to the mitochondrial electron-transport chain, or it can reduce pyruvate to lactate, which exits the cell to provide substrate for hepatic gluconeogenesis [92].

Pyruvate can also be transported into the mitochondrial matrix, where it is converted into a two-carbon acetyl coenzyme A (acetyl CoA) molecule (Figure 1-4B) [89]. This reaction is an

oxidative decarboxylation reaction. It converts the three-carbon pyruvate into a two-carbon acetyl CoA molecule, releasing carbon dioxide and transferring two electrons that combine with NAD^+ to form NADH [89, 92].

Acetyl CoA enters the tricarboxylic acid (TCA) cycle to produce CO_2, H_2O, one ATP, three NADH and one $FADH_2$. Mitochondrial NADH and $FADH_2$ provide energy for ATP production through oxidative phosphorylation by the electron-transport chain (Figure 1-4C) [89].

Electrons from NADH and $FADH_2$ are transferred through protein complexes embedded in the inner mitochondrial membrane by a series of enzymatic reactions (Figure 1-4D, Figure1-5)[89, 90]. The electron transport chain consists of four enzyme complexes (Complex I – Complex IV), cytochrome c and the mobile electron carrier ubiquinone. NADH derived from both cytosolic glycolysis and mitochondrial TCA cycle activity donates electrons to NADH:ubiquinone oxidoreductase (complex I). Complex I ultimately transfers its electrons to ubiquinone. Ubiquinone can also be reduced by electrons donated from several $FADH_2$-containing dehydrogenases, including succinate:ubiquinone oxidoreductase (complex II) and glycerol-3-phosphate dehydrogenase. Electrons from reduced ubiquinone are then transferred to ubiquinol:cytochrome c oxidoreductase (complex III) by the ubisemiquinone radical-generating Q cycle. Electron transport then proceeds through cytochrome c, cytochrome c oxidase (complex IV) and finally to O_2. Electron transfer through complexes I, III and IV generates a proton gradient that drives ATP synthase (chemiosmosis). The electron transport chain couples the transfer of electrons between a donor (NADH and $FADH_2$) and an electron acceptor (O_2) with the transfer of protons H^+ across the inner mitochondrial membrane, enabling the process of oxidative phosphorylation [89, 92].

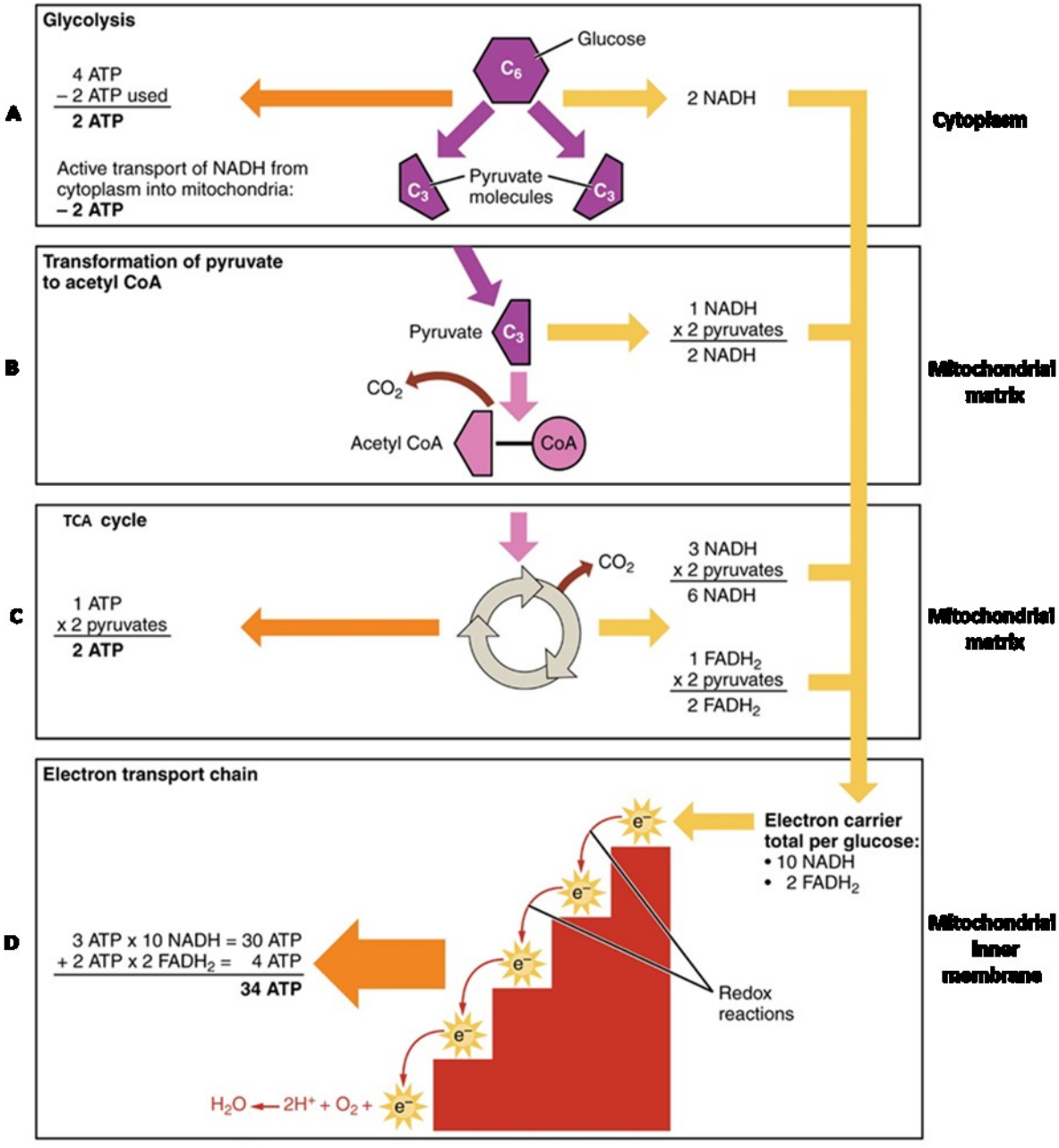

Figure 1-4 Glucose Metabolism. (A) Glycolysis, the breakdown of one molecule of glucose resulting in two molecules of pyruvate, two ATP and two NADH in cytoplasm; (B) Transformation of pyruvate to acetyl CoA in mitochondrial matrix. (C) The tricarboxylic acid (TCA) cycle, acetyl CoA enters the TCA cycle to produce CO_2, H_2O, one ATP, three NADH and one $FADH_2$. (D) The electron transport chain: Electrons from NADH and FADH2 are transferred through protein complexes embedded in the inner mitochondrial membrane by a series of enzymatic reactions to O_2. Electron transfer through complexes I, III and IV generates a proton gradient that drives ATP synthase.[89]

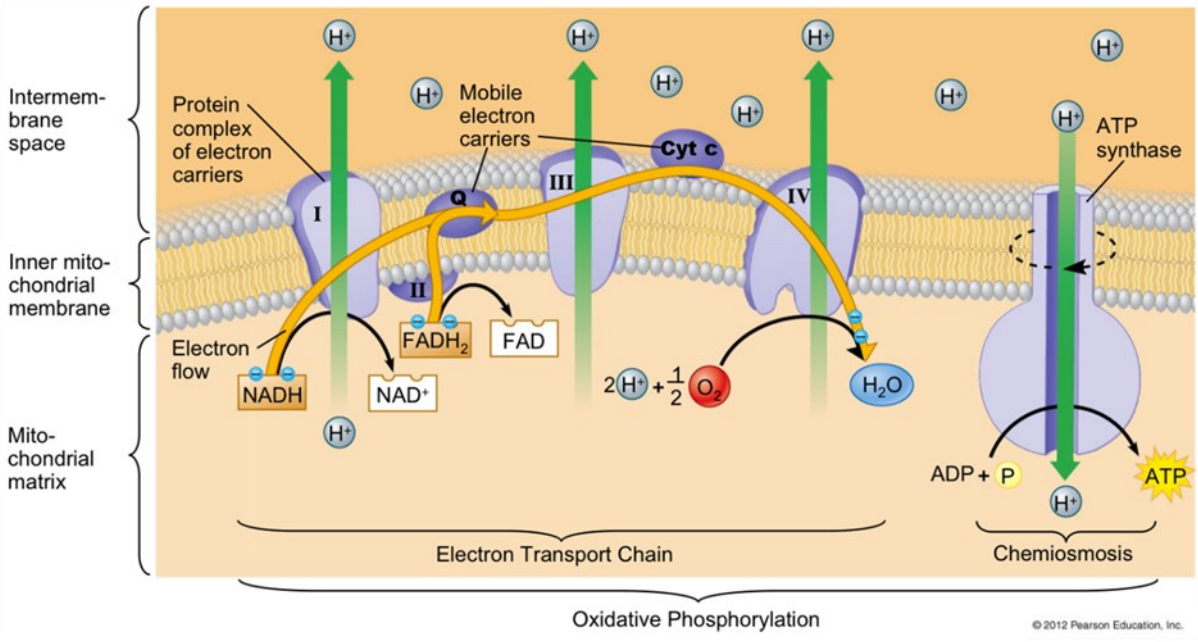

Figure 1-5 Electron Transport Chain. The electron transport chain is a series of electron carriers and ion pumps that are used to pump H^+ out of the inner mitochondrial matrix. NADH donates electrons to NADH:ubiquinone oxidoreductase (complex I). Complex I transfers its electrons to ubiquinone. Ubiquinone can also be reduced by electrons donated from several FADH2-containing dehydrogenases, including succinate:ubiquinone oxidoreductase (complex II) and glycerol-3-phosphate dehydrogenase. Electrons from reduced ubiquinone are then transferred to ubiquinol:cytochrome c oxidoreductase (complex III) by the ubisemiquinone radical-generating Q cycle (Q). Electron transport then proceeds through cytochrome c, cytochrome c oxidase (complex IV) and finally, O_2. Electron transfer through complexes I, III and IV generates a proton gradient that drives ATP synthase (chemiosmosis) [90, 92].

1.3 Diabetes mellitus (DM)

Diabetes mellitus (DM), commonly referred to as diabetes, is a group of metabolic diseases characterized by hyperglycemia resulting from defects in insulin secretion, insulin action, or both [93].

Diabetes can be classified into the following general categories:

Class	Etiology
Type 1 diabetes mellitus (T1DM)	B-cell destruction, usually leading to absolute insulin deficiency
Type 2 diabetes mellitus (T2DM)	A progressive insulin secretory defect on the background of insulin resistance
Gestational diabetes mellitus (GDM)	Diabetes diagnosed in the second or third trimester of pregnancy that is not overt diabetes
Specific types of diabetes due to other causes	Other causes, e.g., monogenic diabetes syndromes, diseases of the exocrine pancreas, and drug or chemical-induced diabetes

T1DM accounts for 5–10% of diabetes and is characterized by absolute insulin deficiency resulted from the destruction of pancreatic beta cells usually caused by cellular-mediated autoimmunity (type 1A). Autoimmune markers such as islet cell antibodies (ICA), antibodies to glutamic acid decarboxylase 65 (GAD 65), insulin and tyrosine phosphatases IA-2 can be detected in the serum. However, some patients have no evidence of autoimmunity and have no other known cause for beta cell destruction (type 1B) [93].

T2DM is the most common type of diabetes in adults and accounts for ~90–95% diabetes. It is due to insulin resistance caused mainly by abdominal fat accumulation, resulting in relative (rather than absolute) insulin deficiency, which ultimately leads to chronic hyperglycemia [93].

In addition to T1DM and T2DM, GDM refers to any degree of carbohydrate intolerance with onset or first recognition during pregnancy [94]. It is classically diagnosed by a fasting oral glucose tolerance test (OGTT) after uptake of 75g glucose with a cut-off plasma glucose of ≥ 140 mg/dl (7.8mmol/l) after 2-hour at 24-28 gestational weeks. This is because insulin resistance increases during the second trimester of pregnancy, and glucose levels will increase in women who do not have the ability to produce enough insulin to adapt to this resistance

[93]. GDM is a problem that affects a significant number of women during pregnancy. It could have lasting health impacts on both mother and fetus.

1.4 Maternal diabetes

Maternal diabetes includes pre-gestational diabetes mellitus (PGDM) and GDM. PGDM refers to pre-existing diabetes (Type 1 or Type 2) when women become pregnant. GDM occurs only during pregnancy.

1.4.1 The main short-term complications in the progeny of maternal diabetes

Maternal diabetes complications affecting fetus have been well demonstrated, including macrosomia, perinatal death, congenital malformations, etc.

1.4.1.1 Macrosomia

Macrosomia or large for gestational age (LGA) is a term used to describe excessive fetal growth. LGA refers to a body weight ≥ 90th percentile for gestational age, which is more precise and takes into consideration gestational age at birth, allowing premature newborns with excessive fetal growth to be identified [95].

Macrosomia in newborns of diabetic mothers is characterized by an increase in body fat, muscle mass and organomegaly without increased brain size. The overnutrition resulted from maternal diabetes, obesity, and excess gestational weight gain, contribute to macrosomia. Maternal obesity is highly related to GDM. The risk of GDM is 2.14-8.56-fold higher in overweight to severely obese pregnant women, compared to pregnant women with normal weight [96].

The mechanisms of how maternal diabetes impact on fetal and neonatal physiology is not fully understood. The Pedersen's hypothesis suggested that macrosomia was related to the increased transplacental transfer of maternal glucose, that further stimulates the release of insulin from the pancreatic beta cells of the fetus. As a major fetal growth factor, insulin triggers macrosomia subsequently [97, 98]. Insulin resistance and inflammation also occur in GDM except for hyperglycemia [99]. They both increase the placental transfer of nutrients to the fetus including glucose, amino acids and free fatty acids, to affect fetal growth [100, 101].

1.4.1.2 Intrauterine growth restriction (IUGR) and premature birth

IUGR indicates restricted growth of a fetus in the mother's uterus during pregnancy and can result in a baby being small for gestational age, which is most commonly defined as a weight ≤ 10th percentile for the gestational age.

IUGR is most often caused by poor maternal nutrition or lack of adequate oxygen supply to the fetus and has been reported in cases with severe vascular complications of preexisting T1DM and poor placental perfusion [102]. Increased preconceptional hemoglobin (HbA1c) has been reported to be associated with a reduced fetal weight at birth [103]. The potential mechanism hypothesized in this regard is that in early pregnancy, the elevated glucose concentration impairs placental development, resulting in placental growth restriction, placental functions damage and IUGR. In other respect, accompanying hyperglycemia in the fetus leads to degranulation of the fetal β-cells, causing fetal hypoinsulinemia. Severe hyperglycemia in maternal rats results in hyperglycemia and hypoinsulinemia in the fetuses and IUGR [104].

The IUGR increases a risk of premature birth. In PGDM, the rate of premature birth is increased up to 25% [105]. Pregestational hypertension is related to premature birth in T1DM, whereas in T2DM, the third trimester glycosylated HbA1c is an indicator of prematurity [106]. As reported, GDM and glucose intolerance are risk factors for spontaneous preterm birth independent of other diabetes complications, while the mean maternal glucose is related to the risk of premature birth [107, 108].

1.4.1.3 Perinatal death

The World Health Organization defines perinatal death as the stillbirths (a baby still in the uterus) and mortalities in the first week of life after birth, the perinatal period commences at 22 completed weeks (154 days) of gestation and ends seven completed days after birth (http://www.who.int/maternal_child_adolescent/topics/maternal/maternal_perinatal/en/).

PGDM is highly associated with an increased risk of stillbirth. Such risk is increased 3-5-fold in T1DM in different countries [109] and more than 75% of perinatal deaths are attributed to congenital anomalies or prematurity. In T2DM, the risk of perinatal death seems even higher

than in T1DM (OR = 1.5) [110], and the deaths are mainly due to stillbirth, chorioamnionitis, or birth asphyxia [111]. The risk for stillbirth may be slightly increased in GDM, less than in PGDM (T1DM and T2DM) [109].

The pathophysiology of stillbirth in diabetic pregnancies is still unclear. It is generally accepted that unexplained stillbirths in diabetic pregnancies are associated with the poor glycemic control. A strict blood glucose control has been shown to reduce the number of stillbirths in women with T1DM and T2DM [19]. It is reported that stillbirth can also result from severe placental insufficiency and fetal growth restriction, especially in the presence of maternal vascular complications [112].

1.4.1.4 Congenital malformations

Congenital malformations are defined as aberrations of structure, function, or body metabolism present in a baby at or before birth, affecting many organs.

Maternal diabetes, especially PGDM, has significant effect on the occurrence of congenital malformations [113]. Babies exposed to continuous high glucose concentration are more likely to suffer the cardiovascular abnormalities, nervous system defects, caudal regression syndrome, and skeletal and genital-urinary tract malformations than the healthy controls [114-116]. The risk of congenital malformations with PGDM is 1.9-10-fold higher than for the general population and slightly increased in GDM compared to the total population [117]. It has been shown that intensive glycemic control in diabetic mothers decreases the prevalence of congenital abnormalities to that in the general population [118].

The understanding of the molecular mechanisms of diabetic embryopathy is still incomplete [109]. As reported, maternal hyperglycemia causes excess glucose metabolism in the embryo that may modify various molecular chain reactions: 1) high glucose levels induce an excess production of ROS which has been shown to result in oxidative stress and subsequently increase the risk for fetal abnormalities [119]; and 2) high glucose also promotes the activation of many apoptotic proteins, such as members of the caspase families [120].

1.4.1.5 Maternal diabetes and renal malformations

Maternal diabetes appears to be one of the key factors associated with renal malformations in both human and experimental animals [121]. When the regular pattern of kidney development is interrupted in both humans and experimental animal models by a high glucose level in utero, kidney abnormalities with a low total nephron number may ensue, and incidences of such anomalies seem to be associated with the degree of maternal hyperglycemia [85, 122, 123]. Amri et al. [85] postulated that hyperglycemia in utero impairs nephrogenesis in rats, resulting in a reduced number of nephrons in the kidneys of 14-day-old pups. Similarly, E13 embryos exposed to 30 mM D-glucose for 1-week show decreased metanephric size. The UB tips are swollen, their branches are deformed and thickened, and their tips blunted [124].

Kanwar et al. [125] found that increased apoptosis in E13 metanephroi, when treated with 30 mM D-glucose as compared to when treated with 5mM D-glucose. Moreover, apoptosis was observed in the kidneys of newborn and 1-week-old mice pups from diabetic mothers. In our lab, we previously reported that maternal diabetes might impair UB branching morphogenesis and affected animals have relatively small kidneys/body weight with ~ 40% fewer nephrons, resulting in renal dysplasia or hypoplasia [122, 126]. Clinical investigations have demonstrated a positive correlation between hyperglycemia and fetal malformations [127], whereas good blood glucose control of diabetic mothers during this period decreases the rate of fetal dysmorphogenesis [118].

1.4.2 Mechanisms of hyperglycemia-induced renal malformations

The mechanisms of hyperglycemia-induced renal malformations are not clearly defined. Developing embryos appear to be very sensitive to high ROS levels, especially during early organogenesis. Embryos grow under a relatively low oxygen concentration at E7.5-9.5 in mice and E9-11 in rats [128] and high oxygen levels are toxic to them [129]. Oxidative stress is increased in diabetes and at the same time maternal hyperglycemia causes sustained ROS generation with depletion of antioxidants [130]. In diabetic environments, increased ROS production leads to embryonic dysmorphogenesis, and ROS scavenging enzymes can reduce the rate of abnormalities in cultured E10.5 rat embryos [131]. Hyperglycemia induces embryonic malformations in rats because of glutathione (GSH) depletion, as GSH ester

supplementation decreases the formation of free oxygen radical species, virtually normalizing growth retardation and embryonic dysmorphogenesis [132].

All components of the intrarenal renin-angiotensin system (RAS) expressed in the developing kidney, play important roles in nephrogenesis [133]. RAS suppression by ACE inhibitors leads to renal abnormalities in both structure and function. Ang II receptor blockade also causes renal maldevelopment. In newborn Sprague-Dawley rat pups, administration of the AT1R antagonist losartan from days 1 to 12 of postnatal life reduced the number of nephrons [134]. Interestingly, growth-retarded infants have small kidneys, elevated cord blood renin levels [135] and heightened renin gene expression in the kidneys [136], suggesting that the intrarenal RAS may be elevated after IUGR.

Maternal high glucose level induces excessive production of ROS which has been shown to result in oxidative stress and subsequently triggers the proliferation gene related signaling pathway to impair mesenchymal-to-epithelial conversion in kidney development [122, 123, 137, 138]. Previously, It has been demonstrated that high D-glucose-induced UB branching and Pax2 gene expression could be blocked by ROS inhibitors (catalase and inhibitors of NADPH oxidase) in ex vivo studies [123]. This indicated that there is a transient rapid growth of UB branching triggered by Pax2 gene expression induced by hyperglycemia at the early stage of maternal diabetes.

Hyperglycemia induced ROS promotes the activation of many apoptosis related pathways such as NF-κB (p50/p65) and p53 pathways [124, 127, 128]. By in vivo studies, the researchers have demonstrated that the offspring of diabetic mice have smaller kidneys which displayed significantly more apoptotic podocytes as well as augmented active caspase3 immunostaining in renal tubules compared to control mice offspring [122]. Subsequently, it has been demonstrated by the researchers that maternal diabetes activates the intrarenal RAS and induces NF-κB (p50/p65) involved glomerular apoptosis, resulting in impairment of renal morphogenesis in diabetic offspring [126]. Taken together, hyperglycemia impairs kidney development in utero.

1.5 Diabetic nephropathy (DN)

Chronic hyperglycemia caused by DM, especially T1DM and T2DM, is associated with increased risk of progression to micro (nephropathy, retinopathy, and neuropathy) and macrovascular complications (cardiovascular disease) of diabetes [139]. As a long-term major microvascular complication of uncontrolled hyperglycemia, diabetic nephropathy (DN) affects a large population worldwide.

DN is clinically divided into multiple stages, and the pathophysiologic changes manifest as microalbuminuria and hyperfiltration at early stages and decreased glomerular filtration rate (GFR) as well as enhanced proteinuria collide at the third stage, followed by deterioration to end-stage renal disease [140, 141]. Microalbuminuria is usually the first signal of renal complications and may progress to overt albuminuria [142, 143]. Approximately 25% of people with T2DM have albuminuria, and the rate is persistently rising by 2-3% every year [144, 145]. Albuminuria results from higher intra-glomerular pressure and GBM permeability, and may be indirectly influenced by interactions of GECs with mesangial cell and podocytes in a paracrine fashion [146]. In T2DM, markers of endothelial dysfunction such as endothelin-1 and tissue plasminogen activator were detected in patients with normal urine albumin excretion [147], which gives support to the hypothesis that endothelial dysfunction might not be a simple consequence but may also play a key role in the vasculopathy [148]

1.5.1 Pathogenesis of DN

The mechanisms related to the pathogenesis of DN is multifactorial. The various signaling pathways modulated by a large number of molecules that regulate the bioactivity of one another, are activated during the progression of DN. They may share common downstream pathways, such as the activation of renin-angiotensin system (RAS) and protein kinase C (PKC) and the increased expression of transforming growth factor beta (TGFβ). These common pathways are associated with the generation of reactive oxygen species (ROS) and promote the renal fibrosis and glomerulosclerosis in DN. Various potential target sites, such as angiotensin II (AngII), TGFβ, nicotinamide adenine dinucleotide phosphate (NADPH) oxidase and $p27^{Kip1}$, seem to be involved in the induction and progression of DN [149].

1.5.1.1 Oxidative stress in DN

The reactive oxygen species (ROS) are composed of molecules including molecular oxygen and its derivatives, superoxide anion (O_2^-), hydroxyl radical ($HO^·$), hydrogen peroxide (H_2O_2), peroxynitrite ($ONOO^-$), hypochlorous acid (HOCl), nitric oxide (NO) and lipid radicals [150]. Living organisms possess finely regulated systems to maintain very low ROS levels, i.e. their production and elimination are well balanced resulting in certain steady-state ROS level. However, under certain circumstances this balance can be disturbed, resulting in more ROS generation [151]. Excessive ROS production and overwhelming antioxidant capacity in pathological conditions, oxidize various tissue biomolecules such as DNA, protein, lipids and carbohydrates, thereby disturbing cellular metabolism and its regulation and damaging cellular constituents; this disastrous state has been referred to as oxidative stress [152, 153]. The sources of ROS in the diabetic kidney include mitochondrial respiratory chain, nicotinamide-adenine dinucleotide phosphate (NADPH) oxidases, xanthine oxidase, NO synthase, advanced glycation end products **(**AGEs) and other certain hemoproteins [154].

1.5.1.1.1 Sources of ROS in DN

Mitochondrial respiration

In normal conditions, glucose generates ATP, NADH, and $FADH_2$ via glycolysis and oxidative phosphorylation. The electrons from NADH or $FADH_2$ are transferred to molecular oxygen (O_2) in the mitochondrial respiratory chains complex I - IV to generate ATP through ATP synthase, and only less than 1% of the total O_2 consumption leaks from the respiratory chain to generate ROS. However, intracellular hyperglycemia increases the flux of electron transfer donors (NADH and $FADH_2$) into the mitochondrial respiratory chain by oxidizing glucose-derived pyruvate. The resulting hyperpolarization of the mitochondrial inner membrane potential partially inhibits electron transport in complex III and accumulates electrons to ubisemiquinone to generate O_2^- [150, 155]. Interestingly, specific target cells, including glomerular mesangial cells and retinal capillary endothelial cells are unable to regulate intracellular glucose concentrations adequately in the diabetic milieu [154]. These cells are particularly susceptible to hyperglycemic assault since they are unable to avert intracellular high glucose ambiance in states of the systemic rise in blood glucose levels. As a result, these target cells with the increased flux of glucose in the diabetic state have

accelerated oxidative phosphorylation, and excessive leakage of O_2^-, and are thereby subjected to extraordinary ROS-mediated oxidative stress [153].

NADPH Oxidases

Another important source of ROS is NADPH oxidase. Human isoforms of the NADPH oxidase include Nox1, Nox2, Nox3, Nox4, Nox5, DUOX1, and DUOX2 [156]. All Nox isoforms are transmembrane proteins that transfer electrons across the biological membrane from NADPH to reduce molecular oxygen to O_2^- [153], as illustrated below:

$$NADPH + 2O_2 \xrightarrow{NOX} NADP^+ + H^+ + 2O_2^-$$

O_2^- is produced through the 1-electron reduction of O_2 catalyzed by NADPH oxidase and rapidly dismutates to the more stable H_2O_2 [157]. Among the NADPH oxidase isoforms, Nox4 is the most abundant Nox in the kidney. The mRNA and protein levels of both Nox4 and p22phox mRNA were increased in both distal tubular cells and glomeruli of STZ-induced diabetic rats as compared with control rats [158]. Nox4 protein expression was increased in diabetic kidney cortex compared with non-diabetic controls and antisense oligonucleotides for Nox4 downregulated Nox expression, reduced whole kidney and glomerular hypertrophy, and attenuated fibronectin expression [159]. The role of Nox4-derived ROS in DN is going to be introduced later in details.

1.5.1.1.2 ROS damage in renal cells

Excessively high ROS can activate transcription factors, such as NF-κB, signaling transduction cascades Protein kinase C (PKC) and mitogen-activated protein kinases (MAPK), which result in the extracellular matrix (ECM) accumulation, glomerular mesangial expansion and tubulointerstitial fibrosis [160]. Nam et al. [161] reported that stimulated ROS is significantly higher with NF-κB up-regulation in diabetic patients with DN than in diabetic patients without DN. Ha et al. [162] demonstrated that the antioxidant taurine effectively inhibits membrane translocation of PKC in STZ-induced diabetic rat glomeruli, indicating that ROS activate PKC in the diabetic kidney as well. These observations suggest that increased

ROS induced by hyperglycemia act as intracellular messengers and integral glucose signaling molecules in DN.

ROS-mediated mesangial ECM accumulation in DN

The contribution of ROS in DN perpetuating glomerular hypertrophy and mesangial expansion is supported by many experimental studies [163, 164]. Enhanced ROS level in response to high glucose was found to be associated with increased expression of Nox4 in the mesangial cells [165-167]. Nox4-derived ROS drives uncoupling of endothelial isoform of nitric oxide synthase (eNOS), and a decrease in NO bioavailability in diabetes can initiate fibrotic injury to mesangial cells, suggesting that Nox4 functions upstream of eNOS [167]. Studies have shown that global genetic deletion of Nox4 significantly attenuated the diabetes-induced increased mesangial expansion, glomerulosclerosis, and accumulation of ECM proteins (collagen IV and fibronectin) via a reduction in ROS production in a murine type 1 diabetes model [164, 168].

Involvement of AngII, TGFβ alone or in association with high glucose in the regulation of Nox4-derived ROS-induced signaling in renal cells, including mesangial cells, has also been reported by several studies [164, 169, 170]. TGFβ was found to induce the activity of Nox4 expression, indicating that this growth factor induces production of ROS in kidney myofibroblasts [171]. Renal tissue AngII activates Nox in mesangial cells and angiotensin-converting enzyme (ACE) inhibitors reduce renal and urine ROS production in STZ-induced diabetic rats [172]. Furthermore, there is a link between Nox-derived ROS and certain PKC isoforms, including PKCα and PKCβ, in the pathogenesis of DN [153, 168, 173]. Overactivation of PKCβ was found to upregulate expression of TGFβ and to increase ECM protein components in the glomeruli of diabetic rats via Nox4-dependent ROS formation [174]. Exposure of advanced oxidation protein product (AOPP) to mesangial cells resulted in increased expression of collagen IV, fibronectin, TGFβ, p22phox, and Nox4, as well as increased activity of PKCα, suggesting the involvement of the PKC/Nox-dependent pathway in glomerular injury [175].

ROS-mediated glomerular endothelial dysfunction in DN

The glomerular capillary endothelium is fenestrated and continuous [176]. There are two main functions of the renal endothelium – oxygen/nutrient delivery and filtration [177]. In contrast to other vascular beds, glomerular capillaries act predominantly as a sieve of fluids and solutes. GECs covering 20% of the endothelial surface, serve as a barrier for efficient absorption, secretion, and filtering [176]. With the glomerular endothelial cell strategically location at the interface between the blood compartment and the glomerular mesangium, it serves an important role in regulating glomerular microcirculation. [153]. Modification of glomerular capillaries and endothelial dysfunction are key contributors to epithelial cell injury in the progression of DN.

The imbalance between NO and ROS generation is the main pathophysiologic cause of diabetic endothelial dysfunction. In diabetic conditions, the production of ROS uncouples the eNOS leading to perturbations to or reductions in NO bioavailability, which impairs endothelium-dependent vasodilatation [178]. More interestingly, this eNOS uncoupling further augments O_2^- production and hence deteriorates vascular endothelial function. The O_2^- may also interact with NO, generating $ONOO^-$ which binds to tyrosine and other protein residues yielding cytotoxic compounds such as nitrotyrosine [179]. $ONOO^-$ is increased in T2DM patients, and diabetic mice [180, 181] and peroxynitrite-mediated endothelial dysfunction has been reported in DN [182]. Endothelial cells have also been shown to participate in glomerular inflammation. Glomerular endothelial cells, in response to AngII was found to be associated with increase in ROS production, as well as inflammatory parameters such as NF-κB and MCP-1 [183].

ROS-mediated podocyte injury, apoptosis, and albuminuria in DN

While glomerular hypertrophy, matrix accumulation, mesangial expansion and GBM thickening are classical features of diabetic glomerular lesions, evidence suggests that the onset of albuminuria is closely associated with podocyte injury, which includes foot process effacement, podocyte detachment and depletion [184].

A lot of studies demonstrate the deleterious effect of Nox4-derived ROS in podocyte injury, leading to albuminuria, foot process effacement, and loss of podocytes in DN [164, 167, 185]. Jha et el. [164] have demonstrated that deletion of Nox4 only in podocytes, attenuates the

diabetes-induced increase in albuminuria by ~50% in diabetic mice. This finding strongly supports the view that Nox4-derived ROS in the podocyte play a significant role in the regulation of albuminuria in diabetes. Studies have shown enhanced ROS production through upregulation of Nox4 in podocytes in response to high glucose and TGFβ [159, 164, 185, 186]. TGFβ/Nox4-derived ROS mediates activation of caspase 3 via the Smad2/3 pathway leading to mouse podocyte apoptosis [187]. In another study, high glucose-induced apoptosis of podocytes was found to be mediated via sequential upregulation of Nox4 by cytochrome P450 of the 4A family (CYP4A) [185].

ROS-mediated tubulointerstitial injury in DN

It is believed that downstream of the glomeruli, exposure of plasma proteins in association with chronic hyperglycemia across the tubular compartment of the nephron can trigger profibrotic and proinflammatory mechanisms in tubular epithelial cells, thereby inducing the development of tubulointerstitial fibrosis [188]. Tubulointerstitial fibrosis is characterized by the accumulation of interstitial fibroblasts and excessive ECM deposition in the tubulointerstitial space [189], ultimately leading to disrupted tubular reabsorption [190].

Nox-dependent ROS in renal tubular cells, in response to high glucose, is found to be associated with stimulation of MAPKs and the redox-sensitive transcription factor, NF-κB, leading to upregulation of the proinflammatory gene MCP-1 [191]. One of the potential mechanisms for renal fibrosis is epithelial-mesenchymal transition (EMT) [192]. Hyperglycemia, along with TGFβ, AngII, albumin, and AGEs induces EMT in renal tubular cells with upregulation of alpha-smooth muscle actin (a-SMA) and vimentin and downregulation of E-cadherin [193, 194]. Nox4-derived ROS formation in mouse proximal tubules exposed to high glucose, activates profibrotic processes via Nox4-sensitive p38 MAPK-dependent pathways [158, 195]. TGFβ is a known profibrotic growth factor mediating tubular injury via interaction of TGFβ with Nox4. Lee et al. [196] have shown that Nox4-mediated ROS generation in the tubular cells in response to TGFβ was ameliorated by activation of the AMPK pathway. Similar to the glomeruli, both PKCα and PKCβ, in association with Nox4 contribute to tubulointerstitial fibrosis in diabetes [168, 197]. TGFβ seems to play a critical role in myofibroblast differentiation via activation of Smad2/3 and

ERK signaling pathways [198, 199]. In addition, the TGFβ/Smad2/3 cascade is tightly regulated by the activation of MAPK in fibroblasts [200]. Another study using renal interstitial fibroblasts demonstrated that TGFβ/Nox4-induced ROS generation contributes to myofibroblast differentiation to a profibrotic phenotype via activation of Smad3 and ERK pathways [171].

1.5.1.2 AngII and DN

AngII is the major effector peptide of RAS in the endothelin system, and it is not only a vasoconstrictor but also an important factor for inducing inflammation and promoting fibrosis and apoptosis [201]. Mesangial cell protein synthesis is stimulated by AngII, with enhanced production of extracellular matrix proteins [202]. It has been demonstrated that AngII was noticeably upregulated in the cytoplasm of renal tubular epithelial cells in the DN group and correlated positively with the degree of renal interstitial fibrosis [203]. AngII overexpression led to tubular hypertrophy, tubular fibrosis, albuminuria and tubular apoptosis [204]. In human endothelial cells, AngII stimulated vascular permeability factor/vascular endothelial growth factor production, contributing to increased capillary permeability and proteinuria in glomerular diseases [205]. All these investigations suggest that overexpression of AngII may be involved in the development of DN.

Hyperglycemia stimulates the production of AngII and develops oxidative stress in human glomerular endothelium [206]. Stimulation of the angiotensin type 1 (AT1) receptor by AngII activates NADPH oxidase and facilitates ROS production in endothelial cells in DM [207]. High glucose stimulated angiotensinogen gene expression is mediated via ROS generation in renal tubular cells [208]. Another group demonstrated that augmentation of angiotensinogen expression in hypertensive rats was caused by ROS [209]. AngII-induced apoptosis is mediated via NADPH oxidase-dependent $ONOO^-$ formation and consequent DNA damage [210]. Apocynin, an inhibitor of NADPH oxidase, abolished AngII-induced apoptosis in embryonic rat cardiomyocytes [211]. These results indicate that AngII-induced cardiomyocytes apoptosis is mediated via, at least in part, ROS production associated with NADPH oxidase. Conversely, ROS may also work as an upstream signaling molecule of

AngII [212]. These effects appear to be the same in renal cells, AngII and ROS, mutually stimulating each other to enhance tissue damage.

1.5.1.3 TGFβ and DN

TGFβ are secreted proteins that exist in at least three isoforms called TGFβ1, TGFβ2, and TGFβ3. They are multifunctional cytokines that regulate proliferation, differentiation, and apoptosis of various cells. They share a receptor complex and signal in similar ways, but their expression levels vary depending on the tissue [213]. TGFβ ligand is synthesized as a precursor homodimer that interacts with its latency-associated peptide (LAP) and a latent TGFβ-binding protein (LTBP), forming a larger complex called the large latent complex (LLC). The process of TGFβ activation includes the release of the LLC from the resource cell and further proteolysis of LAP to release active TGFβ to its receptors at the cell membrane [214]. Upon activation, TGFβ dimers induce heteromeric complex formation between TGFβ receptor II (TGFβRII). Type II receptors then transphosphorylate the TGFβ receptor I (TGFβRI) [215]. Activation of TGFβRI causes phosphorylation and activation of receptor-specific SMAD (R-SMAD) proteins, such as SMAD2 and SMAD3. Together with the common mediator SMAD4 (co-SMAD), R-SMADs translocate to the nucleus where they interact with other transcription factors to regulate transcriptional responses, such as apoptosis, extracellular matrix neogenesis, immunosuppression and G1 arrest in the cell cycle (Figure 1-6) [216].

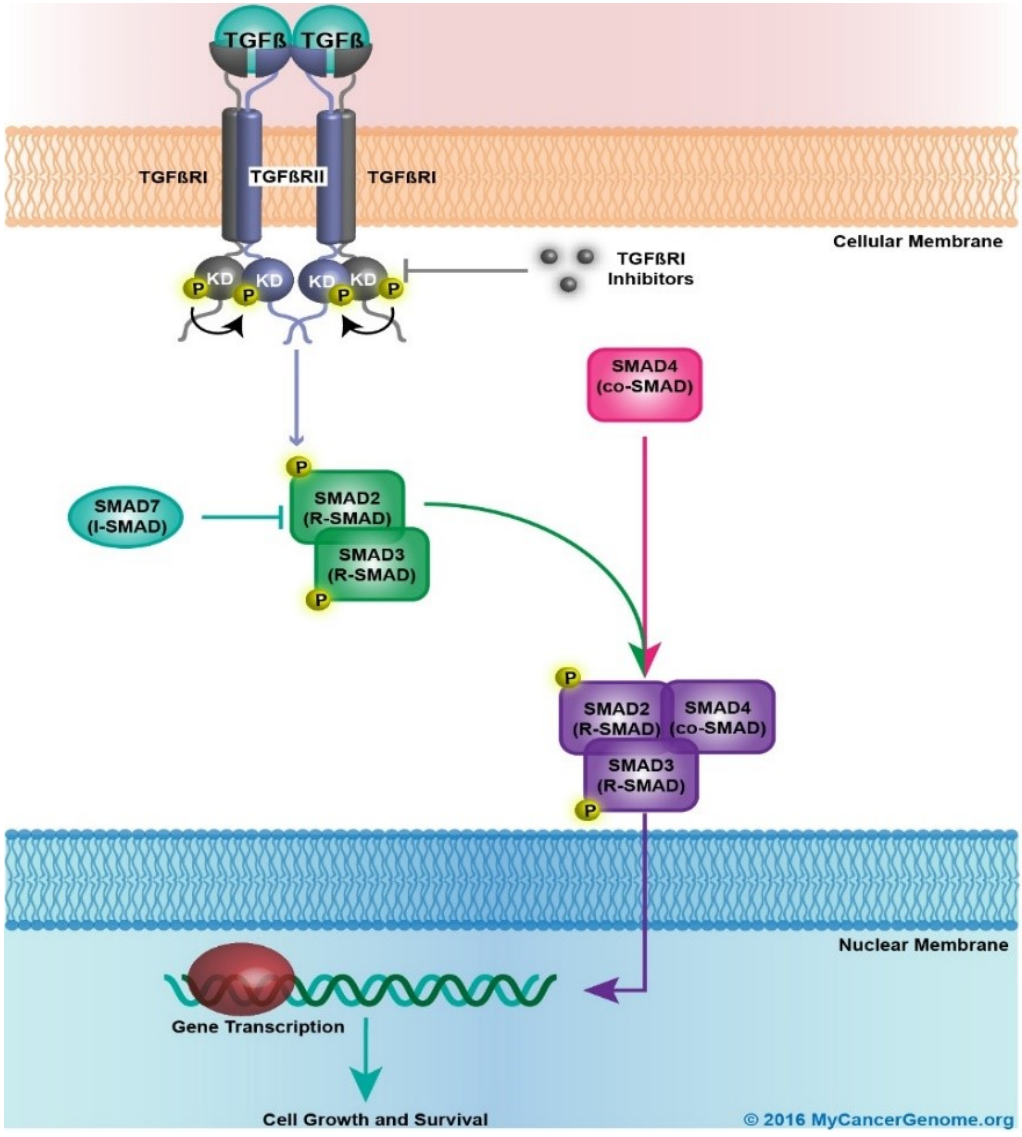

Figure 1-6 Schematic representation of canonical TGFβ signaling pathways. Binding of the TGFβ1 ligand dimer to the TGF-beta receptor type-2 (TGFβRII) promotes dimerization of TGFβRII with TGFβRI and results in phosphorylation of TGFBRI. The activated TGFBRI activates R-SMADs (SMAD2 and SMAD3) via phosphorylation. SMAD2 and SMAD3 trimerize with a co-SMAD (SMAD4). The SMAD trimer enters the nucleus to activate gene transcription and promotes cell growth and survival [215].

TGFβ plays a crucial role in cell proliferation, differentiation, and apoptosis [217]. Studies have suggested that TGFβ1 can facilitate "braking" of the branching program as the UB shifts from a rapid branching stage to a stage where branching slows down and eventually stops [218]. In vitro studies have established that TGFβ1 within the rat metanephros inhibits ureteric duct growth and thereby nephron endowment to shape the structure of the mature

kidney [219, 220]. Convincing evidence suggests that TGFβ1 plays a key role in glomerular endothelial cell damage [92, 221], the production of ECM and the development of renal interstitial fibrosis in DN [222-225]. In addition, TGFβ1 has been implicated in DN-related EndoMT transition [226, 227].

TGFβ signaling is activated by a large number of mediators that have been identified to induce renal injury in DN such as ROS, AGEs, PKC, and AngII [228, 229]. TGFβ is recognized as the major cytokine responsible for the ECM pathobiology seen in DN and perhaps plays the most crucial role in DN pathogenesis [230]. High glucose induces TGFβ1 overexpression in mesangial cells in culture [231]. Enhanced expression of glomerular TGFβ1 is also observed mainly in podocytes of diabetic animals [232, 233]. It has been proposed that in DN, latent TGFβ1 complexes secreted by mesangial cells may be stored in the mesangial matrix, from which latent TGFβ1 is released and transferred to the podocyte surface [234-236]. TGFβ1 stimulates the synthesis of critical extracellular matrix molecules including type IV collagen, type I collagen, fibronectin, and laminin [237]. It was reported that TGFβ1 also decreases matrix degradation by inhibiting proteases as well as activating protease inhibitors. In addition, TGFβ1 promotes cell-matrix interactions by elevating integrins, the cell surface receptors for matrix [230].

An increase in glomerular capillary pressure may stimulate AngII and TGFβ1 expression in podocytes through mechanical force injury due to glomerular hypertrophy in the early phase of DN [238-240]. AngII may increase the ROS generation through the activation of NADPH oxidases and increases the expression of the TGFβRII and VEGF in podocytes [241]. Furthermore, AngII-induced oxidative stress may activate the latent TGFβ and the TGFβ signaling system in DN [235]. Immunostaining for TGFβ1, TGFβRII, and phosphorylated Smad2/Smad3 is increased in damaged podocytes of sclerotic glomerular [242].

In summary, chronic high glucose in diabetic patients may stimulate mesangial cells to secrete TGFβ, which may be stored in the mesangial matrix. Latent TGFβ complex released from the mesangial matrix may be localized to the podocyte surface and activated by Ang II. Activated TGFβ in podocytes may overproduce collagen IV leading to GBM thickening. In addition,

TGFβ-induced EndoMT transition may also contribute to the development of glomerulosclerosis [226, 243, 244].

1.5.1.4 EndoMT in diabetic nephropathy (DN)

Epithelial-mesenchymal transition (EMT), whereby epithelial cells begin to express the characteristics of mesenchymal cells, has been established for several years. More recently, a similar change in endothelial cells, referred to as endothelial-mesenchymal transition (EndoMT), has been observed [245]. During EndoMT, under the effect of a range of factors, endothelial cells begin to resemble myofibroblasts, with loss of polarity, diminished basement membrane adhesion, endothelial markers (such as CD31 and vascular endothelial cadherin), while exhibiting mesenchymal markers, including α-smooth muscle actin (α-SMA), fibroblast-specific protein 1 (FSP1), vimentin, and nestin, many of which are characteristic of active myofibroblasts [246]. Kidney fibrosis in DN is a significant sign of an advanced stage of disease and may develop in both the tubulointerstitial space and glomerulus. EndoMT has also been suggested to play an important role in organ fibrosis and cancer progression [247]. Evidence of the involvement of EndoMT in DN may be found in the pivotal studies of Zeisberg and Li [248, 249]. Zeisberg et al. presented the first evidence of possible EndoMT in diabetic kidney fibrosis: in a 6-month Streptozotocin (STZ) -induced diabetic mouse model, they found that about 40% of all FSP1-positive and 50% of the α-SMA-positive cells co-labeled with CD31, implying that EndoMT may exist in the development and progression of DN and this phenotypic change occurs very early in the disease process [248]. Li et al. [249], using an endothelial-lineage traceable mouse line, demonstrated that the number of endothelial-origin myofibroblasts, as well as the percentage of myofibroblasts of endothelial origin, was significantly higher in STZ-induced DN than in normal kidneys. Moreover, EndoMT occurred independently of albuminuria, suggesting that renal endothelial cells may play a role in the initiation of renal interstitial fibrosis through the process of EndoMT [249]. Based on these studies, EndoMT was considered as a potential new player in diabetic renal fibrosis. However, confirmation in human disease and elucidation of the underlying molecular mechanisms accounting for EndoMT leading to renal fibrosis remain to be studied. Many of the factors known to increase as part of the diabetic milieu have been implicated, including

TGFβ, AngII, and advanced glycation end products **(**AGEs) [246]. Debate on the source of fibrosis-generating myofibroblasts (either from endothelial cells or vascular pericytes) in vivo is still raging [250].

1.5.2 Apoptosis and DN

Apoptosis is nature's preprogrammed form of cell death. Apoptosis occurs normally during development when damaged tissues are repaired, and as a homeostatic mechanism to maintain cell populations in tissues [251]. Caspases have a key role in the induction of apoptosis as well as in the execution phase of apoptosis, and play a central role in DN [252]. Caspase-dependent apoptosis can be induced by either the intrinsic or the extrinsic pathway. The intrinsic apoptotic pathway is mainly regulated by the anti-apoptotic (Bcl-2, Bcl-XL), the pro-apoptotic (Bax, Bak), and the BH3-only proteins (Bim, Puma, Bid…). The extrinsic pathway involves a death-inducing ligand such as Fas ligand (FasL) or TNFα interacting with their corresponding death receptor on the plasma membrane. Both pathways finally activate the effector caspases 3, leading to apoptosis (Figure 1-7) [253, 254].

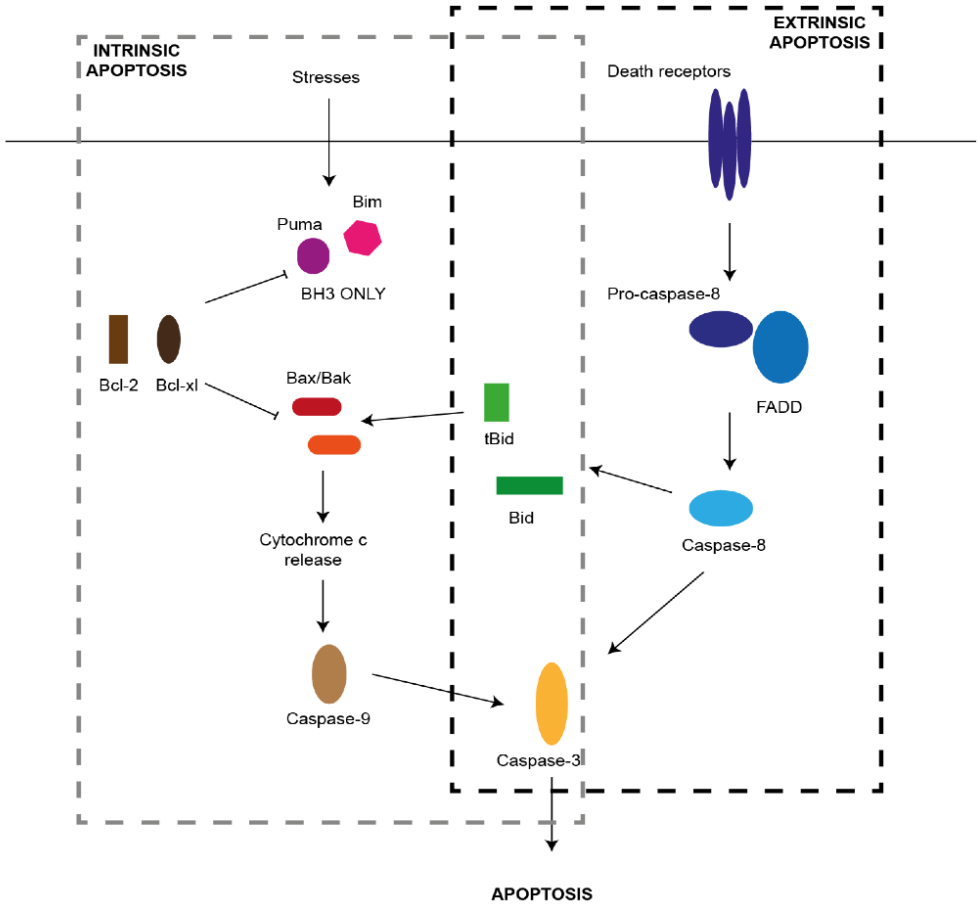

Adopted from *Cells, 2013. **2**(2): p. 266-83*

Figure 1-7 The two pathways (intrinsic and extrinsic) of apoptosis. The intrinsic pathway is activated by cellular stresses such as high glucose and results in activation of the BH3-only members (such as Bim and Puma) that initiate apoptosis signaling by binding to the Bcl-2-like anti-apoptotic proteins (including Bcl-2 and Bcl-xL) and release of Bax and/or Bak to promote loss of mitochondrial outer membrane potential, cytochrome c release and activation of caspase-9, caspase-3 and apoptosis. The extrinsic pathway can bypass the mitochondrial step and is initiated by activation of death receptors, such as Fas, that have an intracellular death domain. This results in formation of a death-inducing signaling complex in which the initiator caspase, caspase-8 is activated by its adaptor FAS-associated death domain (FADD). This results in activation of the caspase cascade and apoptosis. The BH3-only protein Bid communicates between the two pathways. This figure was [254].

Hyperglycemia leads to oxidative stress, and this is the primary trigger for tubular and glomerular cells to go into apoptosis in animal models and cell culture systems [92, 150, 255]. High glucose levels cause ROS-dependent apoptosis of mesangial cells via Bax-mediated mitochondrial permeability and subsequent cytochrome c release [209]. In human and murine

renal mesangial cells, hyperglycemia caused an increased Bax/Bcl-2 ratio, associated with cytochrome c release from mitochondria and subsequent the caspase-3 activation [256]. Apoptosis has been found in podocytes, interstitial cells, endothelial, and tubular epithelial cells in renal biopsies in patients with DN [257]

Enhanced glucose levels increased NADPH oxidase-mediated and mitochondrial-mediated ROS formation that activates proapoptotic p38 MAPK and caspase-3 activation in podocytes in vitro [187]. Susztak et al. [258] have shown that podocyte apoptosis increased markedly with the onset of hyperglycemia in Akita mice and db/db mice, and inhibition of NADPH oxidase-induced ROS formation prevented podocyte apoptosis.

In glomerular endothelial cells, a complex of thrombomodulin and thrombin activates protein C, which subsequently activates the protease-activated receptor-1 (PAR-1) in the proximity of the endothelial protein C receptor (EPCR), resulting in cytoprotective signaling. Hyperglycemia interferes with thrombomodulin-dependent protein C activation, resulting in the release of apoptosis-associated factors like cytochrome c and Smac/Diablo leading to apoptosis of endothelial cells [259, 260].

In renal tubular epithelial cells, high glucose-mediated oxidative stress induced an increased Bax protein expression, which was accompanied by a reduced Bcl-2 expression [261]. This observation is consistent with earlier findings that during diabetes gene expression of pro-apoptotic Bax was increased, whereas anti-apoptotic Bcl-2 expression was down-regulated [262]. Different caspases, in particular, caspase-3 and -9 play a crucial role in high glucose-induced apoptosis of proximal tubular epithelial cells [263]. In summary, apoptosis plays an essential role during the DN progression, particularly through the intrinsic pathway.

1.6 Structure and function of hedgehog interacting protein (Hhip)

Hedgehog-interacting protein (Hhip) encodes a protein of 700 amino acids attached to the cell membrane via a C-terminal glycosylphosphatidylinositol (GPI) anchor. It was initially discovered as a putative antagonist of all three hedgehog (Hh) ligands (Shh, Ihh, and Dhh) by screening a mouse cDNA expression library for proteins that bound to Shh [59].

1.6.1 Structure of Hhip

To understand the functions of Hhip at a molecular level, it is necessary to learn about its structure (Figure 1-8) [264].

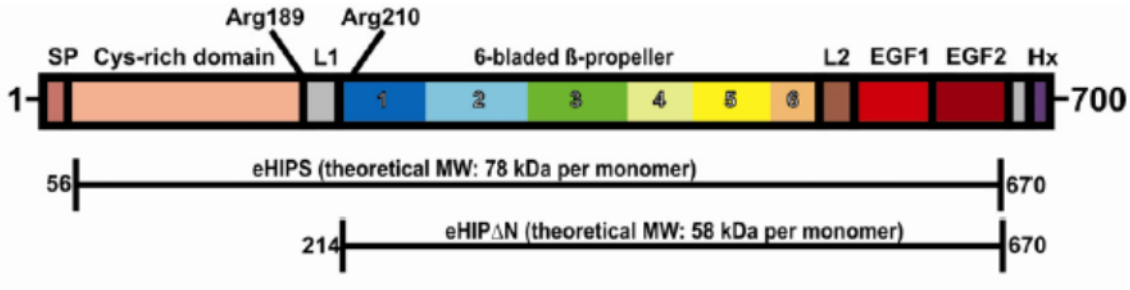

Figure 1-8 Schematic representation of the Hhip domain organization. SP is a signal peptide. During expression, the full-length ectodomain of human Hhip (eHhip, 56-670) segmented. N-terminal truncation of the first 213 amino acid residues (eHhipΔN construct) or mutation of the proteolytic recognition sequences (Arg189, Arg210, and Lys211 to alanine) resulted in proteolytically stable proteins. The stabilized full-length ectodomain is dimeric whereas eHIPΔN is a monomer suggesting a function for the N-terminal cysteine-rich domain in mediating dimerization. The eHhipΔN monomer consists of an N-terminal 6-bladed β-propeller domain (residues 214-583) connected to two epidermal growth factor (EGF) repeat domains (residues 607-637 and 638-670). Twenty-eight residues combine the β-propeller to the EGF repeats. Hx is a membrane attachment helix [264].

In Hhip-Shh complex, Hhip acts as a structural decoy receptor for lipid-modified Shh by inserting its L2 loop into the Shh active site, which contains the Zn^{2+} cation (gray oval). Hhip binding blocks other potential Shh pseudo active site binding proteins such as Ptch1 (Figure 1-5 right). Hhip also blocks Cdon binding due to steric overlap at the Shh Ca^{2+} binding site. Hence, Zn^{2+} makes a key contribution to the interface, whereas Ca^{2+} is likely to prevent electrostatic repulsion between the two proteins. The interplay between Shh Zn^{2+} and Ca^{2+} binding sites may allow extracellular Ca^{2+} concentration to take an essential modulatory role [264, 265].

1.6.2 Function of Hhip

Current data indicate that Hhip is important both during embryonic development and in various diseases of the adult [59, 265-267]. Hhip can function via both canonical- [59, 264-266] and non-canonical Hh pathways [267].

1.6.2.1 Role of Hhip in embryonic development

In mouse embryos Hhip is expressed in cells adjacent to those expressing Shh. Chuang et al. [59] examined the temporal and spatial expression pattern of Hhip in mouse embryos from 7.5 to 14.5 days post-coitum. They found that after Shh expression was detected in several signaling centers, including the notochord, floor plate and zone of polarizing activity (ZPA) of the limb and in several endodermal derivatives, Hhip was all detected next to Shh-expressing cells. Later in development, Shh is expressed in the epithelia of a wide variety of tissues, for instance, the epithelium of the lung, gut, whisker, hair, and rugae. In all cases, Hhip was expressed in the underlying mesenchyme adjacent to Shh-expressing cells. In addition, ectopic expression of Shh leads to ectopic Hhip expression, indicating that Hhip is a transcriptional target of Hh signaling [59].

The fact that Hhip binds Hedgehog proteins directly and that its expression requires Hh signaling suggests that Hhip may modify Hh signaling. Hhip could function either in a negative manner to attenuate a Hh signal or positively to facilitate signal transduction. In the first model, overexpression of Hhip is likely to result in loss of Hh signaling by competition with Ptch1 for Hh binding. Hhip overexpression in chondrocytes leads to severe skeletal defects including short-limbed dwarfism similar to that observed in Ihh mutants [59]. In the second model, Hhip overexpression may enhance signal transduction, possibly by facilitating Hh protein diffusion or increasing the affinity of Hh for other proteins on the membrane such as Ptch1[59].

Deficient Hhip expression results in lung and pancreas malformation [268, 269]. Targeted disruption of Hhip results in neonatal lethality with respiratory failure. Loss of Hhip expression results in increased Shh expression and defective secondary branching in Hhip mutant lungs due to the loss of fibroblast growth factor10 (Fgf10) signaling [269]. Shh signaling negatively regulates Fgf10 expression in the mesenchyme and may play a role in the lung malformation [45]. Hhip null mice exhibited significantly impaired islet formation (45% reduction of islet mass) and decrease of β cell proliferation by 40%. In addition, the spleen is deformed and reduced in mass. The partial reduction of Fgf10 expression in pancreatic mesenchyme is likely to account for some of the pancreatic defects observed in Hhip mutant

mice [268]. These studies suggested that deficient Hhip may contribute to lung and pancreas defect by targeting Fgf10 pathway through increased activation of Shh signaling.

1.6.2.2 Role of Hhip in diseases in adult

In normal condition, Hhip expression is quiescent after birth. An analysis of various human cell lines and primary cells indicated that Hhip is absent or expressed at low levels in other cell types, but expressed at a relatively higher level in endothelial cells [270]. These results are supported by gene chip data analysis of more than 30 normal human tissues showing that Hhip is most highly expressed in blood vessels or vascular-rich tissues such as liver, lung, brain, pancreas, and kidney, suggesting a role for Hhip in the normal function of blood vessels [270].

Abnormal Hhip gene expression is linked to several human diseases, such as chronic obstructive pulmonary disease (COPD) [271-273], pancreatitis [274] and its expression is altered in various cancers [270, 274-276]. Genome-wide association studies (GWAS) identified the association of multiple intergenic single-nucleotide polymorphisms (SNPs) near Hhip on chromosome 4q31 with COPD in population with different genetic background [272, 273, 277]. Studies revealed SNPs as enhancer of the Hhip promotor, modulating the reduced expression of Hhip in the pathogenesis of COPD [271]. Zhou et al [278] applied microarray analysis in human bronchial epithelial cell lines that were silenced with Hhip shRNAs and found silencing of Hhip led to differential expression of 296 genes. Eighteen of the differentially expressed genes associated with COPD were validated by real-time PCR in vitro. Seven of 11 validated genes tested in human COPD and control lung tissues demonstrated significant gene expression differences. Network modeling demonstrated that the extracellular matrix and cell proliferation genes influenced by Hhip tended to be interconnected [278].

Evidence have shown that the down-regulation of Hhip transcription is due to DNA hypermethylation and/ or loss of heterozygosity, and Hh signal activation through the inactivation of Hhip is implicated in the pathogenesis of human hepatocellular carcinoma [275]. In addition, results for Hhip expression and methylation analysis in medulloblastoma cell lines and primary tumors suggest not only epigenetic regulation of Hhip but also the possibility of an activated Shh signal that might down-regulate this gene, at least in this

specific childhood brain tumor. It has been reported that the Hhip promoter has 11 consensus sequences for binding of the basic helix-loop-helix (bHLA) transcription factor, which is indirectly downregulated by Shh signaling in vascular remodeling [279, 280].

Hhip was expressed in normal pancreatic tissues mainly in the cytoplasm of islet cells and blood vessels. In contrast, nuclear localization of increased Hhip was detected prominently in cancer cells of pancreatic ductal adenocarcinoma patient [274]. In vitro studies indicated that recombinant Hhip had a very minor growth-inhibitory effect on only two pancreatic cancer cell lines and silencing of Hhip mRNA expression resulted only in a slight growth stimulatory effect. Pancreatic cancer cells seem to have developed strategies to avoid the inhibitory effects of Hhip on Hh signaling in pancreatic cancer cells, thereby providing a growth advantage [274]. Loulier et al. [281] shown that, in the adult striatum of the brain, the majority of Hhip-expressing cells corresponds to neurons expressing the neuronal form of nitric oxide synthase (nNOS). It is possible that some Hhip functions in the adult brain might not be related to Shh signaling. Hhip has recently been identified as an inhibitor of Wnt-8 and eFgf/Fgf-8 signaling during olfactory and lens placode formation in Xenopus [282]. Therefore, Hhip might be involved in some other signaling pathways in addition to Hh, which requires further identification.

To date, the functional role of Hhip expression in both developing and mature kidneys in diabetes condition is barely known. A genome-wide diabetes profiling database (http://diabetes.wisc.edu) reveals that Hhip mRNA is upregulated in the islets of diabetic ob/ob mice at 4 weeks and 10 weeks of age as compared to lean animals, but is not increased in other tissues such as liver, adipose tissue, muscle, and hypothalamus. However, hyperglycemia is not prominent in this model. We screened the gene profiling of neonatal kidneys of offspring from non-diabetic, diabetic and insulin treated diabetic mice. Among the genes showing significant differences between the groups in our murine maternal diabetes model, Hhip (fold change, 1.536; p=0.007) was upregulated in kidneys of offspring from diabetic dams but was normalized in insulin-treated dams, meanwhile it is highly related to development, signal transduction and proliferation in the analysis of functional pathway

clustering. Therefore, we focused on the role of Hhip expression in both developing and mature kidneys in diabetic condition.

1.7 Animal models of DN and maternal diabetes research

STZ has been generally administered to induce T1DM. It is a compound that has selective toxicity toward pancreatic β cells because its glucose moiety is avidly transported into β cells by Glucose transporter 2 (GLUT2). After it enters the β cells, STZ can damage pancreatic β cells, leading to hypoinsulinemia and hyperglycemia [283]. In addition to pancreatic β-cells, STZ may also have toxic effects on other organs, including the kidney [284]. Therefore, the administration of high doses of STZ to mice should be avoided. To minimize the nonspecific toxicity of STZ, five daily intraperitoneal injections of STZ (40 mg/kg b. wt.) have been used to induce diabetes [285]. At later stages, STZ-induced diabetic mice may exhibit significant weight loss, a different degree of proteinuria and serum creatinine increase, depending on the genetic background [286]. Furthermore, STZ-induced diabetic mice do not develop hypertension. This method has also been employed to elucidate the effect of maternal diabetes on fetal growth and development. The phenotype of the offspring is associated with the STZ dose given during pregnancy [287]. The Low-dose (25, 30, 40, 50 mg/kg b. wt.) STZ results in mild-maternal diabetes, and fetal macrosomia [288, 289]. In contrast, high-dose (150 mg/kg b. wt.) STZ induces insulin deficiency in diabetes and fetal microsomia [290].

Akita mice have Ins2+/C96Y mutation, which is a single nucleotide substitution in the Ins2 gene [291]. This point mutation causes misfolding of the insulin protein, progressive loss of β cell function, β cell mass reduction, and overt hyperglycemia, resulting in T1DM [292]. Akita mice develop diabetic symptoms, such as hyperglycemia, polydipsia, and polyuria, soon after weaning (3 weeks) without obesity. The diabetic symptoms progress continuously in males, but the females exhibit mild symptoms [293]. There are some reports of kidney injury in Akita mice. They developed mild levels of albuminuria and structural changes, such as thickening of glomerular basement membrane, mesangial matrix expansion and podocytes loss at 6 months of age [258, 294, 295]. Many studies have reported that oxidative stress in the kidneys of Akita mice plays an essential role in the pathogenesis of diabetic nephropathy [296-298].

The db/db mouse model is currently the most widely used mouse for DN in settings of T2DM and exhibits many features similar to human DN. The db gene encodes for a G-to-T point mutation of the leptin receptor, resulting in abnormal splicing and defective signaling of the leptin [299]. The mice become obese around 3 to 4 weeks of age. Elevations of plasma insulin begin at 10 to 14 days and of blood glucose at 4 to 8 weeks, with moderate to severe elevation of albuminuria at 8-25 weeks of age [300]. After 16 weeks, a very consistent threefold increase happens in mesangial matrix expansion [301]. DN in these mice is characterized by albuminuria, podocyte loss, and mesangial matrix expansion [302]. Heterozygous leptin receptor-deficient ($Leprd^{db/+}$) mice develop spontaneous glucose intolerance during pregnancy, and the offspring of these mothers are macrosomia [303, 304]. Heterozygous $Lepr^{db/+}$ mice are a good model to study the fundamental role of maternal diabetes in macrosomia and modulation of renal morphogenesis in their offspring.

Another T2DM model, the ob/ob recessive obese mouse carries a mutation in leptin, the ligand for the leptin receptor. Renal lesions and function change in C57BL/6J ob/ob mice are said to be relatively mild [305]. High-fat diet induced obesity and insulin resistance in C57BL6 mice provide a commonly used approach to study T2DM. However, hyperglycemia is not prominent in this model [305]. High-fat diet induced rats are another experimental model used to demonstrate glucose intolerance in mothers during pregnancy, emphasizing that obesity is one of the most important risk factors for GDM. The combination of high fat sucrose diet with a minimal dose (25 mg/kg b. wt.) of STZ in developing GDM animal model was proposed and proved successfully [289].

In the present study, db/db and multiple low doses (40 mg/kg) of intraperitoneal (IP) STZ injected mice have been applied, and maternal diabetic animal models by a single IP STZ injection at a dosage of 150 mg/kg at E13 in Hoxb7-GFP mice have been generated. Compared to low-dose STZ, a single high-dose STZ creates a severely high glucose environment in utero, resulting in fetal microsomia [124, 306].

1.8 Objectives

Maternal diabetes creates a high glucose intrauterine environment that directly affects kidney development. We previously reported that the offspring of severe maternal diabetes mice have

relatively small kidneys/body weight with ~ 40% fewer nephrons [122, 126, 307]. To identify novel proteins or pathways through which maternal diabetes impairs nephrogenesis, we screened gene profiling of neonatal kidneys of offspring from non-diabetic, diabetic and insulin treated diabetic mice. Among the genes showing significant differences between the groups in the murine maternal diabetes model, Hhip (fold change, 1.536; p=0.007) was upregulated in kidneys of offspring from diabetic dams but was normalized in insulin-treated dams. At the same time, it is highly related to development, signal transduction and proliferation in the analysis of functional pathway clustering. So, the first question is whether the elevated Hhip plays a role in the maternal diabetes modulated kidney formation.

Hhip expression is quiescent after birth; only a limited amount of Hhip could be detected in mature ECs [270]. The abnormal Hhip expression has been linked to several human diseases, such as pancreatitis [274], chronic obstructive pulmonary disease [267, 271, 277] and various tumors [270, 308]. Since GECs injury is the hallmark of early renal injury in DN, and Hhip is mainly expressed in ECs at mature stage. The second question is if the increased Hhip in diabetic condition plays a role in GECs injury during the early development of nephropathy.

To date, the functional and pathophysiological role of Hhip expression in the developing and mature kidney has been poorly elucidated. We hypothesize that elevated Hhip plays roles in maternal diabetes modulated nephrogenesis and in the progression of DN. Therefore, the aims of the study would be: 1. To investigate whether Hhip gene expression induced by maternal diabetes could interfere with Shh signaling to impact on kidney formation and study the potentially involved mechanisms. 2. To address whether the upregulated renal Hhip expression in the diabetic condition contributes to the progression of nephropathy and study its related mechanism(s) in vivo and in vitro.

Chapter 2: Published Article 1

Maternal Diabetes Modulates Kidney Formation in Murine Progeny: Role of Hedgehog Interacting Protein (Hhip)

Diabetologia (2014) 57:1986–1996

Xin-Ping Zhao[1], Min-Chun Liao[1], Shiao-Ying Chang[1], Shaaban Abdo[1], Yessoufou Aliou[1], Isabelle Chenier[1], Julie R. Ingelfinger [2] and Shao-Ling Zhang [1§]

[1]Université de Montréal
Centre de recherche du Centre hospitalier de l'Université de Montréal (CRCHUM)
Tour Viger, 900 rue Saint-Denis, Montréal, QC, Canada H2X 0A9

[2] Harvard Medical School
Pediatric Nephrology Unit
Massachusetts General Hospital
55 Fruit Street, Boston, MA 02114-3117, USA

[§] To whom correspondence should be addressed: Shao-Ling Zhang, Ph.D.

Tel: (514) 890-8000 ext. 15633
Fax: (514) 412-7204
Email: shao.ling.zhang@umontreal.ca

Short Title: Hedgehog interacting protein (Hhip) modulate kidney formation

Key words: Hhip gene expression, Maternal diabetes, Nephrogenesis

2.1 Abstract

Aims/hypothesis We hypothesized that maternal diabetes impairs kidney formation in offspring via augmented expression of hedgehog interacting protein (Hhip). Our gene-array results were performed in neonatal kidneys from our murine model of maternal diabetes and indicated that Hhip expression was significantly modulated by maternal diabetes.

Methods We systematically examined the functional role of Hhip in kidney formation in our murine maternal diabetes model and elucidated the potential mechanisms related to dysnephrogenesis in vitro.

Results The kidneys of the offspring of diabetic dams, compared with those of the offspring of control non-diabetic dams, showed retardation of development—small kidneys and less ureteric bud (UB) branching morphogenesis. Augmented Hhip expression was observed in the offspring of diabetic dams, initially localized to differentiated metanephric mesenchyme and UB epithelium and subsequently in maturing glomerular endothelial and tubulointerstitial cells. The heightened Hhip targeting TGFβ1 signaling was associated with dysmorphogenesis. In vitro, Hhip overexpression decreased sonic hedgehog and paired box gene 2 proteins (Shh and Pax2, respectively) and increased transcriptional nuclear factor-kappa B (NF-κB, p50/p65), phosphorylation of p53, and TGFβ1 expression. In contrast, overexpression of Pax2 inhibited Hhip and NF-κB and activated Shh, N-myc and $p27^{Kip1}$ expression. Moreover, high glucose stimulated Hhip expression and then targeted TGF β1 signaling. Thus, Pax2, via a negative autocrine feedback mechanism, attenuated the stimulatory effect of high glucose on Hhip expression.

Conclusions/interpretation Maternal diabetes modulates kidney formation in young progeny mediated, at least in part, via augmented Hhip expression.

2.2 Introduction

Renal malformations are responsible for 34–59% of chronic kidney disease in children and for 31% of pediatric end-stage renal disease in the USA [82, 309, 310]. Of the many factors associated with congenital abnormalities of the kidney and urinary tract, diabetes mellitus during gestation seems to be one of the key players in both human and experimental settings [121]. For example, when the normal pattern of kidney formation is interrupted in both humans and experimental animal models (e.g. by a high ambient in utero glucose level), kidney abnormalities with a low total nephron number may ensue, either in isolation or as part of multiple malformation syndromes. The incidence of such anomalies appears to be proportional to the degree of maternal hyperglycemia [85, 122, 123]. The underlying mechanisms of such findings are incompletely delineated [114, 122, 124].

We previously reported that severe maternal diabetes (maternal blood glucose concentration >30 mmol/l) in a murine model (C57/BL6 background) impairs kidney formation and is associated with an intrauterine growth restriction (IUGR) phenotype in the offspring. Affected pups have relatively small kidneys/body weight with ~ 40% fewer nephrons [122, 126, 307]. We performed screening gene profiling of IUGR neonatal kidneys from offspring of dams with diabetes vs kidneys from offspring of control non-diabetic dams (Affymetrix Gene Chip Mouse Gene 1.0ST array platform, Affymetrix, Santa Clara, CA, USA), aiming to identify the novel proteins or signaling pathways through which maternal diabetes impairs nephrogenesis.

We analyzed our ontology database data using the following: the Affymetrix Expression Console (www.affymetrix.com) to normalize the gene database; the Robust Multi-Array Analysis (RMA) algorithm (Partek, St. Louis, Missouri, USA, www.partek.com) to compute expression values; a TM4 Multi Array Viewer (Boston, MA, USA, www.tm4.org) to analyze differential expression (p-value threshold of 0.01 and false discovery rate of 0.05). Of the genes showing significant differences between the groups in our murine maternal diabetes model, Hhip (fold change, 1,536; p=0.007) was upregulated in the neonatal kidneys of offspring from diabetic dams but was expressed normally in insulin-treated dams, as it is

highly related to development, signal transduction and proliferation in the analysis of functional pathway clustering.

Hhip, which encodes hedgehog interacting protein (Hhip), a transmembrane glycoprotein, was discovered by screening a mouse cDNA expression library for proteins that bound to sonic hedgehog protein (Shh) [59]. As a putative antagonist of the hedgehog signal pathway, Hhip binds to proteins from three mammalian hedgehogs—Shh, Indian hedgehog (Ihh) protein, and desert hedgehog (Dhh) protein—to attenuate their bioactivity [59]. Of the three mammalian hedgehog genes, only the expression of Shh and Ihh has been reported in the developing murine kidney. However, the absence of a renal phenotype in Ihh-deficient mice indicates that it might not have a key role in kidney development [46]. Shh signaling optimally controls the expression of three distinct classes of genes expressed in the nephrogenic zone that are required for normal renal development: early kidney inductive and patterning genes (Pax2, Sall1); cell-cycle modulators (Ccnd1, N-myc) and the signaling effectors of the hedgehog pathway (Ci homologues, Gli1, Gli2) [50].

The protein encoded by Hhip is expressed in vascular endothelial cells [270] and in cells adjacent to those expressing Shh, positioning it to bind to the Shh [59]. To date, although evidence indicates that cellular expression of Hhip inhibits the activation of Shh signaling and promotes angiogenesis during the formation of a variety of tumors [270, 308], the functional role of Hhip expression in developing and mature kidney is incompletely understood.

In the present studies, we first validated the changes in Hhip expression in pregnancies complicated with diabetes and then investigated whether ectopic Hhip gene upregulation induced by maternal diabetes could interfere with Shh targeting gene signaling [50]. We also investigated whether upregulation of Hhip had an impact on kidney formation from birth to 3 weeks in young offspring since in rodents nephrogenesis continues until postnatal day 10 (i.e. murine gestational period between 19 and 21 days) [85]. We then examined potentially involved mechanisms using both in vivo and in vitro studies.

2.3 Research design and methods

Animal models We used the Hoxb7–green fluorescent protein (GFP) transgenic (Tg) (Hoxb7-GFP-Tg, C57/BL6 background) mouse for the current study; this mouse is fertile with a normal phenotype at birth and during adult life [122, 123]. Hoxb7-GFP-Tg mice (GFP expression specifically in ureteric bud [UB] driven by Hoxb7 promoter), provided by F. Costantini (Columbia University Medical Center, New York, NY, USA) [311, 312], were engineered to allow UB branching morphogenesis to be visualized in real time in vivo as reported previously [122, 123].

As reported previously, we used a murine maternal diabetes model [122, 123, 126] induced by a single intraperitoneal injection of streptozotocin (STZ) (Sigma-Aldrich Canada, Oakville, ON, Canada) at a dose of 150 mg/kg of body weight at E13 gestation age. Neonatal kidneys of offspring from three groups of dams (non-diabetic, diabetic and diabetic dams treated by insulin implantation at E15 [Linshin, Scarborough, ON, Canada]) were used.

Animal care and the procedures used were approved by the Institutional Animal Care Committee of the CRCHUM. Mice were housed under standard humidity and lighting conditions (12 h light-dark cycles) with free access to standard mouse chow and water.

Cell lines The MK4 cell line [126, 137] was obtained from S. S. Potter (Children's Hospital Medical Center, Cincinnati, OH, USA) and is representative of late embryonic metanephric mesenchyme (MM), as it undergoes mesenchymal to epithelial conversion. MK4 cells express genes typical of late MM, including Pax2, Pax8, Wnt4, Cdh6, collagen IV and Lfb3 (also known as Hnf1) [313]. Mouse UB tip cells were provided by J. Barasch (Columbia University, New York, NY, USA) and were generated from micro dissected UBs of E11.5 mouse embryos transgenic for simian virus 40 large T antigen (Immorto-mouse) and which express epithelial and ureteric genes (Ret, Met) without hepatocyte growth factor [314]. The plasmids pcDNA3.1/Hhip and pcDNA3.1/Pax2 were gifts from A. McMahon (Harvard University, Cambridge, MA, USA) [59] and P. Goodyer (McGill University, Montreal, QC, Canada) [138], respectively.

We used both MK4 and UB tip cells to represent the MM and UB epithelium, respectively, and examined Hhip gene expression and Hhip regulation with or without a high glucose (25 mmol/l D-glucose) insult in MK4 cells. Unless otherwise indicated, all control cells were

incubated in low glucose (5 mmol/l D-glucose) medium containing 20 mmol/l D-mannitol to ensure equi-osmolar control.

Counting of UB tips and measurement of neonatal kidney size Neonatal kidneys of offspring from three groups of dams (non-diabetic, diabetic and diabetic dams treated by implanted insulin) were dissected aseptically and the number of UB tips in each group was assessed as reported previously [123]. Neonatal kidney size (length [mm], width [mm] and area [mm2]) was measured from the two-dimensional GFP images of freshly isolated neonatal kidneys using Image-J 1.48 (NIH, USA, http://imagej.nih.gov/ij/).

Real-time quantitative PCR Real-time quantitative PCR (qPCR) (the Fast SYBR green mastermix kit and the 7500 Fast real-time PCR system; Applied Biosystems, Life Technologies, Foster City, CA, USA) was performed as reported previously [122, 123, 126]. The final real-time qPCR product was also reviewed by Typhoon Trio Variable Mode Imager (GE Health Care, Bio-Sciences, Uppsala, Sweden). The following primers were used: Hhip forward 5′ CCCATCGGCTCTTCATTCTA-3′, reverse 5′-CCTTTCGTCTCCTCCCTTTA-3′ (NM_020259.4).

Western blot, immunohistochemistry, and immunofluorescence Western blot analysis, immunohistochemical staining, and immunofluorescence were performed essentially according to an established procedure as reported previously [122, 123, 126, 137]. The following antibodies were used: monoclonal anti-Hhip and β-Actin antibodies (Sigma-Aldrich Canada); Dolichos biflorus agglutinin (DBA)– FITC (Vector Laboratories, Burlington, ON, Canada) staining for UB identification [123]; anti-Shh, -nuclear factor-kappa B (NF-κB) (p50/p65), N-myc, CD31 and p53 antibodies (Santa Cruz Biotechnology, Santa Cruz, CA, USA); anti-paired box gene 2 protein (Pax2) antibody (Covance, Richmond, CA, USA); anti-phospho-p53 (Ser 15) (Abcam, Cambridge, MA, USA); anti-$p27^{Kip1}$ (BD Transduction Laboratories, Mississauga, ON, Canada); anti- TGFβ1 antibody (R&D Systems, Burlington, ON, Canada); phospho-Smad2 (Ser465/467)/Smad3 (Ser423/425) antibody (New England Biolabs, Whitby, ON, Canada) and Smad2/3 antibody (Cedarlane-Millipore, Burlington, ON, Canada).

Statistical analysis Statistical significance between the experimental groups was analyzed by one-way ANOVA, followed by the Bonferroni test, using Graphpad Software, Prism 5.0 (www.graphpad.com/prism/Prism.htm). Three or four separate experiments were performed for each protocol. Data are expressed as means±SD. A probability level of $p \leq 0.05$ was considered to be statistically significant.

2.4 Results

UB branching morphogenesis We compared UB branching morphogenesis in neonatal kidneys of three subgroups of Hoxb7-GFP-Tg murine lines' offspring (Con-offspring, the offspring of non-diabetic dams; Dia-offspring, the offspring of diabetic dams; Ins-offspring, the offspring of diabetic dams treated by insulin implantation) (Fig. 1a). At birth, maternal blood glucose concentration (mmol/l) was as follows: nondiabetic dams, 9.03±1.75; diabetic dams, 29.36±2.54; diabetic dams treated by insulin implantation, 15.8±1.36.

Compared with Con-offspring, Dia-offspring with IUGR phenotype had smaller neonatal kidney/body weight ratio as previously reported [122], smaller kidney size (Fig. 1b) and fewer UB tips (Con-offspring, 859.8±7.74; Dia-offspring, 669.9±18.96) (Fig. 1c). The impairment of UB branching was ameliorated by insulin administration to the mothers (Ins-offspring, 807.7±20.52) (Fig. 1c).

Hhip gene expression and localization in vivo We subsequently validated and confirmed Hhip mRNA expression by real-time qPCR (Fig. 1d, e) and Hhip protein expression by immunohistochemistry (Fig. 2a) and immunofluorescence staining (Fig. 2b). Consistent with the data obtained from our prior microarray analysis, Hhip expression was significantly increased in the neonatal kidneys of IUGR Dia-offspring.

We next followed the time course of intrarenal Hhip expression and its localization pattern during late kidney formation in the offspring (from day 1 to 3 weeks). In the kidneys of Con-offspring, Hhip expression was detected in both UB and MM lineages on day 1 (Fig. 2) and in the collecting duct system at 1 week (Fig. 3). After kidney formation was completed (3 weeks), very limited Hhip expression was observed and was localized to mature glomerular endothelial and adjacent tubulointerstitial cells (Fig. 4).

In contrast, the enhanced Hhip expression remained in the nephrogenic zone and was detected in both UB and MM epithelium in the kidneys of Dia-offspring (Fig. 2a). An increased amount of secreted Hhip and intracellular Hhip was detected adjacent to UB tips (Fig. 2b) and UB trunks (Fig. 2c) (DBA–FITC staining for UB identification [123]) in the neonatal kidneys. By 1 week of age, this increased Hhip expression was progressively evident in glomeruli, ultimately forming a nodular expression pattern (Fig. 3). At 3 weeks, the Dia-offspring had only small amounts of Hhip in the tubulointerstitium (Fig. 4a) but Hhip was strongly expressed in glomerular endothelial cells in the neonatal kidney cryosections, as assessed by immunofluorescence (confirmed by co-localization with CD31, a marker of endothelial cells) (Fig. 4b). Furthermore, the pattern of Hhip expression in the kidneys of Ins-offspring was essentially the same as that in the Con-offspring.

Hhip expression and regulation in vitro. Western blotting showed that Hhip, Shh, and Pax2 were basally expressed in both MK4 and UB cells as well as in cells transfected with the empty vector plasmid, pcDNA3.1 (1 μg/ml) (Fig. 5a), a control for the rest of transfection experiments. Overexpression of Hhip by transient transfection of pcDNA3.1/Hhip (1 μg/ml) into both MK4 and UB tip cells (Fig. 5b) inhibited both Shh and Pax2 expression. Conversely, overexpression of Pax2 by transient transfection with pcDNA3.1/Pax2 (1 μg/ml) increased Shh and decreased Hhip expression (Fig. 5b).

We tested the effect of a high-glucose milieu (25 mmol/l D-glucose) on Hhip and Shh expression in MK4 (Fig. 5c) and UB tip cells (Fig. 5d). High glucose persistently stimulated Hhip expression in a time-dependent manner, whereas Shh expression was only initially increased by high glucose within 24 h, then decreased rapidly after 48 h in both cell lines (Fig. 5c, d).

We then performed studies using the MK4 cell line, as it is derived from MM lineages, to examine high-glucose milieu regulation on Hhip expression, since we had noted that the augmented Hhip expression in the offspring of dams with diabetes was seen in the developing proximal portion of the nephron, which is mainly derived from differentiated MM lineages. High glucose (25 mmol/l D-glucose) stimulated Hhip expression in a time- and dose-dependent manner in naive MK4 cells but other glucose analogues such as L glucose, D-

mannitol and 2-deoxy-D-glucose did not (Fig. 6a–c). We also observed that insulin (10^{-6} mol/l) inhibited the stimulatory effect of high glucose on Hhip gene expression (as assessed by western blotting of Hhip) in MK4 cells (Fig. 6d).

We used MK4 cells transfected with the plasmid, pcDNA3.1 (MK4-vector) (1 μg/ml) as controls since the basal expression in naive and transfected MK4 cells were essentially identical (Fig. 5). A high-glucose milieu stimulated transcriptional NF-κB (p50/p65) and phosphorylation of p53 in MK4-vector cells. Overexpression of Hhip in MK4 cells alone significantly increased NF-κB (p50/p65) and p53 expression, including phosphorylation of p53 (Fig. 7a), and this activation was further enhanced by exposure to high glucose. In contrast, overexpression of Pax2 inMK4 cells significantly decreased Hhip and NF-κB (p50/p65) expression; further, this inhibition was unaffected by high glucose (Fig. 7b). In addition, overexpression of Pax2 in MK4 cells resulted in significantly increased Shh, N-myc and $p27^{kip1}$ expression and high-glucose exposure had no additional effect.

TGFβ1 expression in vivo and in vitro. In vitro, we observed overexpression of Hhip in MK4 cells resulted in increased TGFβ1 and phosphorylated Smad2/3 expression and that this activation was further enhanced by high-glucose media (Fig. 8a). Recombinant TGFβ1 upregulated Hhip and phosphorylated Smad2/3, but downregulated $p27^{Kip1}$ expression in a dose-dependent manner in naive MK4 cells (Fig. 8b). In vivo studies validated these findings—TGFβ1 expression was significantly increased in the kidneys of Dia-offspring from day 1 to 3 weeks of age (Fig. 8c). The heightened TGFβ1 expression displayed a similar immunohistochemical pattern to Hhip in mature glomerular endothelial and adjacent tubulointerstitial cells (Fig. 8d).

2.5 Discussion

The present study suggests that heightened ectopic Hhip expression targets NF-κB, p53, and TGFβ1 expression, which is associated with dysmorphogenesis in young Dia-offspring. We would suggest that overexpression of Pax2 may create a negative autocrine feedback on Hhip regulation and may attenuate the stimulatory effect of high glucose on Hhip expression in vitro.

Using the Hoxb7-GFP-Tg mouse model to permit visualization of UB branching morphogenesis in neonatal kidneys, which continue to form nephrons after birth, we previously reported that maternal diabetes may impair UB branching morphogenesis. This ultimately impairs kidney formation [122, 126], resulting in renal dysplasia or hypoplasia, likely via increased cell apoptosis or decreased cell proliferation in the differentiated MM and UB epithelium [122, 126]. The underlying mechanisms appear to be associated with impaired mesenchymal-to-epithelial conversion linked to Pax2 and N-myc interaction [122, 123, 137, 138] and/or excessive nascent nephron apoptosis via activation of NF-κB (p50/p65) and p53 pathways [122, 126].

Consistent with our previous studies [122, 126] with the same phenotype in neonatal kidneys, we validated the data obtained from our screening microarray analysis and observed that Hhip expression was significantly increased in the neonatal kidneys of Dia-offspring. Those data led us to speculate whether the augmented Hhip expression induced by high glucose milieu either directly or indirectly controls Shh targeting genes involved in cell proliferation, cell fate, and cell communication, influencing processes such as epithelial-mesenchymal transition [315, 316]. We further speculated as to whether or not the increased Hhip expression could activate NF-κB (p50/p65) and p53 signals and then impact on kidney formation.

During normal kidney development, the balance of Hhip-Shh signaling appears to be critical in the control of a series of sequential events of nephrogenic processes [52, 55]. Upon high glucose insult, for example, in our murine model, the offspring of diabetic dams had a markedly different expression pattern of Hhip when compared with offspring of normal non-diabetic dams. As compared with the limited Hhip expression in Con-offspring (i.e. neonate—UB and MM lineages; age 1 week—collecting duct system), a significant amount of Hhip was detected in the nephrogenic zone of the still developing kidneys of Dia-offspring at the neonatal stage (i.e. secreted Hhip adjacent to UB tips) and at 1 week old (i.e. a nodular expression pattern in glomeruli). These data suggested that Hhip might delay or disorient the usual gradient Shh expression pattern establishment from distal (high) to proximal (low) [52, 55] since Hhip is expressed in cells adjacent to those expressing Shh to antagonize its activity [59]. Our in vitro studies in MK4 and UB tip cells with or without high-glucose media

elucidated a potential counterbalance between Hhip and Shh gene expression in both differentiated UB and MM epithelium, and hint that this interaction is critical in the nephrogenic process. Thus, the examination of the functional role of Hhip during the entire period of nephrogenesis with respect to Shh signaling in different renal cell lineages, as well as in the in utero high-glucose environment, merits further investigation.

Alternatively, the heightened Hhip expression might alter the Shh-controlled expression of kidney formation genes, such as Pax2, Sall1, N-myc, Ccnd1, Gli1 and Gli2 [50], in the nephrogenic zone, subsequently resulting in the development of renal abnormalities. For instance, Pax2 as a 'kidney-specific' master gene is expressed in both UB and MM lineages, normally optimizing UB branching and mesenchymal to epithelial transition during kidney development [317-319]. Mutation or deficiency of Pax2 causes an increase in cellular apoptosis [14, 15, 320], associated with renal hypoplasia [320-322]. In the current study, we observed that overexpression of Hhip significantly downregulated genes such as Shh and Pax2; in contrast, overexpression of Pax2 increased Shh and decreased Hhip gene expression in both UB and MK4 cells, underscoring the functional interaction between Hhip, Shh, and Pax2.

Thus, we focused on a differentiated MM epithelium (i.e. MK4 cells), since the augmented Hhip expression remained in the developing proximal portion of the nephron in the Dia-offspring, which is mainly derived from differentiated MM lineages. We designed further experiments to elucidate whether the excess amount of Hhip with or without high glucose could modulate the mesenchymal-to-epithelial conversion and nascent nephron apoptosis by studying the MM cell proliferation genes (i.e. Shh, Pax2, N-myc and $p27^{kip1}$ genes) and apoptosis genes (i.e. genes encoding NF-κB [p50/p65] and p53). Indeed, upon exposure to high D-glucose, but not other glucose analogues, there was specific stimulation of Hhip gene expression in a time- and dose-dependent manner. Insulin appears to inhibit the stimulatory effect of high glucose on Hhip gene expression in vitro. Moreover, our current data suggest that Pax2 may be involved in a negative autocrine feedback loop to prevent the high-glucose stimulatory effect on Hhip gene expression by promoting MM cell proliferation genes (i.e.

Shh, Pax2, N-myc and $p27^{kip1}$ genes) and inhibiting MM cell apoptosis genes (i.e. genes encoding NF-κB [p50/p65] and p53).

In the current study, we observed that the distribution of Hhip expression is similar to that of TGFβ1 and that FTGFβ1 expression was significantly increased in young Dia-offspring with dysmorphogenesis occurring, suggesting that there is a functional interaction between Hhip and TGFβ1. It is well known that TGFβ1 decreases renal branching morphogenesis via its negative feedback mechanisms [218, 219]. Compelling evidence suggests that TGFβ1 plays a key role in glomerular endothelial cell damage [92, 221], production of extracellular matrix and the development of renal interstitial fibrosis in diabetic nephropathy [223-225]. In studies in vitro, we further demonstrated that the increase of Hhip expression either by overexpression of Hhip or by the induction of a high-glucose milieu might target TGFβ1 signaling, which, in turn, may lead to events such as phosphorylation of Smad2/3 and decreases in $p27^{Kip1}$ expression.

In conclusion, the present studies suggest that impaired nephrogenesis induced by maternal diabetes is associated with augmented Hhip gene expression. Hhip targets TGFβ1 signaling, resulting in kidney formation impairment in young Dia-offspring. Pax2 appears to be involved in a negative autocrine feedback loop on Hhip gene expression, attenuating the stimulatory effect of high glucose on Hhip gene expression.

`

2.6 Legends and Figures

Figure 2-1

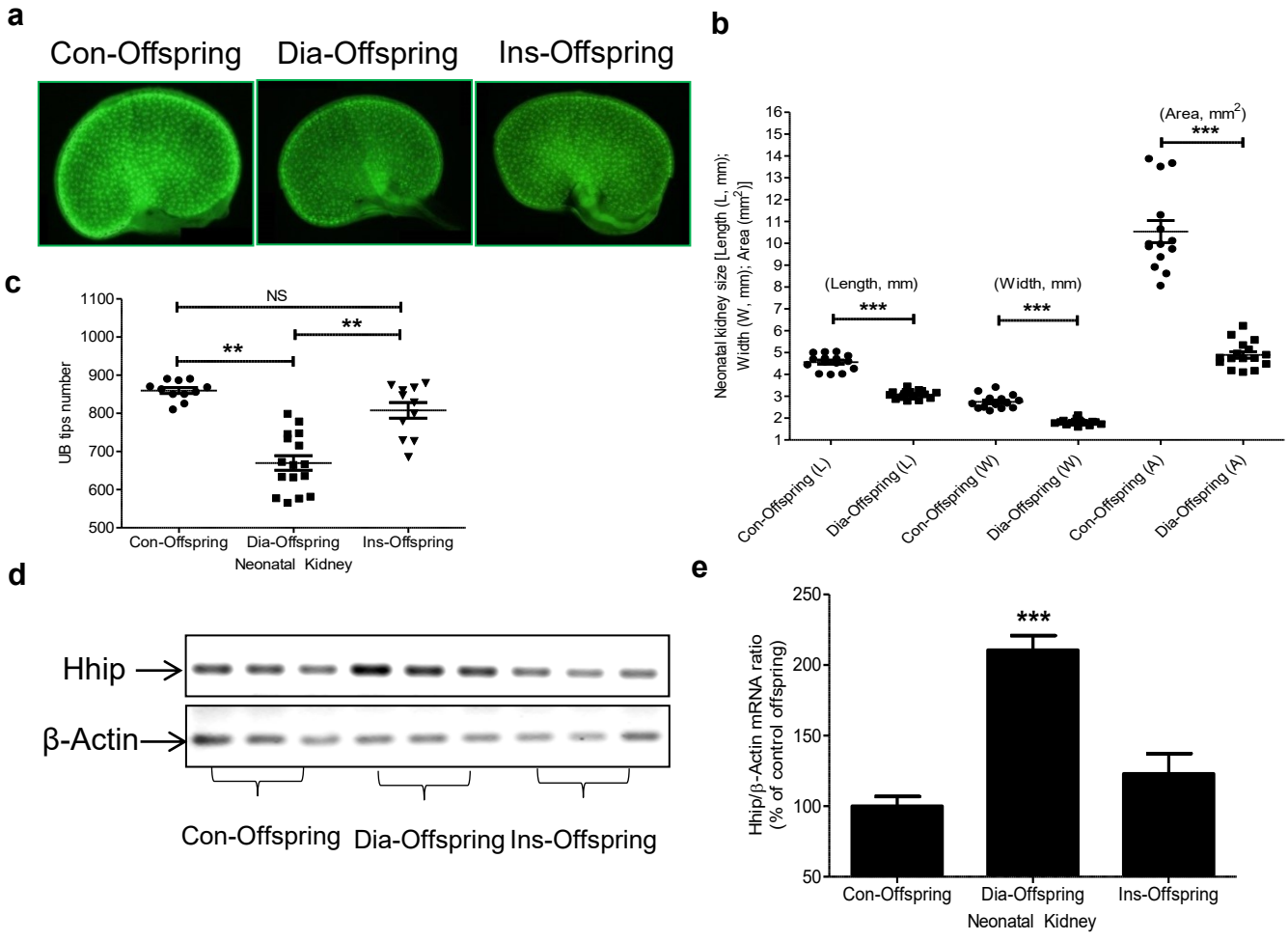

Figure 2-1 (a) GFP images of the freshly isolated neonatal kidney (magnification×4). (b) Neonatal kidney size; Length, L; Width, W; Area, A. (c) The number of UB tips in the neonatal kidney. Circles, Con-offspring; squares, Dia-offspring; inverted triangles, Ins-offspring. (d, e) Real-time qPCR image. (d) Typhoon gel. (e) The relative density of Hhip mRNA was compared with its own β-actin mRNA. Con-offspring values were considered as 100%. Each point represents the mean ± SD of three independent experiments. **p≤0.01; ***p≤0.001analysis of Hhip mRNA expression in neonatal kidney.

Figure 2-2

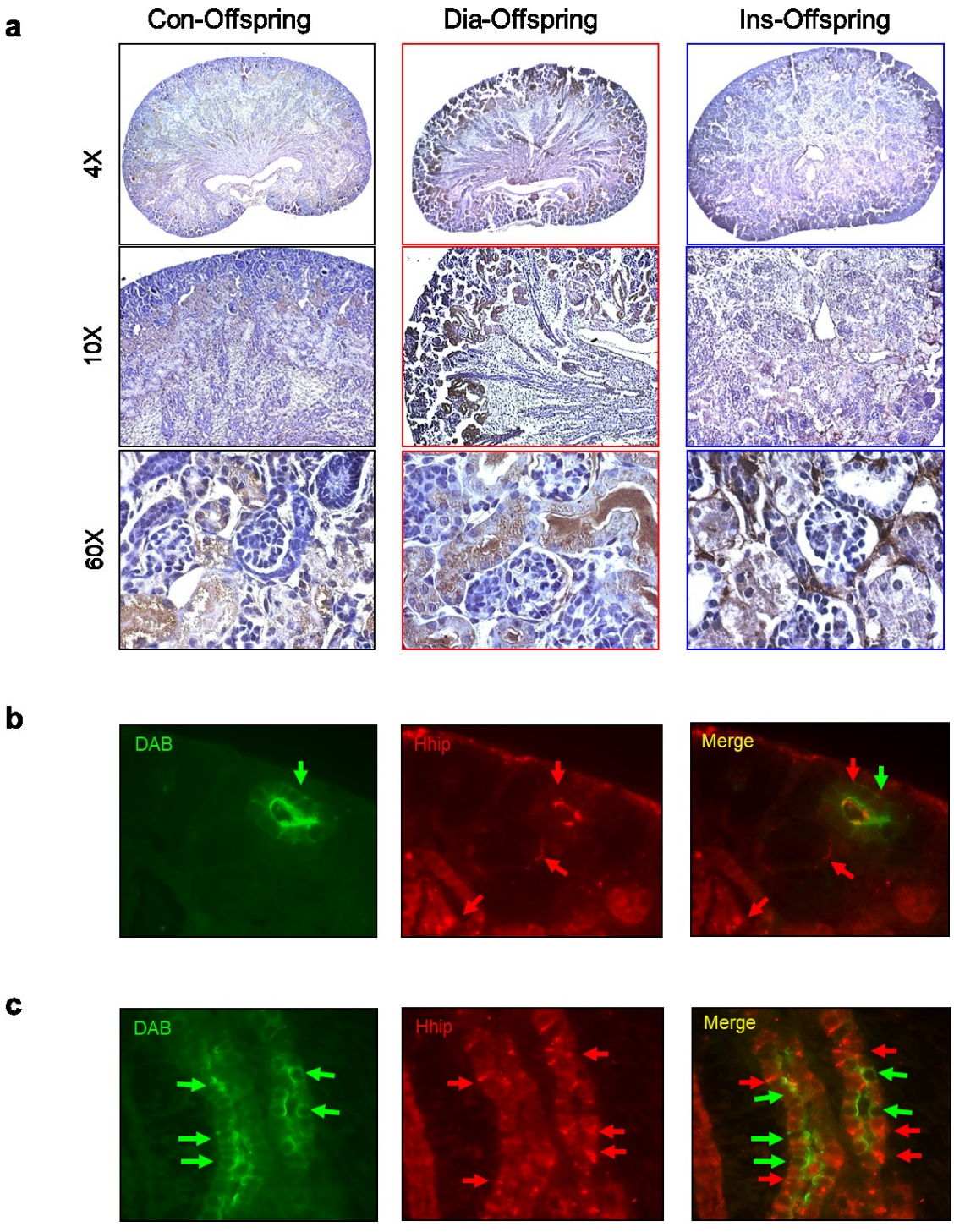
a
Con-Offspring
Dia-Offspring
Ins-Offspring
4X
10X
60X
b
DAB
Hhip
Merge
c
DAB
Hhip
Merge

Figure 2-2 (a) Immunohistochemical staining showing Hhip expression in neonatal kidneys. Black frame, Con-offspring; red frame, Dia-offspring; blue frame, Ins-offspring (magnification ×4, ×10 and ×60, as shown). (b, c) Co-localisation, by immunofluorescence, of Hhip (red arrows) and DBA (green arrows) as well as Hhip/DBA merge in UB tips in renal cortex (b) and UB trunks in renal medulla (c) of the neonatal kidneys of Dia-offspring (magnification ×60)

Figure 2-3

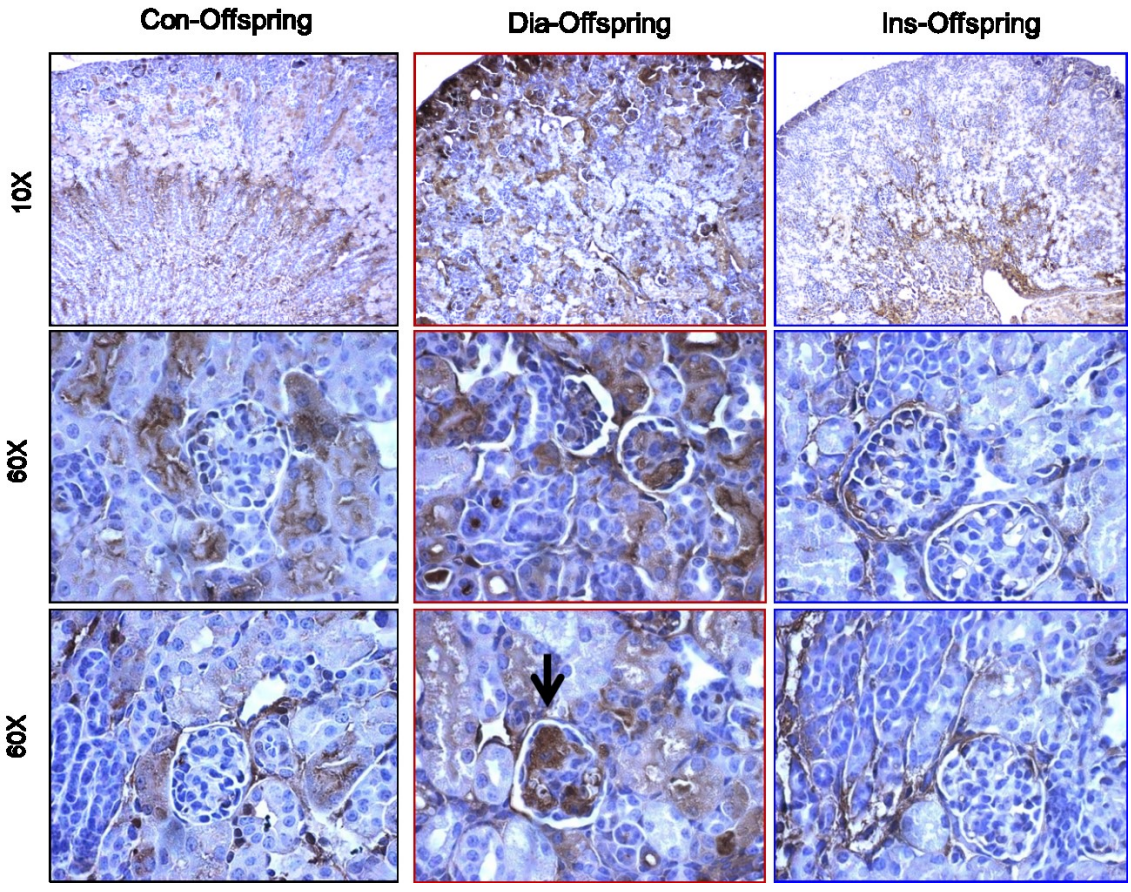

Figure 2-3 Immunohistochemical staining showing Hhip expression in 1-week-old kidneys. Black frame, Con-offspring; red frame, Dia-offspring; blue frame, Ins-offspring (magnification ×10 and ×60). The glomerular nodular Hhip expression is indicated by the arrowhead

Figure 2-4

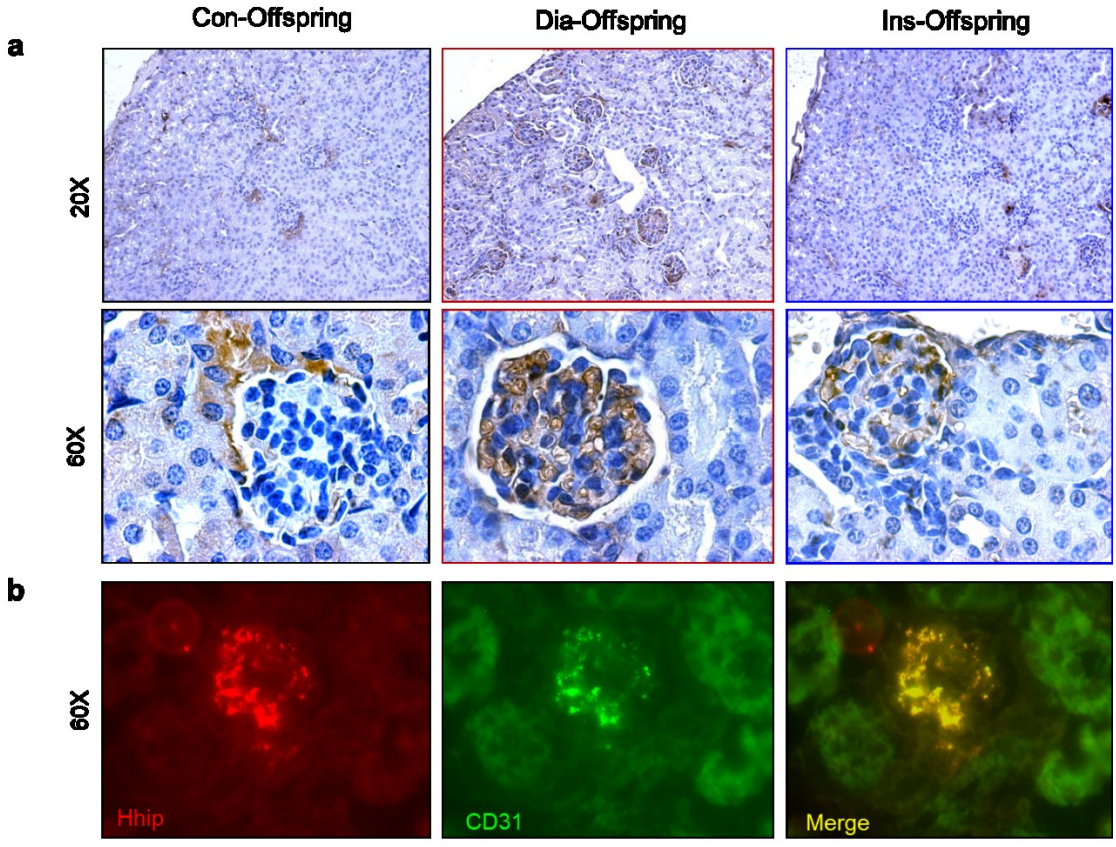

Figure 2-4 Hhip expression in 3-week-old kidneys. (a) Immunohistochemical staining showing Hhip. Black frame, Con-offspring; red frame, Dia-offspring; blue frame, Ins-offspring (magnification ×20 and ×60). (b) Co-localization, by immunofluorescence, of Hhip (red) and CD31 (green), as well as Hhip/CD31 merge (yellow), in 3-week-old kidneys of Dia-offspring (magnification ×60)

Figure 2-5

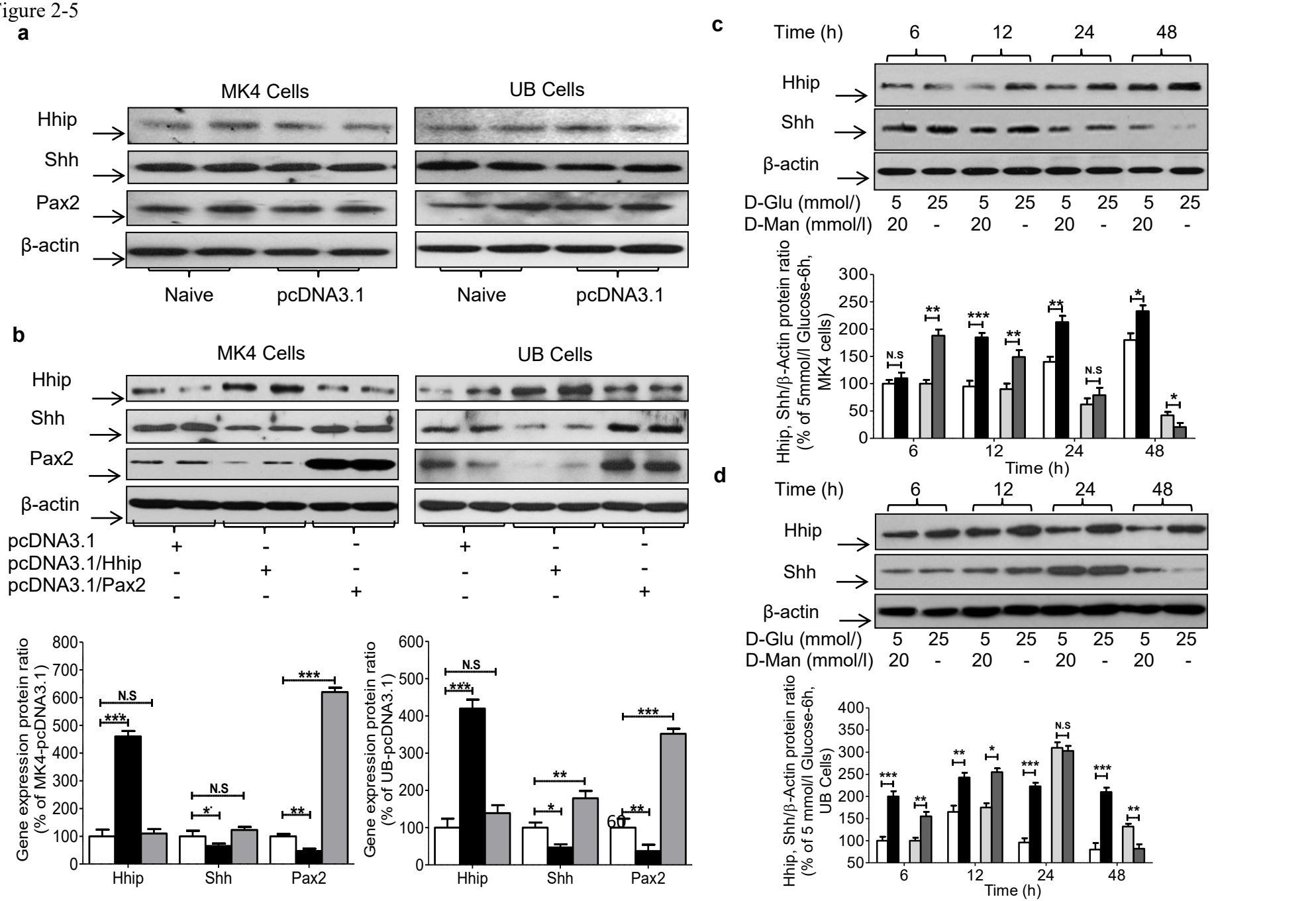
a
MK4 Cells
UB Cells
Hhip
Shh
Pax2
β-actin
Naive
pcDNA3.1
Naive
pcDNA3.1
b
MK4 Cells
UB Cells
Hhip
Shh
Pax2
β-actin
pcDNA3.1
pcDNA3.1/Hhip
pcDNA3.1/Pax2
Gene expression protein ratio (% of MK4-pcDNA3.1)
Hhip
Shh
Pax2
Gene expression protein ratio (% of UB-pcDNA3.1)
Hhip
Shh
Pax2
c
Time (h)
6
12
24
48
Hhip
Shh
β-actin
D-Glu (mmol/)
D-Man (mmol/l)
Hhip, Shh/β-Actin protein ratio (% of 5mmol/l Glucose-6h, MK4 cells)
Time (h)
d
Time (h)
Hhip
Shh
β-actin
D-Glu (mmol/)
D-Man (mmol/l)
Hhip, Shh/β-Actin protein ratio (% of 5 mmol/l Glucose-6h, UB Cells)
Time (h)

Figure 2-5 Hhip, Pax2 and Shh protein expression analyzed by western blot. (a) Basal expression in naive MK4 and UB cells as well as the cells transfected with pcDNA3.1 plasmid (1 μg/ml). (b)MK4 and UB tip cells were transfected with the plasmids pcDNA3.1 (white bars), pcDNA3.1/Hhip (black bars) and pcDNA 3.1/Pax2 (grey bars) at 1 μg/ml, respectively; the gene expression protein ratio in cells transfected with pcDNA3.1 plasmid was considered to be 100%. (c, d) The time course of high glucose effect on Hhip and Shh expression in naive MK4 cells (c) and UB tip cells (d) was analysed by western blot using 20 mmol/l D-mannitol (D-Man) as an osmotic control (white bars, 5 mmol/l D-glucose [D-Glu]/Hhip; black bars, 25 mmol/l D-glucose/Hhip; light-grey bars, 5 mmol/l D-glucose/Shh; dark-grey bars, 25 mmol/l D-glucose/Shh). The gene expression protein ratio in 5 mmol/l glucose medium at the 6 h incubation period was considered to be 100%. Each point represents the mean ± SD of three independent experiments. *$p \leq 0.05$; **$p \leq 0.01$; ***$p \leq 0.001$

Figure 2-6

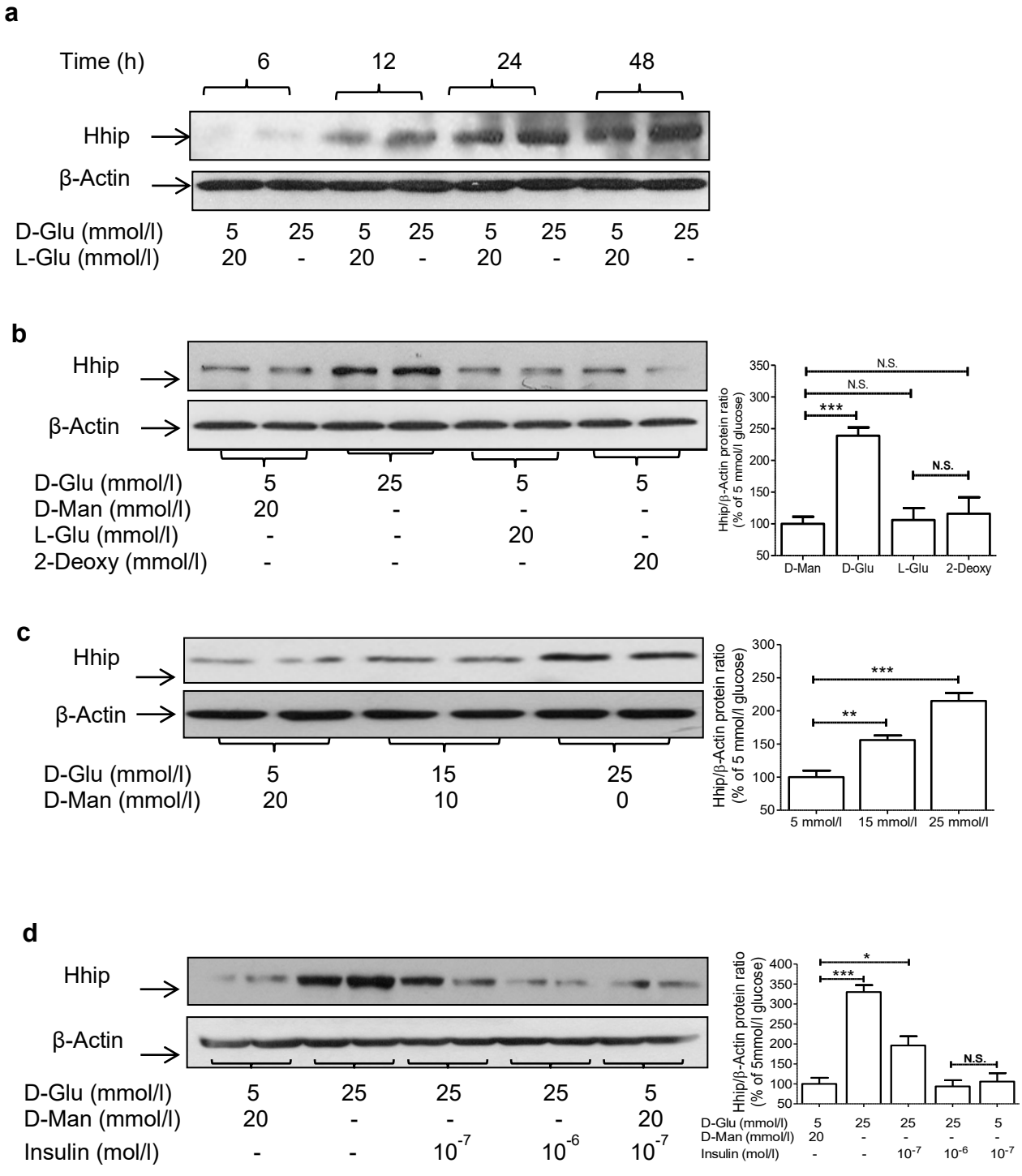
a
Time (h)
6
12
24
48
Hhip
β-Actin
D-Glu (mmol/l)
L-Glu (mmol/l)
b
Hhip
β-Actin
D-Glu (mmol/l)
D-Man (mmol/l)
L-Glu (mmol/l)
2-Deoxy (mmol/l)
Hhip/β-Actin protein ratio (% of 5 mmol/l glucose)
N.S.
***
D-Man
D-Glu
L-Glu
2-Deoxy
c
Hhip
β-Actin
D-Glu (mmol/l)
D-Man (mmol/l)
**
5 mmol/l
15 mmol/l
25 mmol/l
d
Hhip
β-Actin
D-Glu (mmol/l)
D-Man (mmol/l)
Insulin (mol/l)
*

Figure 2-6 Effects of high D-glucose (25 mmol/l, D-Glu) on Hhip expression in naive MK4 cells. (a) Time course analyzed by western blot using 20 mmol/l L-glucose (L-Glu) as an osmotic control. (b) Effect of the glucose analogues D-glucose (D-Glu), L-glucose (L-Glu), D-mannitol (D-Man) and 2-deoxy-D-glucose (2-Deoxy), on Hhip expression analyzed by western blot. (c) Dose-dependent effect of glucose analyzed by western blot. (d) Insulin's inhibitory effect analyzed by western blot. The gene expression protein ratio in 5 mmol/l glucose medium with 20 mmol/l D-mannitol at the 24 h incubation period was considered to be 100%. Each point represents the mean ± SD of three independent experiments. *$p \leq 0.05$; **$p \leq 0.01$; ***$p \leq 0.001$

Figure 2-7

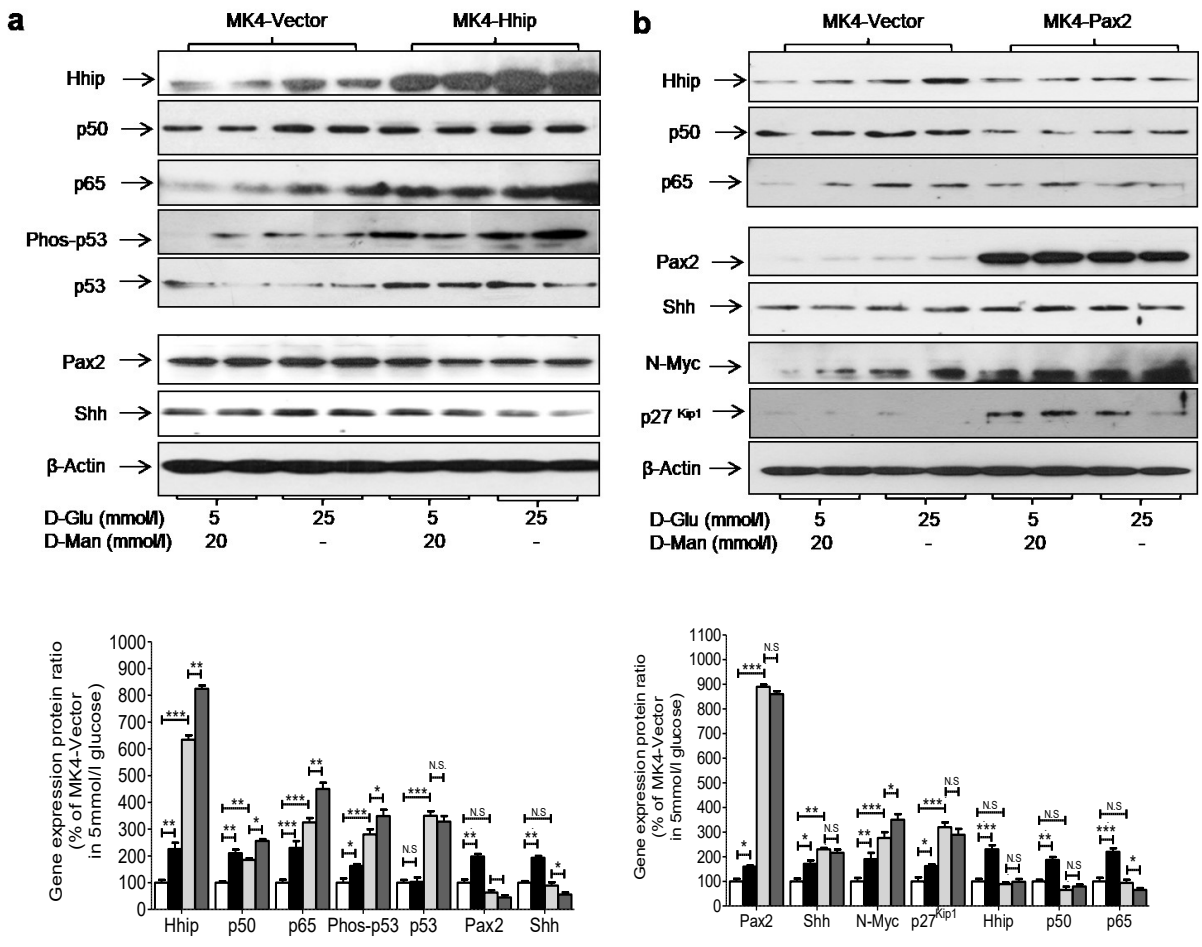

Figure 2-7 Effect of high glucose on different genes of MK4 transfected cells analyzed by western blot. (a) MK4 cells transfected with the plasmids pcDNA3.1 (1 μg/ml) (MK4-Vector) in D-glucose (D-Glu) 5 mmol/l (white bars) and 25 mmol/l glucose (black bars) or pcDNA3.1/Hhip (1 μg/ml) (MK4-Hhip) in 5 mmol/l glucose (light-grey bars) and 25mmol/l glucose (dark-grey bars). (b)MK4-Vector in 5 mmol/l glucose (white bars) and 25 mmol/l glucose (black bars); MK4 cells transfected with the plasmid pcDNA3.1/Pax2 (1 μg/ml) (MK4-Pax2) in 5 mmol/l glucose (light-grey bars) and 25 mmol/l glucose (dark-grey bars). The gene expression protein ratio in MK4-Vector cells in 5 mmol/l glucose medium with 20 mmol/l D-mannitol (D-Man) were considered to be 100%. Each point represents the mean ± SD of three independent experiments. *p≤0.05; **p≤0.01; ***p≤0.001.

Figure 2-8

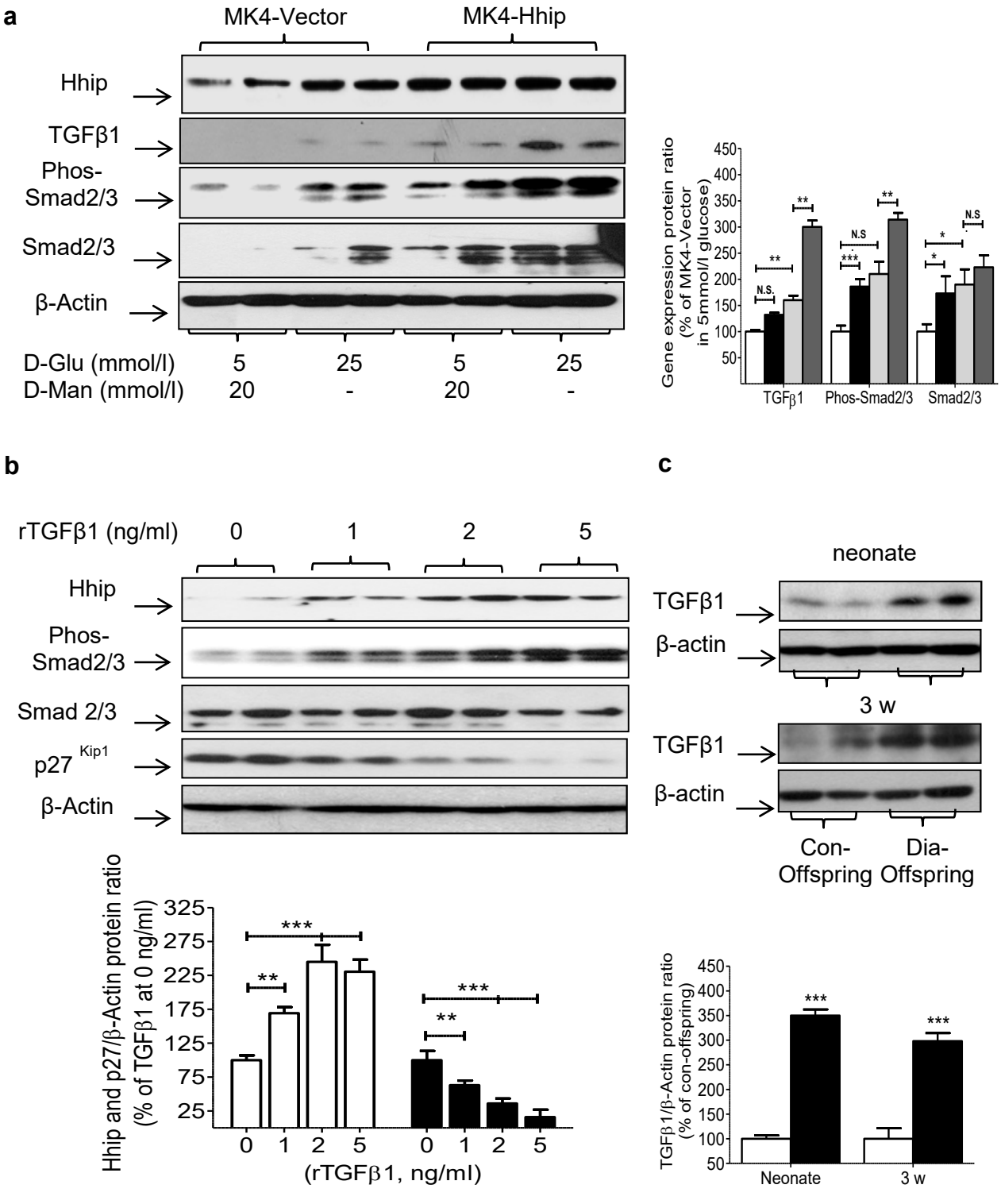
a
MK4-Vector
MK4-Hhip
Hhip
TGFβ1
Phos-Smad2/3
Smad2/3
β-Actin
D-Glu (mmol/l) 5 25 5 25
D-Man (mmol/l) 20 - 20 -
Gene expression protein ratio (% of MK4-Vector in 5mmol/l glucose)
TGFβ1
Phos-Smad2/3
Smad2/3
b
rTGFβ1 (ng/ml) 0 1 2 5
Hhip
Phos-Smad2/3
Smad 2/3
p27 Kip1
β-Actin
Hhip and p27/β-Actin protein ratio (% of TGFβ1 at 0 ng/ml)
(rTGFβ1, ng/ml)
c
neonate
TGFβ1
β-actin
3 w
TGFβ1
β-actin
Con-Offspring
Dia-Offspring
TGFβ1/β-Actin protein ratio (% of con-offspring)
Neonate
3 w

Figure 2-8

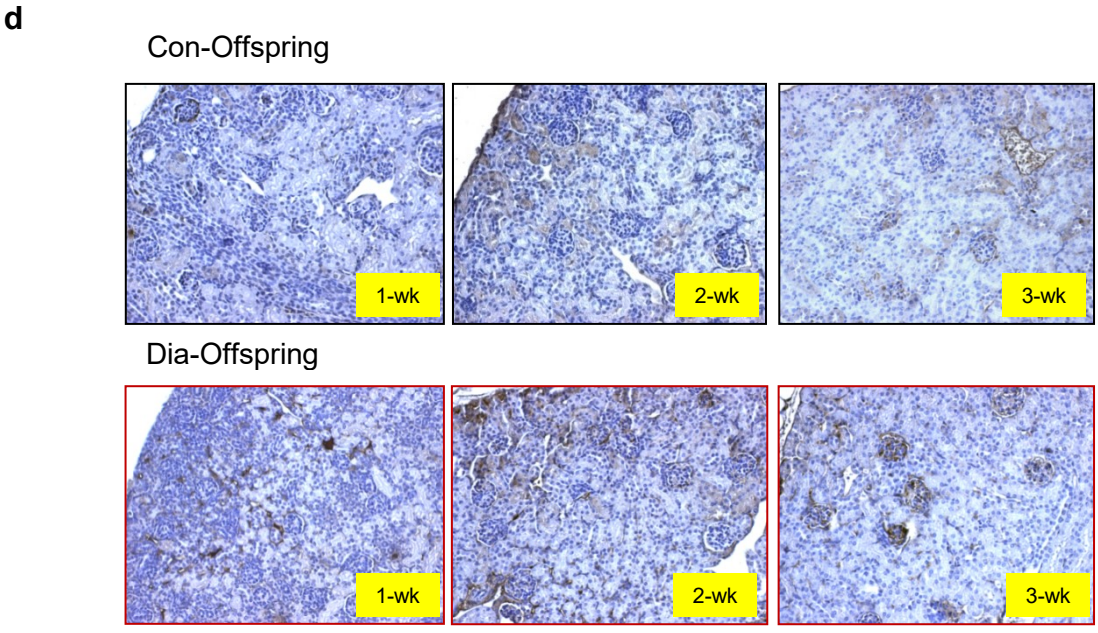

Figure 2-8 Hhip and TGFβ1 expression in vitro (a, b) and in vivo (c, d). (a) TGFβ1 expression in MK4 cells transfected with the plasmids pcDNA3.1 (1 μg/ml) (MK4-Vector) in 5 mmol/l glucose (white bars) and 25 mmol/l glucose (black bars) or pcDNA3.1/Hhip (1 μg/ml) (MK4-Hhip) in 5 mmol/l glucose (light-grey bars) and 25 mmol/l glucose (dark grey bars). The gene expression protein ratio in MK4-Vector cells in 5 mmol/l glucose medium with 20 mmol/l D-mannitol (D-Man) was considered as 100%. (b) The dose–effect of recombinant TGFβ1(rTGFβ1) on Hhip, phospho-Smad2/3, Smad 2/3 and $p27^{Kip1}$ expression in naive MK4 cells. The gene expression protein ratio in rTGFβ1 (0 ng/ml) was considered as 100%. (c)Western blot performed in neonatal and 3-week-old kidneys of Con-offspring and Dia-offspring. Con-offspring values were considered as 100%. (d) Immunohistochemical analysis of TGFβ1 expression in 1-, 2- and 3-week-old kidneys of Con-offspring (black frame) and Dia-offspring (red frame) (magnification ×20). Each point represents the mean ± SD of three independent experiments. *p≤0.05; **p≤0.01; ***p≤0.001

2.7 Acknowledgements

The authors owe special thanks to J. S. D. Chan (CRCHUM, Montreal, QC, Canada) for his unconditional support and valuable comments on this manuscript.

Funding

This project was supported by grants to SLZ from the Canadian Institutes of Health Research (CIHR, MOP115025) and American Society of Nephrology (ASN)-Carl W. Gottschalk Research Scholar Grant as well as the Bourse de chercheure-boursier Juniors 2-Fonds de recherche en santé du Québec (FRSQ) (SLZ). SYC is a Canadian Diabetes Association Doctoral Student. Editorial assistance was provided by the CRCHUM's Research Support Office.

Contribution statement

SLZ is the guarantor of this work, had full access to all study data and takes responsibility for data integrity and the accuracy of data analysis. XPZ and SLZ were principal investigators and were responsible for the study conception and design. SLZ drafted, reviewed and edited the manuscript. XPZ, MCL, SYC, SA, YA, IC and SLZ contributed to the in vivo and ex vivo experiments and collection of data. JRI contributed to data discussion and reviewed/edited the manuscript. All authors were involved in the analysis and interpretation of data.

We demonstrated that hyperglycemia stimulates Hhip expression, impairing nephrogenesis and observed that increased renal Hhip induced by high glucose was predominantly expressed in GECs in mature offspring (3-Week- old) of the diabetic mouse. Since GECs injury is the hallmark of early renal injury in diabetic nephropathy, whether Hhip contributes to the GECs injury, initiating the pathophysiology of diabetic nephropathy is unknown. We speculated that the augmented renal Hhip expression in diabetic condition contributes to the development of nephropathy and explored its potential mechanism(s) by in vivo and in vitro studies.

Chapter 3: Published Article 2

Hedgehog Interacting Protein (Hhip) Promotes Fibrosis and Apoptosis in Glomerular Endothelial Cells in Murine Diabetes

Sci Rep. 2018 Apr 13;8(1):5958. doi: 10.1038/s41598-018-24220-6

Xin-Ping Zhao[1], Shiao-Ying Chang[1], Min-Chun Liao[1], Chao-Sheng Lo, Isabelle Chenier [1], Hongyu Luo[1], Jean-Louis Chiasson[1], Julie R. Ingelfinger [2], John S.D. Chan[1] and Shao-Ling Zhang [1§]

[1]Université de Montréal
Centre de recherche du Centre hospitalier de l'Université de Montréal (CRCHUM)
Tour Viger, 900 rue Saint-Denis, Montréal, QC, Canada H2X 0A9

[2] Harvard Medical School
Pediatric Nephrology Unit
Massachusetts General Hospital
55 Fruit Street, Boston, MA 02114-3117, USA

[§] To whom correspondence should be addressed: Shao-Ling Zhang, Ph.D.

Tel: (514) 890-8000 ext. 15633
Fax: (514) 412-7204
Email: shao.ling.zhang@umontreal.ca

Short Title: Hedgehog interacting protein (Hhip) in diabetic nephrology

Keywords: Hhip Gene Expression, Diabetic nephropathy, endothelial to mesenchymal transition

3.1 Summary

We investigated whether renal hedgehog interacting protein (Hhip) expression contributes to the progression of diabetic nephropathy (DN) and studied its related mechanism(s) in vivo and in vitro. Here, we show that Hhip expression is highly elevated in glomerular endothelial cells of adult type 1 diabetic (T1D) Akita and T2D db/db mouse kidneys as compared to non-diabetic control littermates. Hyperglycemia enhances reactive oxygen species (ROS) generation via NADPH oxidase 4 (Nox4) activation and stimulates renal Hhip gene expression, and that elevated renal Hhip gene expression subsequently activates the TGFβ1-Smad2/3 cascade and promotes endothelial to mesenchymal transition associated with endothelial cell fibrosis/apoptosis in vivo and in vitro. Furthermore, kidneys of low-dose streptozotocin-induced diabetic heterozygous Hhip deficient ($Hhip^{+/-}$) mice displayed a normal albumin/creatinine ratio with fewer features of DN (glomerulosclerosis/fibrosis and podocyte apoptosis/loss) and less evidence of renal compensation (glomerular hypertrophy and hyperfiltration) as compared to diabetic wild type controls ($Hhip^{+/+}$). Thus, our studies demonstrated that renal Hhip expression is associated with nephropathy development in diabetes and that hyperglycemia-induced renal Hhip expression may mediate glomerular endothelial fibrosis and apoptosis in diabetes, which is novel.

3.2 Introduction

In patients with diabetes, endothelial injury leads to multiple macro- and microvascular complications, including diabetic nephropathy (DN). DN accounts for 50% of all end-stage renal disease (ESRD) cases in Canada and the USA [323-325], and the incidence of DN, a progressive kidney disease, is increasing worldwide [326]. In DN, the glomerular filtration barrier, which consists of an inner fenestrated glomerular endothelial cells (GECs) layer, a glomerular basement membrane (GBM) and an outer layer of podocytes with interdigitated foot processes that enwrap the glomerular capillaries, is injured. GEC injury (reduced fenestrated capacity/ability), GBM thickening, and podocyte foot process effacement/detachment are hallmarks of early renal injury in DN [323-325]. Although current treatments such as anti-hyperglycemic agents, statins, renin-angiotensin system (RAS) blockers and other anti-hypertensive agents can slow the progression of DN, such agents have failed to prevent the development of ESRD. Therefore, the identification of new molecules that might be useful to develop targeted preventive therapies for patients at risk for developing DN would be important.

Hedgehog interacting protein (Hhip), a signaling molecule in the hedgehog (Hh) pathway, was originally discovered as a putative antagonist of all 3 secreted Hh ligands, i.e., Sonic (Shh), Indian (Ihh), and Desert (Dhh) [59, 264-266, 327, 328]. Hhip encodes a protein of 700 amino acids attached to the cell membrane via a glycosylphosphatidylinositol (GPI) anchor and is abundantly expressed in vascular endothelial cells-rich tissues, including the kidney [270]. Hhip regulates cell function via either canonical- or non-canonical hedgehog pathways [59, 264-267, 269, 327, 328]. Under certain conditions, cells express Hhip, which then acts cell-autonomously (intrinsically, in the same and/or adjacent cells – in an “autocrine manner”) and non-cell autonomously (acting in other cells – in a “paracrine manner”) to regulate cell and/or organ functions [59, 264-267, 269, 327, 328]. Hhip function is important during organogenesis as an interruption of Hhip gene expression results in developmental anomalies that include skeletal, lung and pancreatic malformations [59, 268, 269, 329]. In contrast, Hhip expression is quiescent after birth, but the abnormal Hhip expression has been linked to several human diseases, such as pancreatitis [274], chronic obstructive pulmonary disease

[267, 271, 277], and various tumors [270, 308]. However, the pathophysiological role of Hhip in the kidney is poorly understood.

We recently discovered that Hhip gene expression is differentially up-regulated in the kidneys of the offspring in our murine model of maternal diabetes, impairing nephrogenesis [330]. Using cultured metanephric mesenchymal cells [313], we demonstrated that high glucose (25 mM D-Glucose) specifically stimulated Hhip gene expression in a time- and dose-dependent manner. The hyperglycemic milieu delayed or disrupted the usual gradient Hhip-Shh expression pattern, and the elevated Hhip gene expression could be reversed by insulin [330], suggesting that Hhip gene expression could be altered by hyperglycemia. In the present study, we hypothesized that hyperglycemia regulates Hhip gene expression and that elevated renal Hhip gene expression contributes to DN development and progression.

Here we examined the role of renal Hhip expression in murine models of diabetes mellitus—T1DM (in Akita mice [331, 332] and in low-dose streptozotocin (STZ) (LDSTZ)-induced diabetic heterozygous Hhip (Hhip+/-) mice [204, 333]) and T2DM (db/db mice) [333-335]. We determined the mechanisms of hyperglycemia-induced renal Hhip gene expression that result in apoptosis of GECs and endothelial to mesenchymal transition (EndoMT)-related renal fibrosis.

3.3 Research design and methods

Animal Models. Adult male wild-type (WT, C57BL/6 J), heterozygous Akita mice with a mutated *insulin2* gene (C57BL/6-Ins2Akita/J), heterozygous *db/m* and homozygous *db/db* mice (C57BLKS) were purchased from Jackson Laboratories (Bar Harbor, ME: http://jaxmice-jax.org). All animals were fed standard mouse chow and water *ad libitum*. These mice were studied from 12 to 20 weeks of age, as reported elsewhere [331-335].

Male heterozygous Hhip ($Hhip^{+/-}$) mice and control littermates ($Hhip^{+/+}$) (Jackson Laboratories, Hhip*tm1Amc*/J; mixed background) were used [59, 268]. The low-dose streptozotocin (STZ, Sigma-Aldrich Canada Ltd., Oakville, ON, Canada) (LDSTZ) model [336], as recommended by the NIH Animal Models of Diabetic Complications Consortium (http://www.diacomp.org/), was performed in $Hhip^{+/+}$ and $Hhip^{+/-}$ mice at 12 weeks of age

(i.e., intraperitoneal injections of STZ at ~45–50 mg per kg body weight (BW) daily for 5 consecutive days). Mice were then euthanized at the age of 16 weeks after a 4-week experimental period. Blood glucose levels were measured with an Accu-Chek Performa glucose meter (Roche Diagnostics, Laval, QC, Canada) in the morning after a 4-hour fast [204, 333]. Mice with blood glucose levels below 16 mmol/l (measured 72 hours following the last STZ injection) were excluded from our analyses.

Systolic blood pressure (SBP) was monitored by the tail-cuff method with a BP-2000 Blood Pressure Analysis System (Visitech Systems Inc., Apex, NC), as reported elsewhere [307, 332, 337]. The non-diabetic and LDSTZ-induced diabetic mice (N = 5–7 mice/group) were acclimated to SBP measurement to minimize stress (training period of 5 days during 3rd week of STZ-induction), and then actual SBP was measured for 5 consecutive days during the 4th week of the experiment (the average SBP of 5 days of measurements were reported). We counted podocyte numbers per glomerulus that were positive for p57 (a marker for podocytes; 5–6 mice/group; 30–40 glomeruli/ animal) and compared the results among the groups in a blinded fashion [338].

All animal protocols were carried out in strict accordance with the recommendations in the NIH Guide for the Care and Use of Laboratory Animals and followed the Principles of Laboratory Animal Care [National Institutes of Health (NIH) publication no. 85-23, revised 1985: http://grants1.nih.gov/grants/olaw/references/phspol.htm]. Animal care and procedures were approved by the Animal Care Committee at the Centre de recherche du centre hospitalier de l'Université de Montréal (CRCHUM).

Cell Lines and Promoter Analysis. The murine SVEC4-10 endothelial cell line (mECs) (ATCC, CRL- 2181) was a kind gift from Dr. Hongyu Luo (CRCHUM, Montreal, QC, Canada). The immortalized mouse podocyte cell line (mPODs) obtained from Dr. Stuart J. Shankland (University of Washington, Seattle, WA, USA) is highly proliferative when cultured under permissive conditions and has been well characterized [338-340].

We cloned the mouse Hhip promoter (pGL4.20/mHhip, N-1542/N+9, NC_000074.6) and rat TGFβ1 promoter (pGL4.20/rTGFβ1, N-1016/+143, NM_021578.2) by PCR. Both pGL4.20/mHhip and pGL4.20/rTGFβ1 promoter activities in mECs under normal (5 mM D-

glucose) and high D-glucose (25 mM D-glucose) ± recombinant Hhip (rHhip) (R&D Systems, Inc.) or rTGFβ1 (R&D Systems, Inc.) conditions were analyzed by luciferase assay.

Immunohistochemical Studies and Reagents. Western blotting (WB), immunohistochemistry (IHC), immunofluorescence (IF) and dihydroethidium (DHE) and terminal deoxynucleotidyl transferase dUTP nick end labeling (TUNEL) staining were performed as described elsewhere [307, 330, 332, 338]. The antibodies used for IHC and IF included the following: anti-Hhip (monoclonal clone 5D11), α-smooth muscle actin (α-SMA) and β-actin antibodies from Sigma-Aldrich Canada; Shh, TGFβ receptor II (TGFβRII), CD31, synaptopodin (Synpo) (P-19) and p57 (H-91) antibodies from Santa Cruz Biotechnology (Santa Cruz, CA, USA); p27Kip1 antibody from BD Biosciences (San Jose, CA, USA); cleaved caspase-3 (Asp175) and caspase-3 antibodies from Cell Signaling (Danvers, MA, USA); anti-TGFβ1 antibody from R&D Systems, Inc. (Burlington, ON, Canada); Phospho-Smad2 (Ser465/467)/Smad3 (Ser423/425) antibody (New England Biolabs, Whitby, ON, Canada); Smad2/3 antibody (Cedarlane-Millipore, Burlington, ON, Canada); and anti-NADPH oxidase 4 (Nox4) antibody (Abcam, Cambridge, MA, USA). GKT137831 (dual inhibitor of both Nox1 and Nox4) was procured from Cayman Chemical (Ann Arbor, MI, USA).

Renal Morphology, Glomerular Filtration Rate, Urinary Albumin/Creatinine Ratio. Kidney sections were stained with Periodic-Acid Schiff (PAS) and Masson's trichrome to reveal renal morphologic changes [332, 337]. The changes of DN features—glomerulosclerosis (based on PAS images, scale from 0 to 4) and glomerular fibrosis (based on Masson staining) were scored with the scorer blinded to the group [332, 337]. Relative staining was quantified with NIH Image J software (Bethesda, MD, USA). The images (N = 6~10 per animal, 6–11 mice/group) were analyzed and quantitated in a blinded fashion [332, 337]. Glomerular filtration rate (GFR) was measured in conscious mice by the fluorescein isothiocyanate-inulin method as reported previously [307, 332], as recommended by the Diabetic Complications Consortium (http://www.diacomp.org/). Urine samples, collected from mice individually housed in metabolic cages, were assayed for albumin/creatinine ratio (ACR) (Albuwell and Creatinine Companion, Exocell Inc., Philadelphia, PA, USA) [307, 332]

Statistical Analysis. For animal studies, groups of 6 to 12 mice were used. *In vitro*, three to four separate experiments were performed for each protocol. All values represent mean ± SEM. Statistical significance between the experimental groups was analyzed by Student's *t*-test or 1-way ANOVA, followed by the Bonferroni test using Prism 5.0 software (GraphPad, San Diego, CA, USA). A probability level of $p < 0.05$ was considered to be statistically significant (*$p \leq 0.05$; **$p \leq 0.01$; ***$p \leq 0.001$; NS, non-significant).

3.4 Results

Hyperglycemia-Induced Renal Hhip Gene Expression. As compared to controls (non-Akita littermates (Fig. 1a–c) and *db/m* mice (Fig. 1d–f)), renal Hhip mRNA and protein expression were significantly increased in the renal cortex of both Akita (Fig. 1a–c) and *db/db* (Fig. 1d–f) mice at the age of 20 weeks. Western blot (WB) revealed that enhanced TGFβ1, TGFβ receptor II (TGFβRII) and Shh protein expression were also apparent in both diabetic models (Figs 1b, S1a, and e, S1b). The increased Hhip, TGFβ1, TGFβRII and Shh protein expression in the renal cortex of Akita mice was normalized with insulin implants in the animals (Figs 1b and S1a). The heightened renal Hhip expression in both Akita and *db/db* mice was subsequently confirmed by immunohistochemistry (IHC) staining (Fig. 1c, 1f, respectively); TGFβ1 had a similar IHC expression pattern in Akita and *db/db* mice kidneys (Fig. 1c, 1f, respectively). Next, we validated our *in vivo* Hhip expression pattern by using 2 cell lines including murine SVEC4-10 endothelial cells (mECs) (ATCC, CRL-2181) (Fig. 1g) and immortalized mouse podocyte cells (mPODs) [338-340] (Fig. 1h). It is apparent that high glucose (25 mM D-Glucose) increases Hhip protein expression in both mECs and mPODs, while it inhibits synaptopodin protein expression in mPODs (Fig. 1h).

In line with the Hhip expression reported in endothelial cells [270], our co-localization experiments (Fig. 2a, immunofluorescence (IF)) showed that hyperglycemia-induced Hhip and TGFβ1-IF expression was predominantly found in GECs (revealed by CD31 co-localization), suggesting that GECs might be the potential source of elevated Hhip expression in diabetic glomeruli. Focusing on mECs (Fig. 2b–e), our data revealed that high glucose stimulates pGL4.20/mHhip promoter (N-1542/N+9, NC_000074.6) activity (Fig. 2b), Hhip mRNA (Fig. 2c) and protein (Fig. 2d–e) expression in a dose-dependent and/or time-

dependent manner. Furthermore, the stimulatory effect of high glucose on TGFβ1 mRNA (Fig. 2c) and protein expression (Fig. 2e) was similar to Hhip expression in mECs, while high glucose had no impact on Shh protein expression within 24 hours (Fig. 2e).

Oxidative Stress and Hhip Expression. Next, we investigated the effect of angiotensin II (Ang II) and hydrogen peroxide (H_2O_2) on Hhip protein expression. We observed that Ang II (Fig. 3a) and H_2O_2 (Fig. 3b) increased the expression of Hhip protein and activated the TGFβ1-Smad2/3 cascade in a dose-dependent manner. Catalase (250 U/ml) attenuated the stimulatory effect of high glucose on Hhip protein expression in mECs (Fig. 3c).

NADPH oxidase 4 (Nox4) is the major H_2O_2-generating enzyme expressed in endothelial cells [341]. The addition of 10 μM of GKT137831 (a dual inhibitor of both Nox1 and Nox4) completely abolished the high glucose effect on *Nox4*, *Hhip* and *TGFβ1*-mRNA expression in mECs (Fig. 3d). The increased Nox4 protein expression in mECs by high glucose was further confirmed by IF staining (Fig. 3e). Similarly, as compared to controls (non-Akita littermates and *db/m* mice), Nox4 protein expression was highly elevated in the renal cortex of both Akita and *db/db* mice at the age of 20 weeks as analyzed by WB (Fig. 3f) and it was profoundly increased in the glomeruli as revealed by Nox4-IHC staining (Fig. 3g).

Recombinant Hhip (rHhip) dose-dependently enhanced the number of DHE-positive cells and apoptotic cells (terminal deoxynucleotidyl transferase dUTP nick end labeling (TUNEL) assay), and increased α-smooth muscle actin (α-SMA) and Nox4 IF-staining (Fig. 4a), as well as the expression of several factors associated with fibrosis and apoptosis in mECs as shown by changes in the expression of fibronectin (Fn1), α-SMA, p27, Nox4 and cleaved caspase-3 (Fig. 4b). The stimulatory effect of rHhip on dihydroethidium (DHE) staining was completely reversed by GKT137831 (10 μM) (Fig. 4c).

The Interaction of Hhip and TGFβ1 in vitro. rHhip directly activated TGFβ1 protein expression in a time-dependent manner without influencing Shh protein expression until 48hrs (Figs 5a and S2a) in mECs. Transient transfection of Hhip siRNA attenuated the high glucose-stimulatory effects on both Hhip and TGFβ1 protein expression in mECs (Figs 5b and S2b). Also, rHhip dose-dependently stimulated pGL4.20/TGFβ1 promoter activity (Fig. 5c) and activated TGFβ1-Smad2/3 cascades (Figs 5d and S2c) in mECs. Furthermore,

blocking TGFβ1 receptors (TGFβ1RI/RII), either by SB431532 (an inhibitor of TGFβ1RI) (Fig. 5e) or TGFβ1RII siRNA (Fig. 5f–g), abolished the stimulatory effect of rHhip (Fig. 5e–f) and high glucose (Fig. 5g) on TGFβ1 protein expression. In contrast, administration of recombinant TGFβ1 (2 ng/ml) had no impact on either pGL4.20/mHhip promoter (N-1016/+143, NM_021578.2) activity (Fig. 5h) or Hhip protein expression (Fig. 5i) in mECs.

Low Dose Streptozotocin (LDSTZ)-Induced Diabetes in Heterozygous Hhip$^{+/-}$ Mice. To validate the effect of endogenous Hhip, we used male heterozygous Hhip (Hhip$^{+/-}$) mice [N.B., Adult Hhip$^{+/-}$ mice are phenotypically indistinguishable from control littermates (Hhip$^{+/+}$), whereas Hhip null mice (Hhip$^{-/-}$) die after birth due to lung defects; thus Hhip$^{+/-}$ were used in the current study [59, 268]]. We examined the renal outcomes in male Hhip$^{+/-}$ vs. Hhip$^{+/+}$ mice undergoing 4 weeks of LDSTZ -induced diabetes from the age of 12 to 16-week old (Fig. 6a). In the non-diabetic condition, adult Hhip$^{+/-}$ mice were indistinguishable from Hhip$^{+/+}$ mice including kidney weight (KW)/tibia length (TL) ratio (Fig. 6b), glomerular filtration rate (GFR) (Fig. 6c), urinary albumin/creatinine ratio (ACR) (Fig. 6d) and renal morphology (Fig. 6e, Periodic-Acid Schiff (PAS), Masson, Nox4-IHC and podocyte numbers). After 4 weeks of diabetes, diabetic Hhip$^{+/+}$ animals had evidence of renal hypertrophy (Fig. 6b), increased GFR (Fig. 6c) and urinary ACR (Fig. 6d), and developed DN features (Fig. 6e) including glomerulosclerosis, glomerular fibrosis as well as elevated oxidative stress (Nox4-IHC). However, such renal changes were attenuated in diabetic Hhip$^{+/-}$ mice (Fig. 6b–e) with normal urinary ACR (Fig. 6d). Systolic blood pressure (SBP) (Fig. 6f), however, remained unchanged among the different groups with or without 4-weeks of diabetes.

3.5 Discussion

In the current study, we systematically examined renal Hhip expression in several diabetic murine models. We demonstrated that Hhip expression is significantly increased in diabetic GECs and that kidney injury is ameliorated in diabetic Hhip$^{+/-}$ mice. Our data support the notion that augmented renal Hhip expression may play an important role in the progression of DN by promoting apoptosis and fibrosis in GECs.

While GEC injury is the hallmark of early renal injury in DN, there is a pressing need to identify novel insights into causal processes that contribute to the onset of diabetes-related glomerular endothelial injury or its progression that may help to identify potential therapeutic targets [323-325]. Here, we are focusing on Hhip, a molecule not previously considered in the development and progression of DN; we found that Hhip appears to be involved in GEC injury in diabetic murine models, a novel finding.

In the kidney, the functional role of renal Hhip expression in both developing and mature kidneys is unknown. Previously, we reported that renal Hhip gene is excessively expressed in the nascent glomeruli of the offspring of diabetic dams. Consequently, those elevated/trapped renal Hhip proteins, via Hhip-TGFβ1 interaction, lead to the impaired kidney development observed [330]. After birth, in normal non-diabetic states, Hhip expression is quiescent, with only a limited amount of Hhip detectable in mature GECs in line with endothelial cells Hhip-expressing property [270], however, it is not detectable in podocytes by immunohistochemistry [330]. In contrast, in animals with diabetes, we observed that renal Hhip expression was significantly elevated in mature kidneys (Akita, db/db, and LDSTZ-induced diabetic models), predominantly localized to GECs (confirmed by CD31 co-localization). We further confirmed the stimulatory effect of high glucose on pGL4.20/mHhip promoter activity, Hhip mRNA and protein expression in a dose- and time-dependent manner; Hhip induces mECs apoptosis and EndoMT in vitro. Moreover, an increased Hhip expression was also observed in mouse podocytes cultured in high glucose milieu. Consistent with our recent findings [338], when Hhip expression is ectopically activated and/or stimulated in podocyte, Hhip could trigger caspase-3 and p53-related apoptotic processes resulting in podocyte loss and activate TGFβ1-Smad2/3 cascades and α-SMA expression to transform differentiated podocytes to undifferentiated podocyte-derived fibrotic cells [338]. Taken together, our data indicate that increased Hhip expression might directly impact diabetes-related glomerular endothelial injury.

Counterbalance between Hhip and Shh signaling appears to be important for maintaining a normal Shh gradient [distal (high) to proximal (low)] in the developing kidney [50, 342], and interruption of the Shh gradient has been shown to result in renal dysplasia/hypoplasia [50]. In

the mature kidney, although Shh has been linked to renal fibrosis [315, 343], given the fact that Hhip expression is quiescent after birth, it is unclear whether high glucose-promoted Hhip gene expression could function dependently and/or independently via Shh/Ptc1-signaling process. Our present studies revealed that Shh expression was highly elevated in the renal cortex of diabetic models (Akita and db/db mice). In vitro, high glucose had no impact on Shh protein expression within 24 hours, and Shh responsed to rHhip at 48 hours, not as early as TGFβ1 at 6 hours, suggesting that high glucose regulation of Hhip and TGFβ1 gene expression may take place prior to the Shh/Ptcl signaling pathway, underscoring the independence of Hhip action.

It has been well-established that hyperglycemia and AngII increase cellular oxidative stress (reactive oxygen species, ROS) and play key roles in the pathogenesis of DN [92, 221, 325]. Our data showed that Ang II and H_2O_2 directly and dose-dependently promote Hhip expression and the TGFβ1-Smad2/3 cascades and that catalase attenuates the stimulatory effect of high glucose on Hhip protein expression. Hhip is known to play a critical role in cell apoptosis, angiogenesis, and tumorigenesis [270, 308, 344]. While several mechanisms involving cross-talk among oxidative stress, hedgehog signaling, and TGFβ1 signaling have been associated with certain pathologic conditions such as diabetic retinopathy [345], brain ischemia [346], renal fibrosis [315, 343], pulmonary fibrosis [347] and cancer-related epithelial to mesenchymal transition and metastasis [348]. Together, these observations led us to hypothesize that Hhip could interact with ROS and/or TGFβ1-signaling to result in EndoMT associated with DN-fibrosis/apoptosis.

TGFβ1 has been implicated in DN-related EndoMT transition [226, 227] and Nox4-derived ROS have a central role in TGFβ1-related EndoMT in renal fibrosis [192]. In contrast to superoxide-generating enzymes Nox1 and Nox2, Nox4 is an H_2O_2-generating enzyme and is highly expressed in murine endothelial cells [341]. Our studies showed elevated Nox4 IHC-staining in the glomeruli of both Akita and db/db mice and that the stimulatory effect of high glucose on Hhip and TGFβ1 mRNA expression in mECs could be completely abolished by GKT137831, demonstrating the involvement of Nox4. Furthermore, rHhip dose-dependently elevated ROS generation as revealed by DHE and Nox4 IF staining in mECs and that H_2O_2

stimulates Hhip production, underscoring a positive feedback loop of Hhip and ROS, probably mediated by Nox4. Consequently, rHhip triggers mECs apoptosis (increases in TUNEL-positive cells and cleaved caspase-3) and fibrosis (increases in Fn1, α-SMA, and p27 expression).

Our studies also revealed that renal Hhip and TGFβ1 had similar expression patterns in diabetic kidneys; in vitro, both Hhip and TGFβ1 genes shared a similar time-course responding to high glucose stimulation in mECs, and rHhip stimulated TGFβ1 transcription and TGFβ1-Smad2/3 cascade signaling, together, underscoring a functional interaction of Hhip and TGFβ1. Indeed, Hhip siRNA attenuated the effect of high glucose on TGFβ1 production. Blocking TGFβ receptors (TGFβ1RI by SB431532 or TGFβ1RII by siRNA) completely attenuated the action of rHhip or high glucose on TGFβ1 expression. At the present, we do not understand how Hhip interacts with TGFβ1. One possibility might be that Hhip acts upstream of TGFβ1 signaling, targeting TGFβ1 gene transcription and translation. This is supported by our data that rHhip stimulates TGFβ1 promoter activity, protein expression, and TGFβ1-Smad2/3 cascade signal. Furthermore, our data showed that rTGFβ1 fails to impact Hhip promoter and protein expression, but it directly promotes fibrotic gene expression (Shh, α-SMA, and p27). Together, these data strongly support the presence of the axis of Hhip-TGFβ1-Shh and its action on DN-related EndoMT.

To further support the role of renal Hhip in DN progression, we extended our investigation in LDSTZ-induced diabetic heterozygous $Hhip^{+/-}$ mice. Our data revealed that adult non-diabetic male $Hhip^{+/-}$ mice exhibit grossly normal renal morphology, similar to control $Hhip^{+/+}$ mice. Diabetic $Hhip^{+/+}$ mice had a significant increase in urinary ACR in a time-dependent manner and exhibited features that were consistent with DN progression (renal hypertrophy, increased GFR, glomerulosclerosis/fibrosis, and podocyte loss). In contrast, diabetic $Hhip^{+/-}$ mice had normal urinary ACR with less pronounced renal morphologic and/or functional changes. Such data indicate that with a lower renal Hhip expression, the kidney is protected from DN development. Consistent with the notion that GEC injury may lead to podocyte damage, and that podocyte loss further exacerbates GEC injury, forming a vicious cycle ultimately leading to DN that has been gaining attention[323-325], our data

indicate that augmented Hhip gene expression is associated with podocyte transition from a normal morphology to an apoptotic and/or fibrotic-like phenotype, and are further supported by the finding that human Hhip is upregulated in glomerular cells, in patients with focal segmental glomerulosclerosis [338]. However, GECs specific gain and/or loss-of-Hhip function/expression murine models would be needed to circumvent the potential pitfall of whole body Hhip-deficient murine model in the future. Taken together, the present data support the concept that Hhip plays a role in diabetic nephropathy; further studies will be needed to elucidate the mechanism(s) of cross-talk between GECs and/or podocyte-derived Hhip functions on EndoMT. Finally, blood pressure remained unchanged, consistent with other studies in an LDSTZ model [305].

In summary, our findings document that Hhip expression is associated with nephropathy development in diabetes and that hyperglycemia-induced renal Hhip expression may mediate glomerular endothelial fibrosis and apoptosis in diabetes.

3.6 Legends and Figures

Figure 3-1

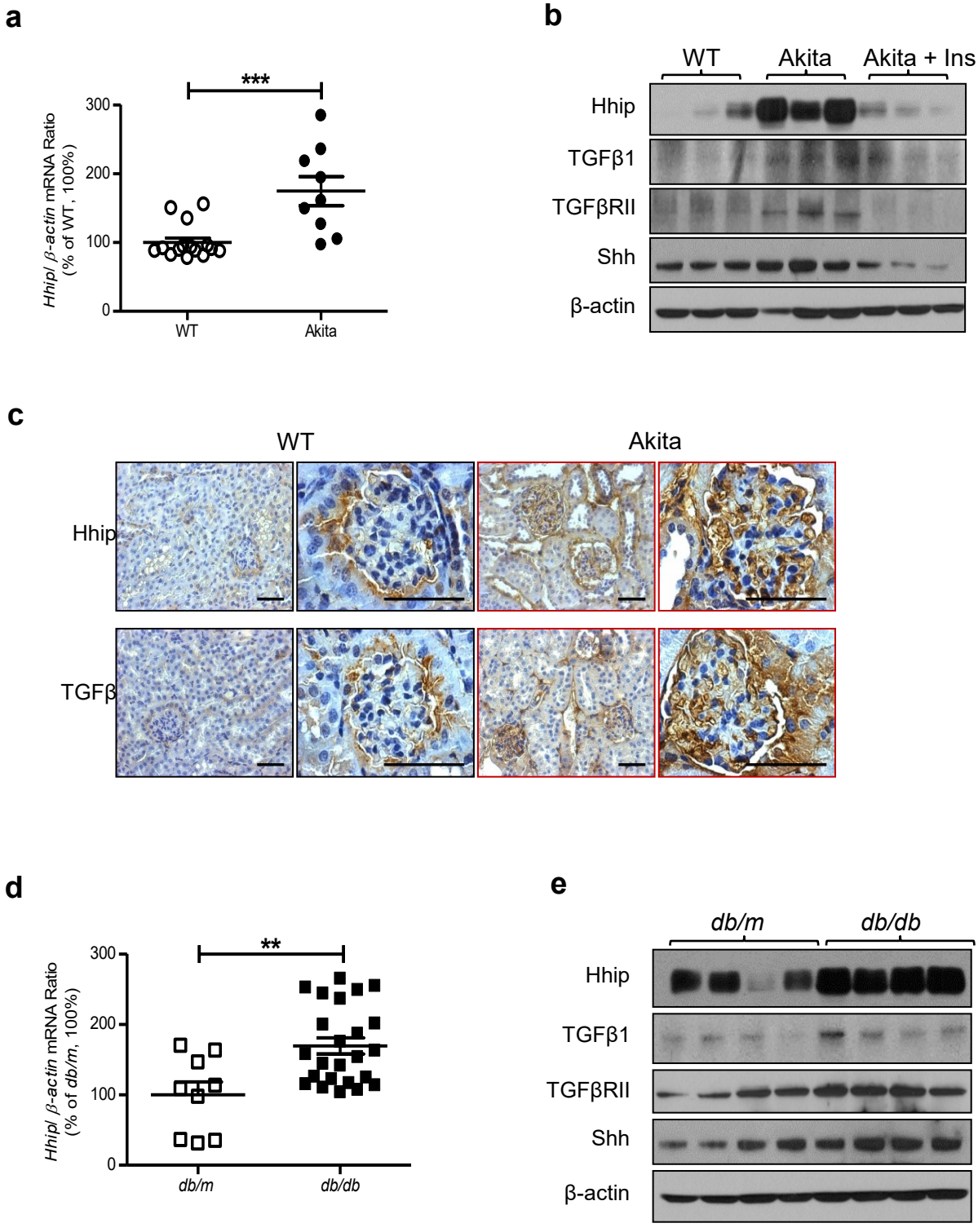

Figure 3-1

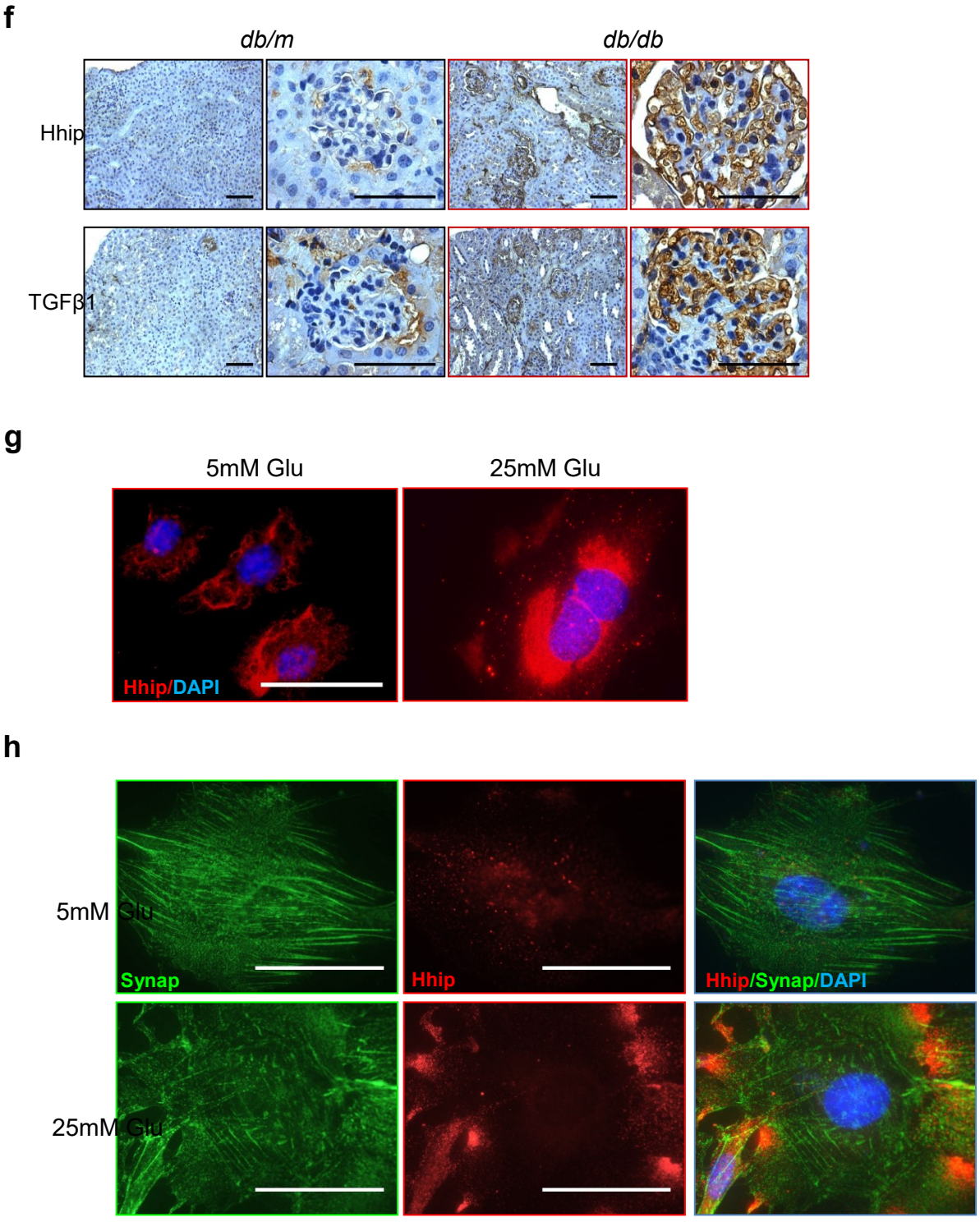
f
db/m
db/db
Hhip
TGFβ1
g
5mM Glu
25mM Glu
Hhip/DAPI
h
5mM Glu
25mM Glu
Synap
Hhip
Hhip/Synap/DAPI

Figure 3-1. Hyperglycemia-induced renal Hhip expression *in vivo* (Akita (a–c) and *db/db* mice (d–f) at the age of 20 weeks) and *in vitro* (mECs (g) and mPODs (h)). (a,d) qPCR of Hhip mRNA expression in renal cortex. Hhip mRNA expression was normalized by their corresponding β-actin mRNA. (b,e) WB analysis of Hhip, Shh, TGFβ1, and TGFβ1RII in the renal cortex. $^{**}P \leq 0.01$; $^{***}P \leq 0.001$ vs. WT or *db/m*; Values represent the mean ± SEM. (c,f) Hhip- and TGFβ1-IHC in the kidneys (scale bar, 50 μm). (g–h) IF staining in mECs (g) and mPODs (h) (scale bar, 50 μm).

Figure 3-2

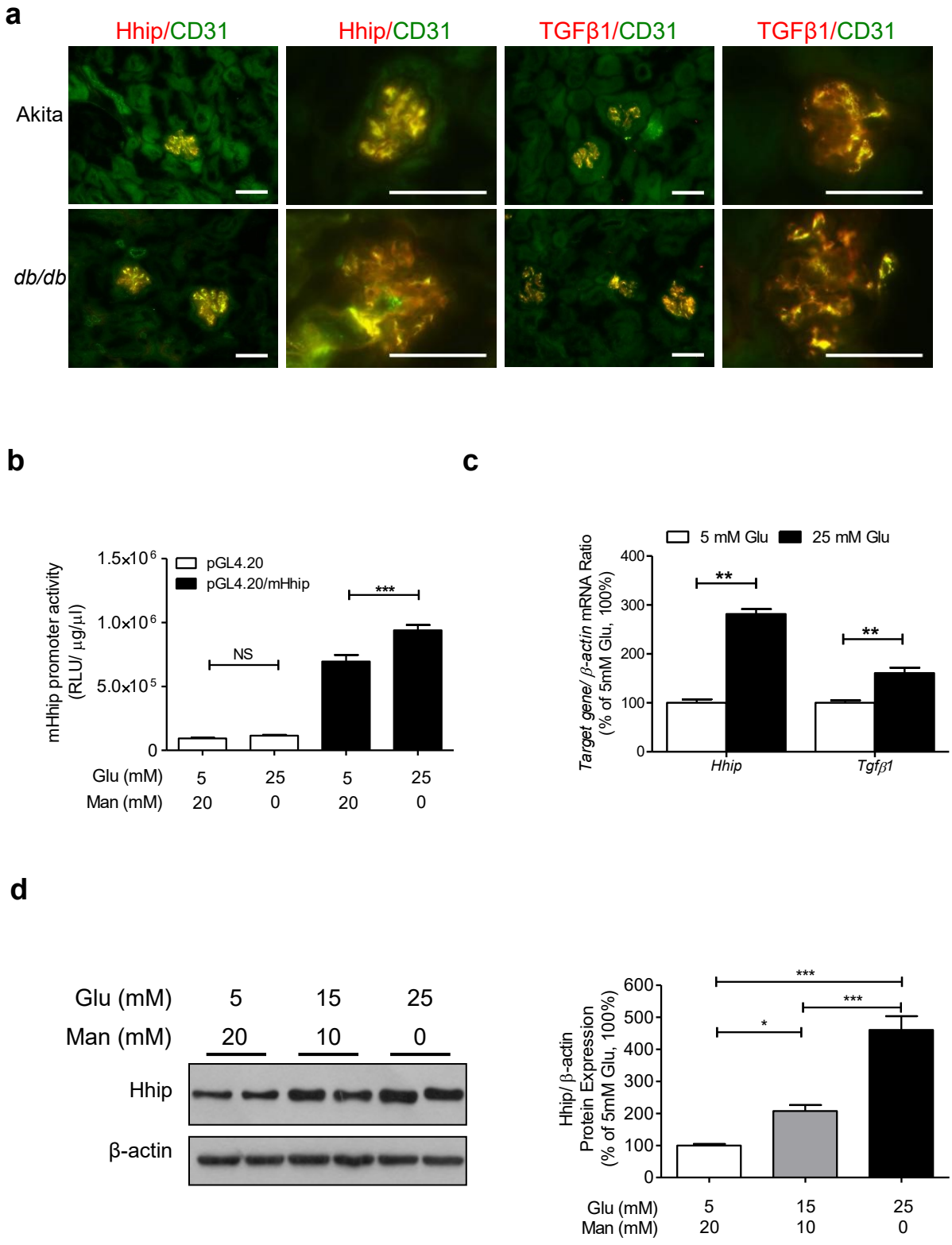
a
Hhip/CD31
Hhip/CD31
TGFβ1/CD31
TGFβ1/CD31
Akita
db/db
b
mHhip promoter activity (RLU/ μg/μl)
1.5x10^6
1.0x10^6
5.0x10^5
0
pGL4.20
pGL4.20/mHhip
NS
***
Glu (mM) 5 25 5 25
Man (mM) 20 0 20 0
c
5 mM Glu
25 mM Glu
Target gene/ β-actin mRNA Ratio (% of 5mM Glu, 100%)
400
300
200
100
0
**
**
Hhip
Tgfβ1
d
Glu (mM) 5 15 25
Man (mM) 20 10 0
Hhip
β-actin
Hhip/ β-actin Protein Expression (% of 5mM Glu, 100%)
600
500
400
300
200
100
0
***
***
*
Glu (mM) 5 15 25
Man (mM) 20 10 0

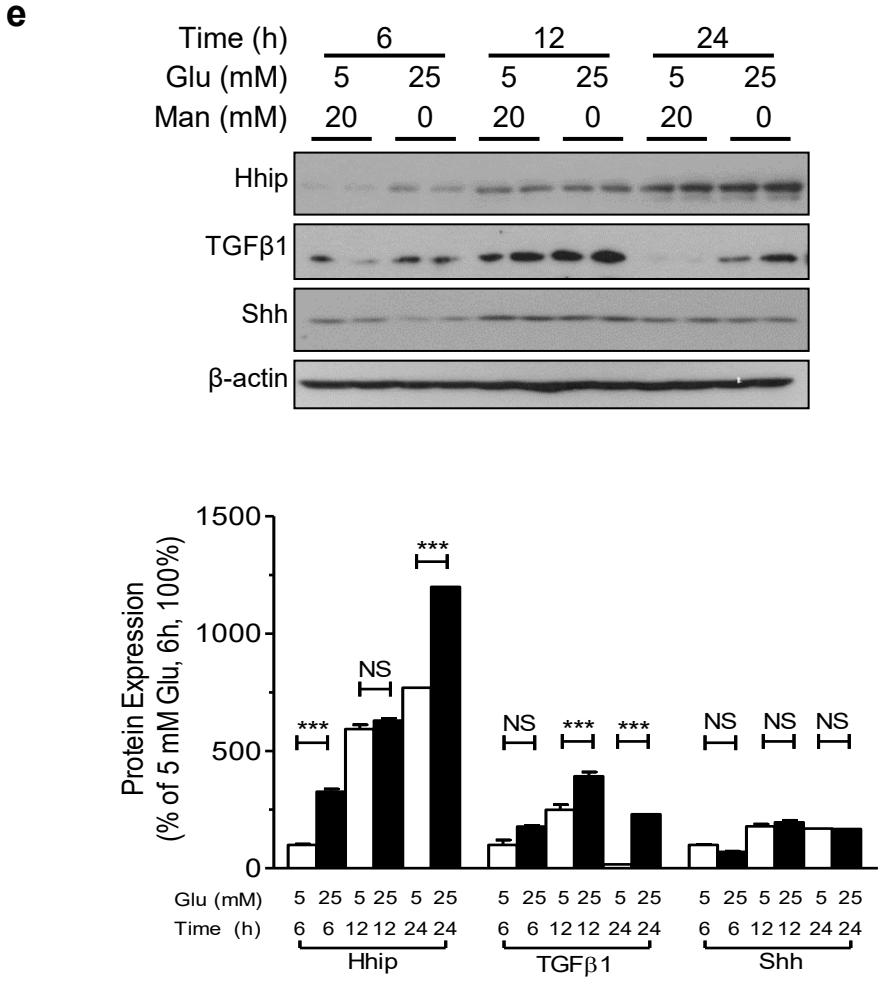

Figure 3-2 *Hhip* gene expression in GECs *in vivo* (**a**) and in mECs *in vitro* (**b**–**e**). (**a**) Hhip- and TGFβ1- colocalization IF-staining with CD31 in the kidney of Akita and *db/db* mice at the age of 20 weeks (scale bar, 50 μm); (**b**) pGL4.2/mHhip promoter activity analyzed by luciferase assay. ***$P \leq 0.001$; NS, non-significant; Values represent the mean ± SEM. (**c**) qPCR of Hhip mRNA. Hhip mRNA expression were normalized by their corresponding β-actin mRNA; (**d**,**e**) WB analysis in glucose dose- (**d**) and time- (**e**) dependent manner, *$P \leq 0.05$; **$P \leq 0.01$; ***$P \leq 0.001$ vs. mECs cultured in 5 mM glucose (100%); Values represent the mean ± SEM.

Figure 3-3

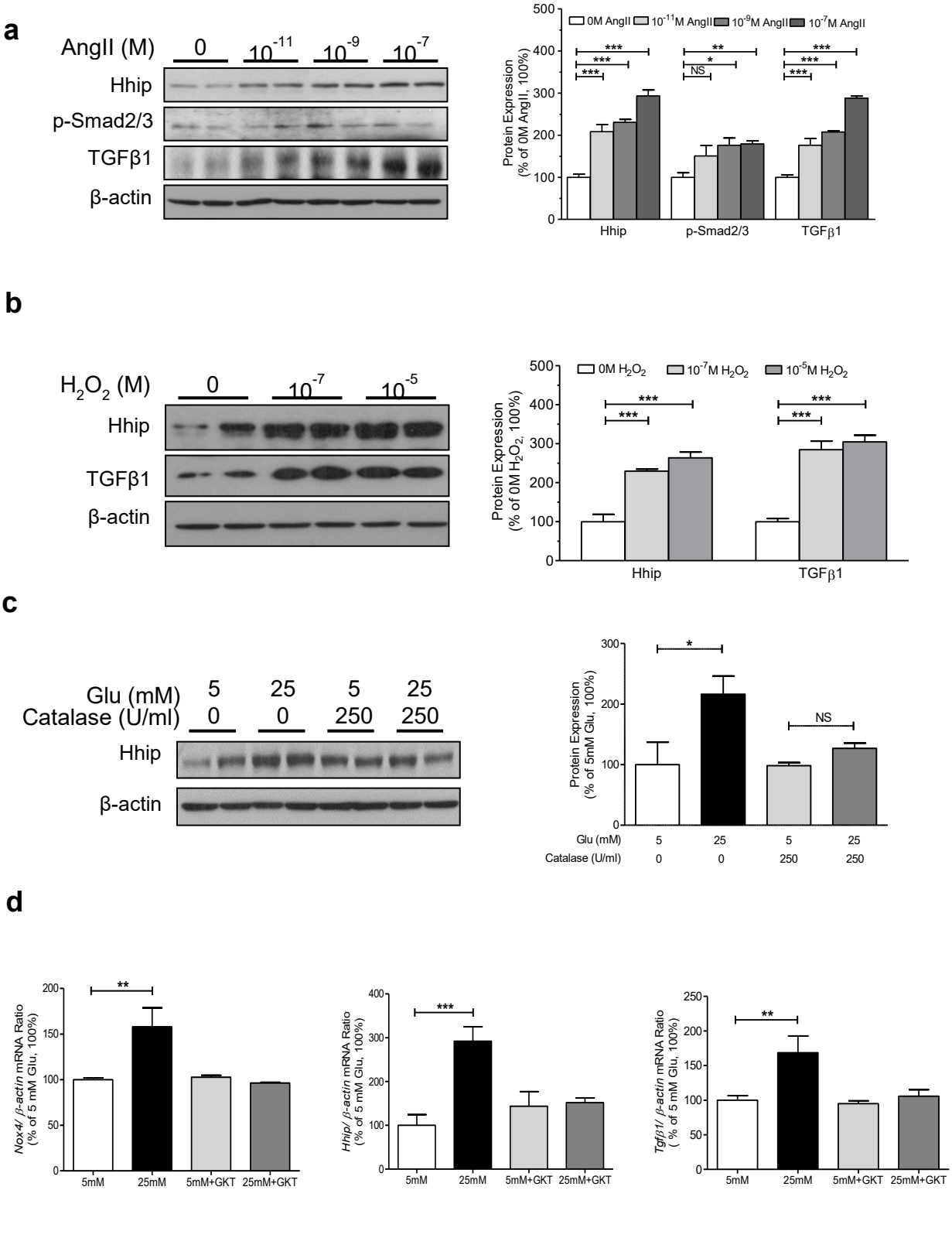
a
AngII (M)
0
10-11
10-9
10-7
Hhip
p-Smad2/3
TGFβ1
β-actin
0M AngII
10-11M AngII
10-9M AngII
10-7M AngII
Protein Expression
(% of 0M AngII, 100%)
Hhip
p-Smad2/3
TGFβ1
b
H2O2 (M)
0
10-7
10-5
Hhip
TGFβ1
β-actin
0M H2O2
10-7M H2O2
10-5M H2O2
Protein Expression
(% of 0M H2O2, 100%)
Hhip
TGFβ1
c
Glu (mM)
Catalase (U/ml)
Hhip
β-actin
Protein Expression
(% of 5mM Glu, 100%)
NS
d
Nox4/ β-actin mRNA Ratio
(% of 5 mM Glu, 100%)
Hhip/ β-actin mRNA Ratio
(% of 5 mM Glu, 100%)
Tgfβ1/ β-actin mRNA Ratio
(% of 5 mM Glu, 100%)
5mM
25mM
5mM+GKT
25mM+GKT

Figure 3-3

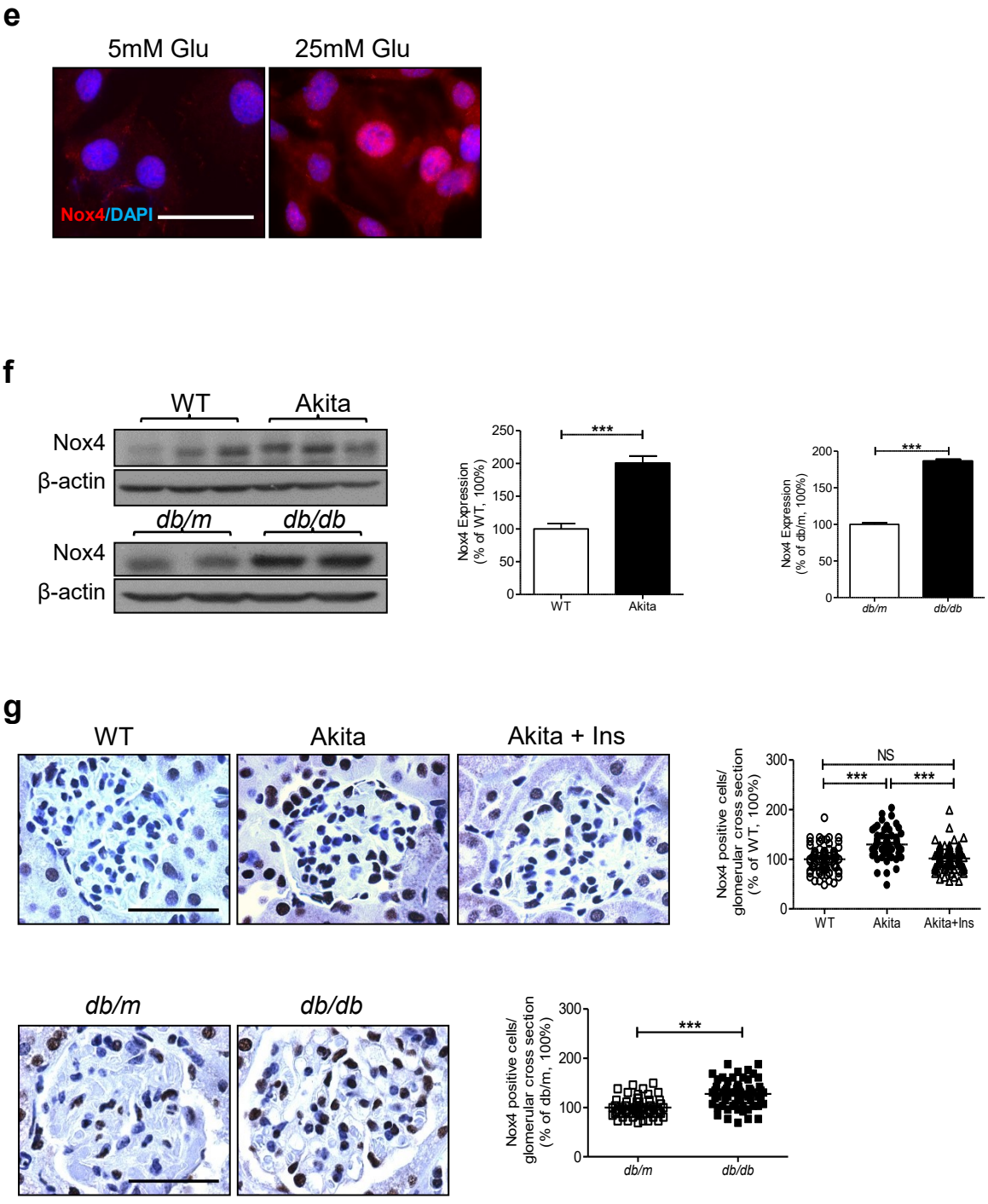
e
5mM Glu
25mM Glu
Nox4/DAPI
f
WT
Akita
Nox4
β-actin
db/m
db/db
Nox4
β-actin
Nox4 Expression (% of WT, 100%)
***
WT
Akita
Nox4 Expression (% of db/m, 100%)
***
db/m
db/db
g
WT
Akita
Akita + Ins
Nox4 positive cells/ glomerular cross section (% of WT, 100%)
NS
***
***
WT
Akita
Akita+Ins
db/m
db/db
Nox4 positive cells/ glomerular cross section (% of db/m, 100%)
***
db/m
db/db

Figure 3-3 The interaction of Hhip and Nox4 *in vitro* and *in vivo*. (**a**–**c**) WB in mECs. (**a**) Ang II dose-dependent manner. (**b**) H2O2 dose-dependent manner. (**c**) High glucose ± Catalase (250U/ml) on Hhip protein expression. *$P \leq 0.05$; **$P \leq 0.01$; ***$P \leq 0.001$; NS, non-significant vs. mECs cultured in 5 mM glucose (100%); Values represent the mean ± SEM. (**d**) qPCR of Nox4, TGFβ1, and Hhip- mRNA expression in mECs. mRNA of genes were normalized by their corresponding β-actin mRNA. **$P \leq 0.01$; ***$P \leq 0.001$; NS, non-significant vs. mECs cultured in 5 mM glucose (100%); Values represent the mean ± SEM. (**e**) Nox4-IF staining in mECs (scale bar, 50 μm). (**f**) WB of Nox4 protein expression in renal cortex of Akita and *db/db* mice at the age of 20 weeks. ***$P \leq 0.001$ vs. WT or *db/m*; Values represent the mean ± SEM. (**g**) Nox4-IHC in the kidneys of Akita and *db/db* mice at the age of 20 weeks (scale bar, 50 μm). Semi-quantification of Nox4 positive stained cells per glomerulus. ***$P \leq 0.001$; NS, non-significant.

Figure 3-4

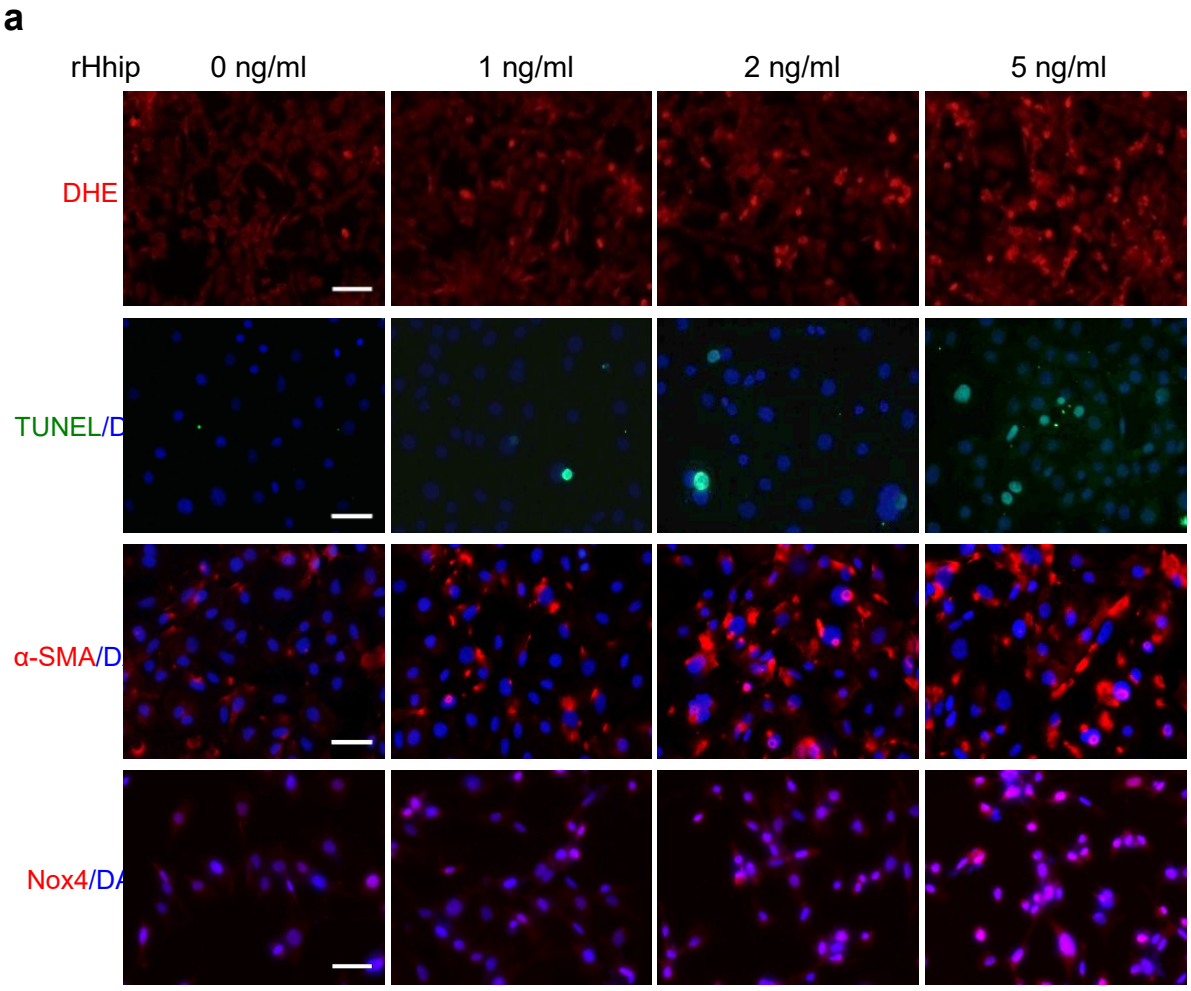
a
rHhip
0 ng/ml
1 ng/ml
2 ng/ml
5 ng/ml
DHE
TUNEL/D
α-SMA/D
Nox4/DA
b
rHhip (ng/ml)
0
1
2
5
Fn1
α-SMA
p27
Nox4
β-actin
Casp-3 (cleaved)
Casp-3 (total)
rHhip (ng/ml) 0 1 2 5
Protein Expression (% of 0 ng/ml rHhip, 100%)
800
700
600
500
400
300
200
100
0
***
**
NS
*
Fn1
α-SMA
Nox4
Casp-3

Figure 3-4

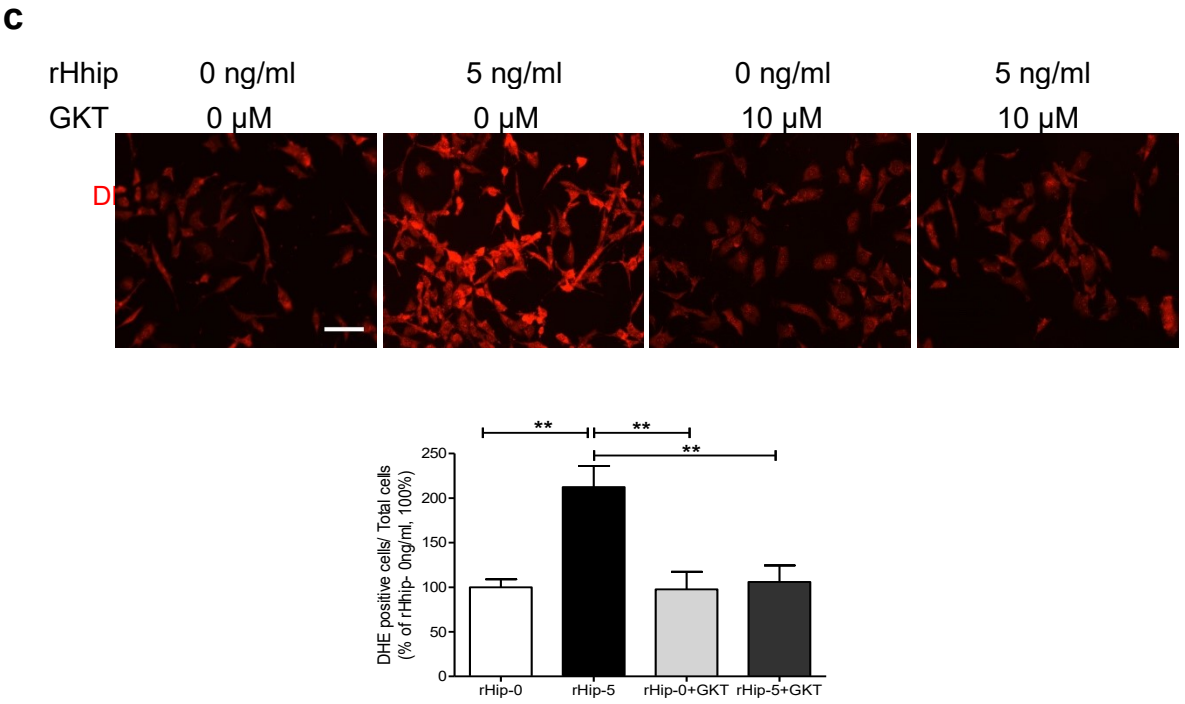

Figure 3-4 rHhip effect in mECs. (**a**) rHhip dose-dependent effect analyzed by DHE staining, TUNEL, α-SMAand Nox4-IF staining (scale bar, 50 μm). (**b**) rHhip dose-dependent effect on a variety of proteins expression analyzed by WB. *$P \leq 0.05$; **$P \leq 0.01$; ***$P \leq 0.001$; NS, non-significant vs. mECs cultured in 5 mM glucose (100%) without rHhip (0 ng/ml); Values represent the mean ± SEM. (**c**) The inhibitory effect of GKT137831 (10 μM) on DHE staining with or without rHhip (5 ng/ml) (scale bar, 50 μm). **$P \leq 0.01$; ***$P \leq 0.001$; NS, non-significant vs. mECs cultured in 5 mM glucose (100%) without rHhip (0 n

Figure 3-5

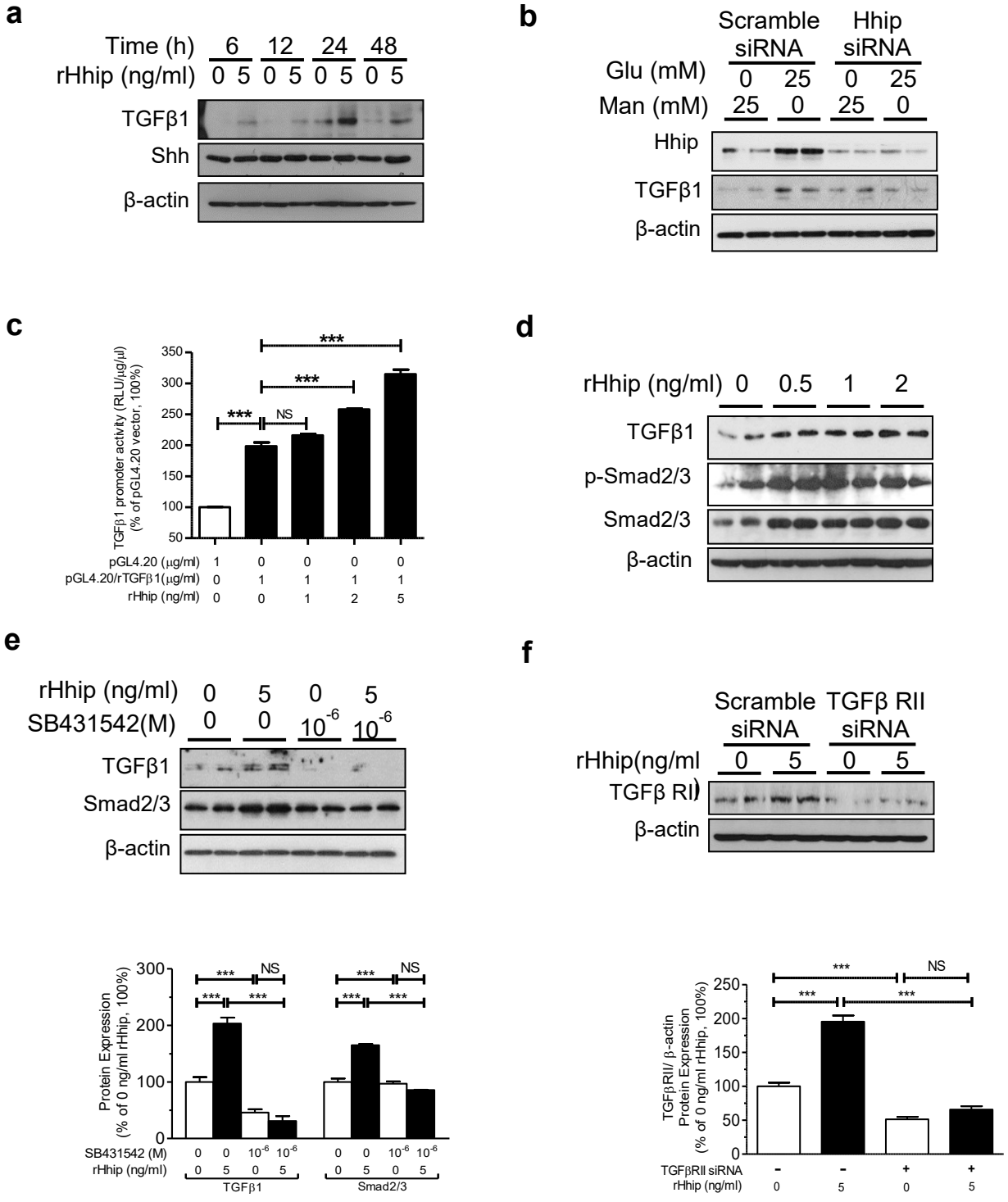
a
Time (h) 6 12 24 48
rHhip (ng/ml) 0 5 0 5 0 5 0 5
TGFβ1
Shh
β-actin
b
Scramble siRNA
Hhip siRNA
Glu (mM) 0 25 0 25
Man (mM) 25 0 25 0
Hhip
TGFβ1
β-actin
c
TGFβ1 promoter activity (RLU/μg/μl) (% of pGL4.20 vector, 100%)
350
300
250
200
150
100
50
***
***
***
NS
pGL4.20 (μg/ml) 1 0 0 0 0
pGL4.20/rTGFβ1(μg/ml) 0 1 1 1 1
rHhip (ng/ml) 0 0 1 2 5
d
rHhip (ng/ml) 0 0.5 1 2
TGFβ1
p-Smad2/3
Smad2/3
β-actin
e
rHhip (ng/ml) 0 5 0 5
SB431542(M) 0 0 10-6 10-6
TGFβ1
Smad2/3
β-actin
Protein Expression (% of 0 ng/ml rHhip, 100%)
300
200
100
0
***
NS
***
***
***
NS
***
***
SB431542 (M) 0 0 10-6 10-6 0 0 10-6 10-6
rHhip (ng/ml) 0 5 0 5 0 5 0 5
TGFβ1
Smad2/3
f
Scramble siRNA
TGFβ RII siRNA
rHhip(ng/ml 0 5 0 5
TGFβ RII
β-actin
TGFβRII/ β-actin Protein Expression (% of 0 ng/ml rHhip, 100%)
250
200
150
100
50
0
***
NS
***
***
TGFβRII siRNA - - + +
rHhip (ng/ml) 0 5 0 5

Figure 3-5

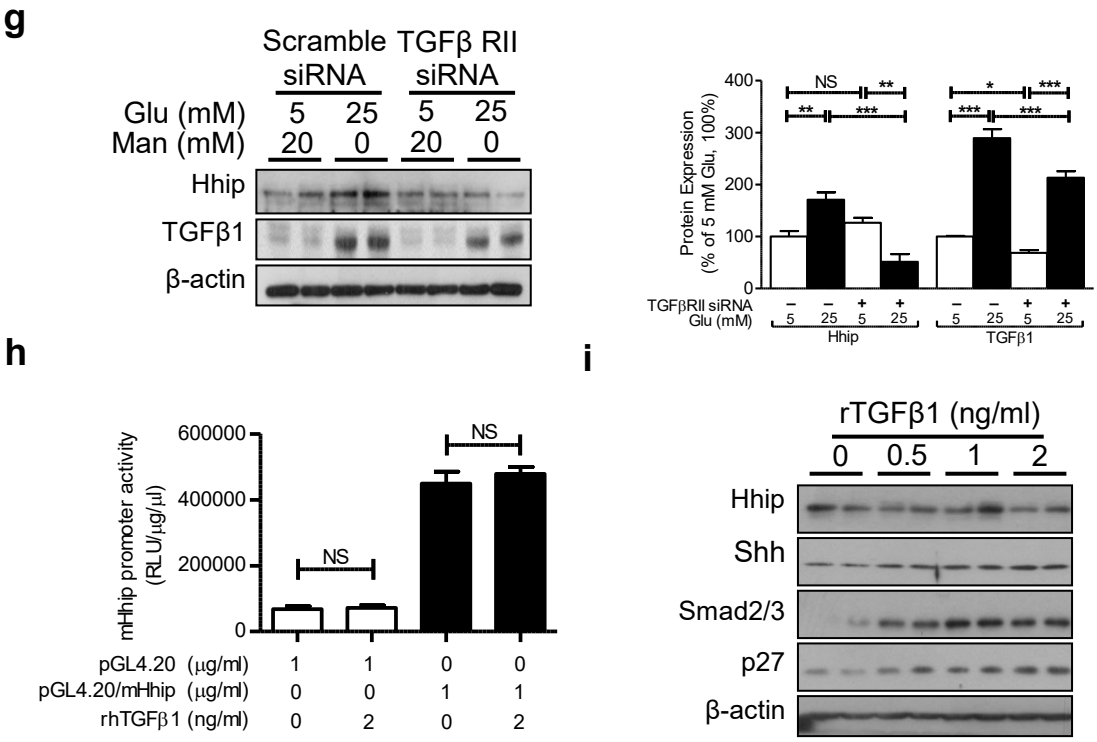

Figure 3-5 The interaction of Hhip and TGFβ1 signaling in mECs *in vitro*. (**a**) rHhip treatment in a time-course on Shh and TGFβ1 protein expression analyzed by WB. ***$P \leq 0.001$ vs. mECs cultured in rHhip (0 ng/ml) at 6 h (100%), NS, non-significant; Values represent the mean ± SEM. (**b**) WB analysis of Hhip siRNA treatment. (**c**) rHhip effect on pGL4.2/rTGFβ1 promoter activity analyzed by luciferase assay. ***$P \leq 0.001$ vs. mECs transfected with pGL4.20 (1 μg/ml) (100%); Values represent the mean ± SEM. (**d**) rHhip effects on TGFβ1 and phosphorylation of Smad 2/3 expression analyzed by WB. (**e**) WB analysis of rHhip ± SB431532 treatment. ***$P \leq 0.001$ vs. mECs cultured in rHhip (0 ng/ml) (100%), NS, non-significant; Values represent the mean ± SEM. (**f**) WB analysis of rHhip ± TGFβII siRNA treatment. ***$P \leq 0.001$ vs. mECs cultured in rHhip (0 ng/ml) (100%), NS, non-significant; Values represent the mean ± SEM. (**g**) WB analysis of TGFβII siRNA treatment. *$P \leq 0.05$; **$P \leq 0.01$; ***$P \leq 0.001$; NS, non-significant vs. mECs cultured in 5 mM glucose without TGFβRII siRNA (100%); Values represent the mean ± SEM. (**h**) rTGFβ1 effect on pGL4.2/mHhip promoter activity analyzed by luciferase assay. NS, non-significant. (**i**) rTGFβ1 dose-dependent effect on protein expression analyzed by WB.

Figure 3-6

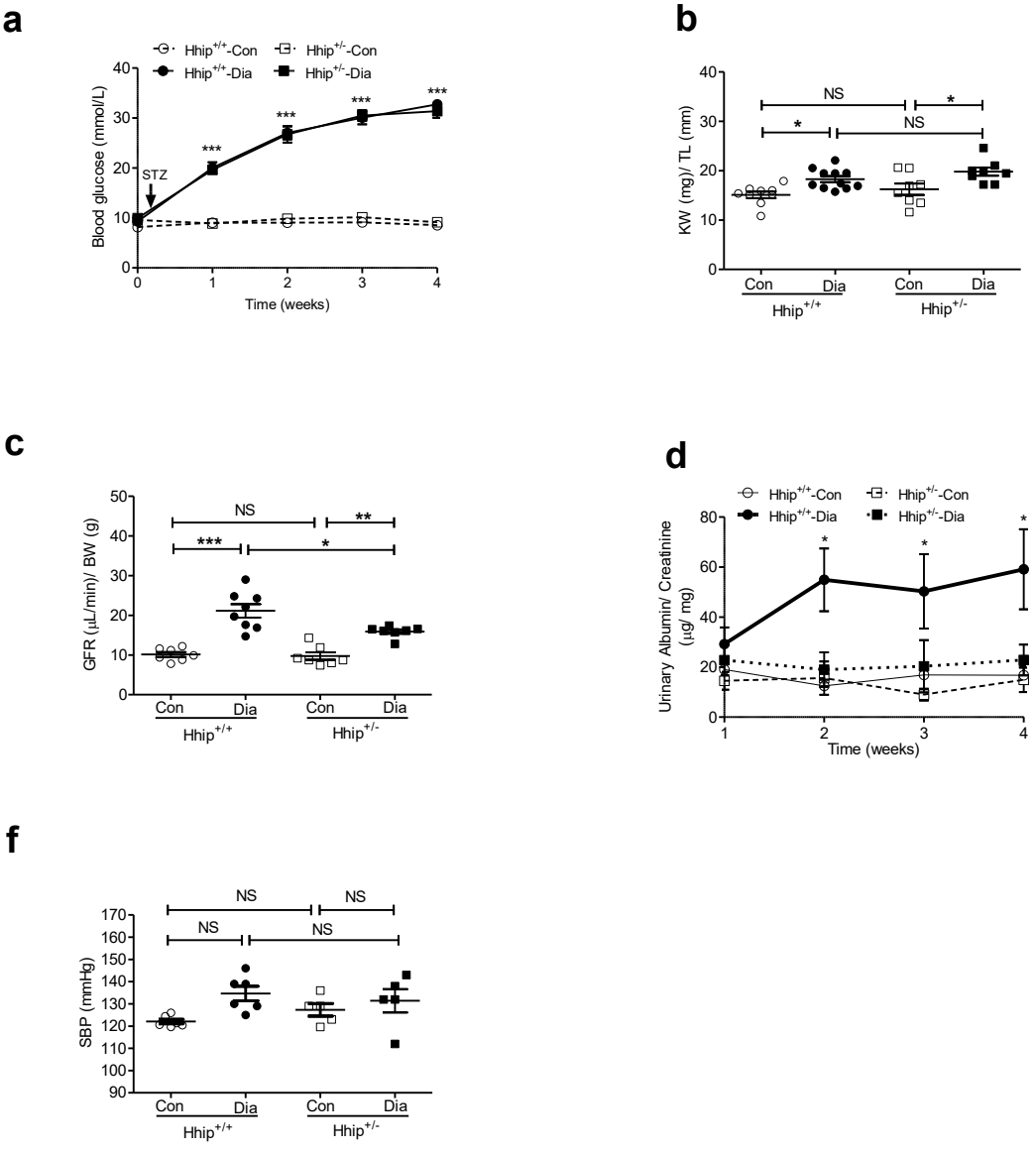
a
Hhip+/+-Con
Hhip+/+-Dia
Hhip+/--Con
Hhip+/--Dia
Blood glucose (mmol/L)
STZ
Time (weeks)
b
KW (mg)/ TL (mm)
NS
Con
Dia
Hhip+/+
Hhip+/-
c
GFR (μL/min)/ BW (g)
d
Urinary Albumin/ Creatinine (μg/ mg)
Time (weeks)
f
SBP (mmHg)

Figure 3-6

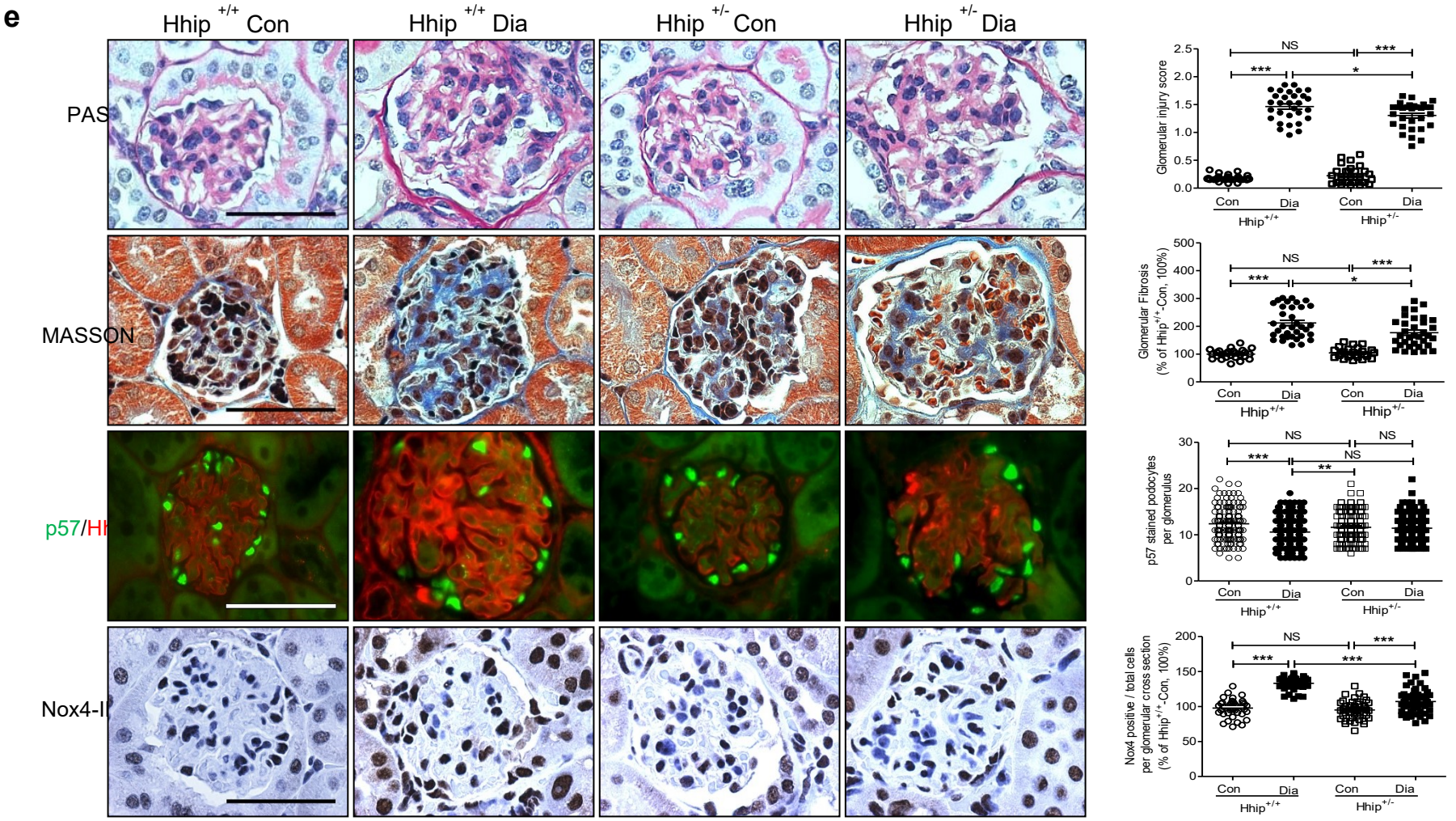
e
Hhip +/+ Con
Hhip +/+ Dia
Hhip +/- Con
Hhip +/- Dia
PAS
MASSON
p57/HI
Nox4-I
Glomerular injury score
Glomerular Fibrosis (% of Hhip+/+-Con, 100%)
p57 stained podocytes per glomerulus
Nox4 positive / total cells per glomerular cross section (% of Hhip+/+-Con, 100%)
NS
***
*
**
Con
Dia
Hhip+/+
Hhip+/-

Figure 3-6 4 weeks of the LDSTZ-induced diabetic model in male $Hhip^{+/+}$ and $Hhip^{+/-}$ mice from the age of 12 to 16 weeks. (**a**) Glycemia measurement. (**b**) The ratio of KW/TL. (**c**) GFR measurement. (**d**) Urinary ACR measurement. (**e**) Renal morphology. PAS staining (scale bar, 50 μm) with semi-quantification of glomerulosclerosis injury score. Grade 0, normal glomeruli; Grade 1, presence of mesangial expansion/ thickening of the basement membrane; Grade 2, mild/moderate segmental hyalinosis/sclerosis involving less than 50% total glomerular area; Masson staining (scale bar, 50 μm) with semi-quantification of glomerular fibrosis; p57/Hhip co-IF staining with semi-quantification of p57 positive stained cells per glomerulus. Nox4-IHC staining with semi-quantification of Nox4 positive stained cells per glomerulus. (**f**) SBP (mmHg) measurement. NS, non-significant vs. $Hhip^{+/+}$-Con; Values represent the mean ± SE

Supplemental Figure 1

Fig. S1a

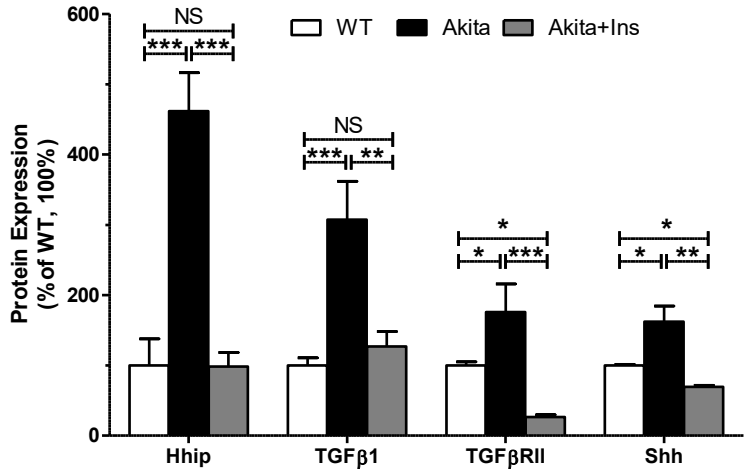

Fig. S1b

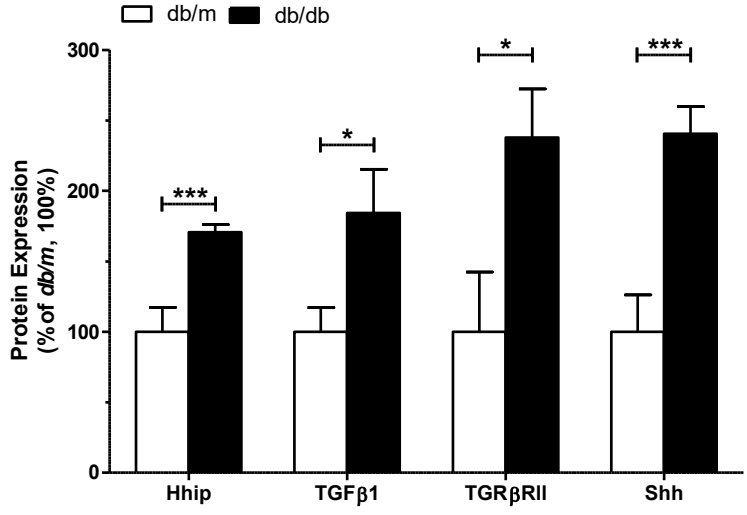

Fig. S1. Semi-quantification of WB analysis in Akita (S1a--Figure 1b) and db/db mice (S1b--Figure 1e). *P ≤ 0.05; **P ≤ 0.01; ***P ≤ 0.001; NS, non-significant; Values represent the mean ± SEM.

Supplemental Figure 2

Fig. S2a

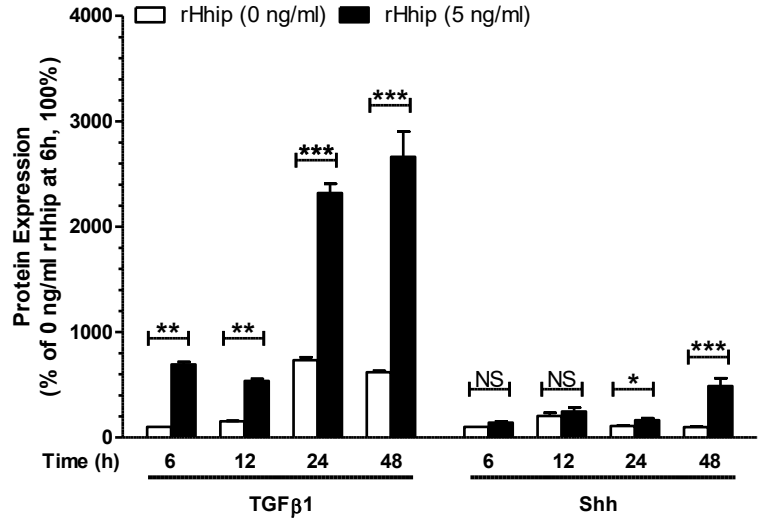

Fig. S2b

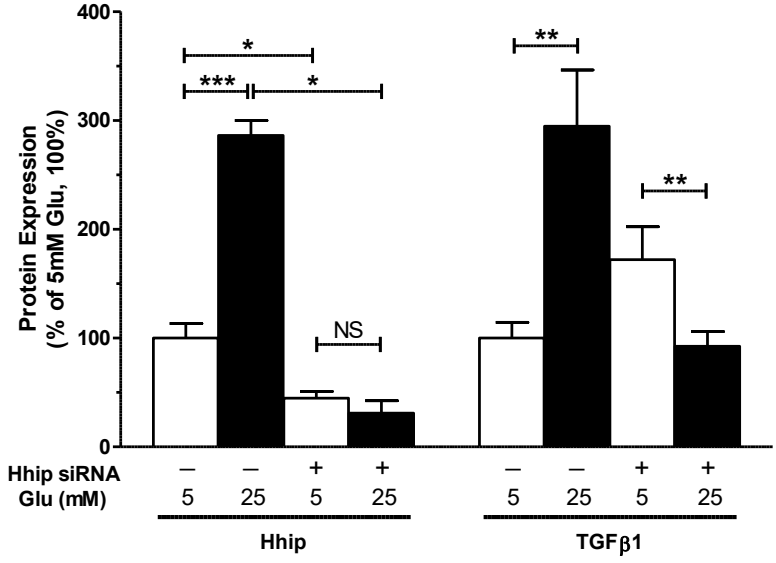

Fig. S2c

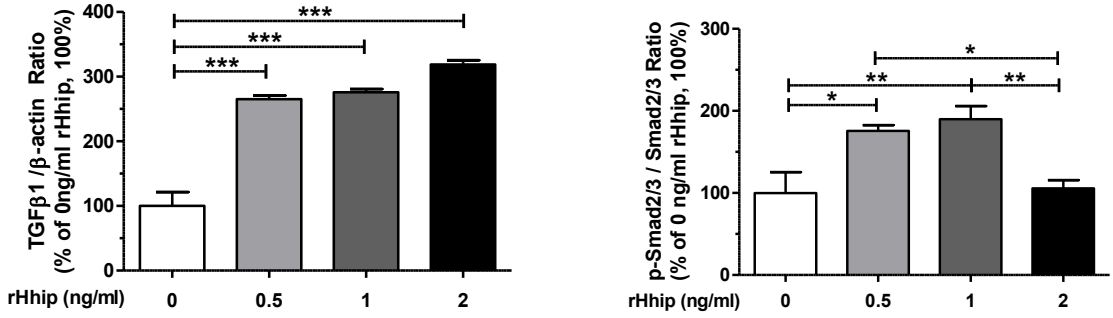

Fig. S2. Semi-quantification of WB analysis (S2a-S2c). S2a (Figure 5a); S2b (Figure 5b) and S2c (Figure 5d), *P ≤ 0.05; **P ≤ 0.01; ***P ≤ 0.001; NS, non-significant. Values represent the mean ± SEM.

Supplemental Figure 3

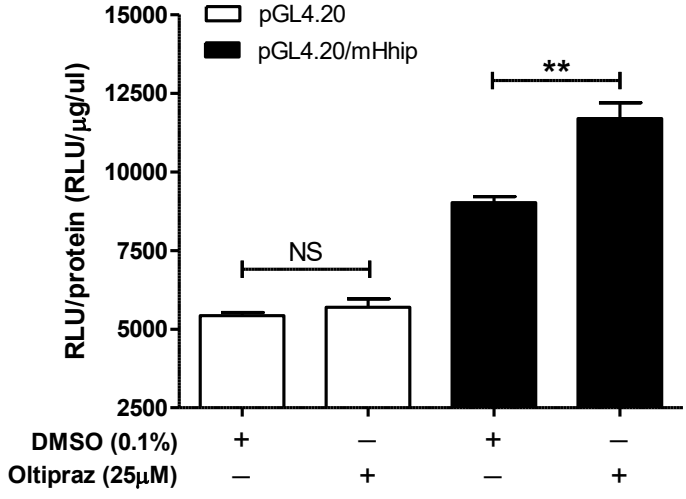

Fig. S3. Oltipraz (an Nrf2 activator, 25μM) stimulates pGL4.20/mHhip promoter activity analyzed by luciferase assay, **P ≤ 0.01; ***P ≤ 0.001; NS, non-significant vs. mECs transfected with pGL4.20 (1μg/ml) (100%); Values represent the mean ± SEM.

3.7 Acknowledgements

This project was supported by grants to SLZ from the Canadian Institutes of Health Research (CIHR PJT153348), Kidney Foundation of Canada (KFOC160019) and Renal Consortium of University of Montreal. Editorial assistance was provided by the CRCHUM's Research Support Office.

Author Contributions

S.L.Z. is the guarantor of this work, had full access to all study data, and takes responsibility for data integrity and the accuracy of data analysis. X.P.Z., S.Y.C., M.C.L., C.S.L., I.C., contributed to research data and discussion; H.L., J.L.C., J.R.I., J.S.D.C., contributed to discussion and reviewed/edited manuscript.

Chapter 4: General Discussion

Maternal diabetes creates a high-risk intrauterine environment that has direct implications in congenital renal malformations. To identify novel proteins or signaling pathways through which maternal diabetes might impair kidney development, we screened the gene profiling of kidneys of the neonatal offspring from diabetic and control mice. The result revealed the expression of Hhip was significantly enhanced in kidneys of offspring from diabetic dams but was normalized in insulin-treated dams, while being highly related to development, signal transduction and proliferation in the analysis of functional pathway clustering. As an antagonist of the hedgehog signal pathway, Hhip binds to Shh which plays a critical role in cell differentiation, growth and tissue patterning in kidney development and kidney fibrosis to attenuate its activity [59, 315]. It is reported that Hhip is predominantly expressed in vascular endothelial cells [270] and cells adjacent to those expressing Shh [59]. While GECs injury is the hallmark of early renal injury in DN, to recognize potential therapeutic targets, it is necessary to identify some novel perceptions on factors that may promote the onset of glomerular endothelial injury in the progression of DN [323-325]. To our knowledge, the functional role of Hhip in both developing and mature kidneys in diabetic condition is barely addressed. The present project focused on the role of Hhip in maternal diabetes modulates kidney formation and GECs injury in the progression of DN.

In our studies, we first confirmed that renal Hhip expression was upregulated by maternal diabetes, then investigated that enhanced Hhip expression targets Shh as well as Pax2 to slow down the mesenchymal-to-epithelial transition, and triggers NF-κB, p53, and TGFβ1 expression, promoting apoptosis and contributes to renal malformations in the young Dia-offspring. We suggest that overexpression of Pax2 attenuates the stimulatory effect of high glucose on Hhip expression in vitro, may form negative autocrine feedback on Hhip regulation.

We next systematically examined Hhip expression in the kidney of several diabetic murine models and observed that Hhip is significantly increased in diabetic GECs, and kidney injury is ameliorated in diabetic $Hhip^{+/-}$ mice. Our data suggest that augmented renal Hhip expression induced by hyperglycemia may play an important role in the progression of DN by promoting apoptosis and fibrosis in GECs.

4.1 The role of Hhip in maternal diabetes modulated nephrogenesis

4.1.1 High glucose induces Hhip expression in the kidney of Dia-offspring and in vitro

Our previous studies established that maternal diabetes might impair UB branching morphogenesis, resulting in renal dysplasia or hypoplasia in a murine model [122, 126]. In the present study, we observed that Hhip expression was significantly upregulated in the neonatal kidneys of Dia-offspring, and Dia-offspring had a smaller neonatal kidney/body weight ratio with smaller kidney size and fewer UB tips in keeping with our previous report [122]. Insulin administration to the diabetic mothers ameliorated the impairment of UB branching. The enhanced Hhip expression was detected in both UB and MM epithelium in the neonatal kidneys of Dia-offspring. Surprisingly, increased intracellular Hhip, as well as secreted Hhip was observed adjacent to UB tips and trunks. Then eventually apparent Hhip expression was detected in glomeruli around 1 week, and was ultimately strongly expressed in GECs at 3 weeks compared to the bare Hhip expression in control groups. Based on these observations, we speculated whether the increased Hhip expression induced by the high glucose, directly or indirectly affects Shh targeting genes which are involved in cell proliferation, cell fate, and cell communication [315, 316].

Since the augmented Hhip expression in the Dia-offspring was seen in both MM epithelium and UB, we performed experiments in vitro applying the MK4 and UB tip cell line to examine the regulation of high glucose on Hhip expression. The data revealed that Hhip expression responded to high glucose in a time- and dose-dependent manner in naive MK4 cells rather than other glucose analogues. Moreover, after giving insulin, the stimulatory effect of high glucose on Hhip gene expression was inhibited in MK4 cells. These data confirmed that high glucose could induce Hhip expression directly in vitro.

Taken together, Hhip was significantly upregulated in the kidney of Dia-offspring.

4.1.2 Hhip induced by hyperglycemia limits mesenchymal-to-epithelial conversion in nephrogenesis

Shh signaling plays a crucial role in cell differentiation, growth, and tissue patterning. In normal kidney development, the balance of Hhip-Shh signaling is essential in the control of a

series of sequential events [52, 55]. In our murine model, compared with the limited Hhip expression in Con-offspring, significantly increased Hhip was detected in kidneys of Dia-offspring with a distribution of progressive transfer from distal (low) to proximal (high) with passage of time, from neonate to 3-weeks old. It is reported that Shh expression pattern gradationally changes from distal (high) to proximal (low) in developing kidneys [52, 55]. As an antagonist, Hhip is supposed to express in cells adjacent to those expressing Shh to attenuate its bioactivity [59], which is consistent with our observations. These data suggest that Hhip might delay or disorient the Shh signaling by inhibiting its activity during kidney formation, and may play other roles later on, in mature diabetic kidney.

Renal hypoplasia is observed in mice in which Shh is specifically inactivated in the ureteric cell lineage. Furthermore, Shh is required for mesenchymal cell proliferation [52]. It is reported that inhibition of Hhip promoter methylation can efficiently inhibit human gastric cancer cell proliferation and migration via antagonizing the activity of Shh singling [349]. Our in vitro study revealed that Shh expression was initially upregulated by high glucose within 24 h, then downregulated rapidly after 48 h in both MK4 and UB tip cells. However, Hhip was progressively increased from 6 h to 48 h. This indicated a potential counterbalance between Hhip and Shh expression in both differentiated UB and MM epithelium, suggesting that this interaction is crucial in kidney development. Although Hhip is a downstream gene of Hh signaling, studies reported that Hhip is downregulated in human aortic endothelial cells forming tubes on Matrigel while the mRNA levels of Shh receptor Ptch1 were increased [270], suggesting that the trend of Hhip expression does not necessarily reflect a general regulation of Hh-responsive genes. To some respect, this is consistent with our results that high D-Glucose stimulates Hhip expression while decreasing Shh expression in MK4 and UB tip cells. It is reported that overexpression of Hhip in cells results in less Shh secreted into the media [308], and Hhip expressed in responding cells inhibits the activation of the Shh signaling pathway [270]. Consistent with these studies, we observed that overexpression of Hhip significantly downregulated Shh expression in MK4 cells in vitro, suggesting augmented renal Hhip induced by hyperglycemia may downregulate Shh expression directly. Thus, the functional role and mechanisms of the counterbalance between Hhip and Shh under the high

glucose intrauterine condition during nephrogenesis in different renal cell lines require further investigation.

Shh directly controls the expression of three distinct classes of genes that are required for normal renal development. They are early kidney inductive and patterning genes (Pax2, Sall1), cell cycle modulators (CyclinD1, N-myc) and the signaling pathway effectors (Gli1, Gli2) [21]. The elevated Hhip expression might affect the expression of Shh-targets genes in the nephrogenic zone, subsequently leading to the onset of abnormal renal morphogenesis. Pax2 as a 'kidney-specific' master gene expressed in both UB and MM, plays a fundamental role in UB branching and mesenchymal-to-epithelial transition during kidney formation [317-319]. Pax2 deficiency results in renal agenesis or hypoplasia with increased cellular apoptosis [14, 15, 17, 320-322]. In the current study, we observed that overexpression of Hhip significantly downregulated Shh as well as Pax2 expression. These data indicated that upregulated Hhip may function both canonically (binding to Shh) and noncanonically (reducing the Shh as well as Pax2 expression) as an antagonist of the Shh pathway to attenuate the signaling, further to slow down the cell proliferation and patterning during kidney formation. In addition, overexpression of Pax2 decreased Hhip gene expression in both UB and MK4, whereas it significantly upregulated Shh, N-myc and $p27^{kip1}$ expression in MK4 cells with high glucose having no further inductive effect. These data suggest that Pax2 may create a negative autocrine feedback loop to prevent the high glucose stimulatory impact on Hhip gene expression, promoting MM cell proliferation genes as a protector.

Bush et al. [218] demonstrated that TGFβ1 in the appropriate matrix context could facilitate "braking" of the branching program as the UB shifts from a rapid branching stage to a stage where branching slows down and eventually stops as a negative feedback. It was also established that TGFβ1 within the rat metanephros inhibits ureteric duct growth and thereby nephron endowment, to shape the structure of the mature kidney by in vitro studies [219, 220]. In our study, we observed that renal TGFβ1 expression was significantly increased in young Dia-offspring with a similar distribution to Hhip expression, suggesting that there may be a functional interaction between Hhip and TGFβ1 in nephrogenesis. We further demonstrated that either overexpression of Hhip or high glucose induced Hhip expression might target

TGFβ1 signaling to phosphorylate Smad2/3 and downstream genes expression. In this regard, Hhip could stimulate TGFβ1 expression to activate the downstream genes directly. Conversely, recombinant TGFβ1 induced Hhip expression dose-dependently, and downregulated $p27^{kip1}$ expression in MK4 cells. Hhip might be involved in a positive feedback loop on TGFβ1 expression as a TGFβ1 signaling target gene. Given that transcription of Hhip and Ptc-1 are both activated by Hh signaling, it is likely that the decrease in Hhip expression in endothelial cells on Matrigel is mediated by a pathway independent of Hh signaling [270]. These evidence leads us to speculate that Hhip and TGFβ1 might interact mutually to slow down the mesenchymal-to-epithelial conversion during nephrogenesis modulated by maternal diabetes. Further studies on the specific interaction between TGFβ1 and Hhip in hyperglycemia condition are required. Moreover, Hhip may influence an individual's susceptibility to COPD by regulating ECM remodeling and cell growth pathways. The expression levels of multiple extracellular matrix-related genes were significantly changed by Hhip shRNAs based on gene enrichment analysis [278]. These observations may also provide supportive evidence for the regulation of Hhip to TGFβ1.

In summary, upregulated renal Hhip induced by hyperglycemia limits mesenchymal-to-epithelial conversion by targeting the expression of Shh as well as its downstream genes directly or indirectly. Heightened Hhip also interacts with TGFβ1signaling to slow down the UB branching, contributing to renal hypoplasia induced by maternal diabetes.

4.1.3 Hhip induces NF-κB (p50/p65) and p53 invoved apoptosis in high glucose milieu

Normally, apoptosis is necessary during kidney development in association with cell proliferation and differentiation. It is already known that NF-κB is a regulator of programmed cell death by apoptosis or necrosis [71]. Overexpression of p53 during kidney development promotes apoptosis and causes smaller kidneys with half the normal number of nephrons in the murine model and defects in the human kidney [78, 79]. Consistent with the reported fact that STZ-induced diabetes during pregnancy leads to a highly significant reduction of nephron numbers in offspring, and high-glucose milieu triggers increased apoptosis in diabetic embryopathy [85, 350-352], our previous studies showed that the neonatal kidneys of Dia-offspring had fewer nephrons on average compared to the controls, with increased apoptosis

detected in collecting tubules, UB and podocyte associated with activation of NF-κB (p50/p65) and p53 pathways [122, 126]. Nie et al. [344] demonstrated that the endothelial apoptosis induced by Hhip was reversed when the Hhip was silenced with an Hhip small interfering RNA. In this regard, we speculated whether or not the increased Hhip expression could activate NF-κB (p50/p65) and p53 signals and subsequently, its impact on kidney development.

We performed experiments using MK4 cells to demonstrate whether the excessive expression of Hhip with or without high glucose could modulate nascent nephron apoptosis by studying the MM cell apoptosis genes NF-κB [p50/p65] and p53. Our data revealed that high glucose stimulated transcriptional NF-κB (p50/p65) and phosphorylation of p53. Overexpression of Hhip alone significantly increased the expression of NF-κB (p50/p65), p53 and phosphorylation of p53. In addition, this activation was further enhanced when the cells were exposed to high glucose. These observations validated the role of Hhip in apoptosis consistent with the previous report [344]. In contrast, overexpression of Pax2 in MK4 cells significantly decreased Hhip and NF-κB (p50/p65) expression, and this inhibition was unaffected by high glucose, suggesting that Pax2 may be involved in a negative feedback loop to prevent the stimulatory effect of high glucose on Hhip gene expression further to inhibit the expression of MM cell apoptosis genes. Consistent with our observation, it is reported that both TGFβ1 and Hhip target NF-κB pathway [215]. In this case, whether there is a possibility that Hhip activates NF-κB through the stimulation of TGFβ1 in a non-canonical signaling pathway, requires further evidence.

Together, Hhip induced by hyperglycemia induces NF-κB [p50/p65], p53 involved apoptosis during nephrogenesis, modulated by maternal diabetes.

4.1.4 Summary and conclusion on the role of Hhip in maternal diabetes modulated nephrogenesis

To summarize, the present studies suggest that maternal diabetes forms a high glucose intrauterine milieu which can induce ectopic Hhip expression in the kidney of the offspring. Heightened Hhip attenuates the Shh pathway and targets TGFβ1signaling to slow down the mesenchymal-to-epithelial conversion, as well as targets NF-κB, p53, promoting apoptosis in

developing kidneys. Overexpression of Pax2 may create negative autocrine feedback on Hhip regulation and attenuate the stimulatory effect of high glucose on Hhip expression in vitro.

In conclusion, elevated Hhip impairs nephrogenisis modulated by maternal diabetes.

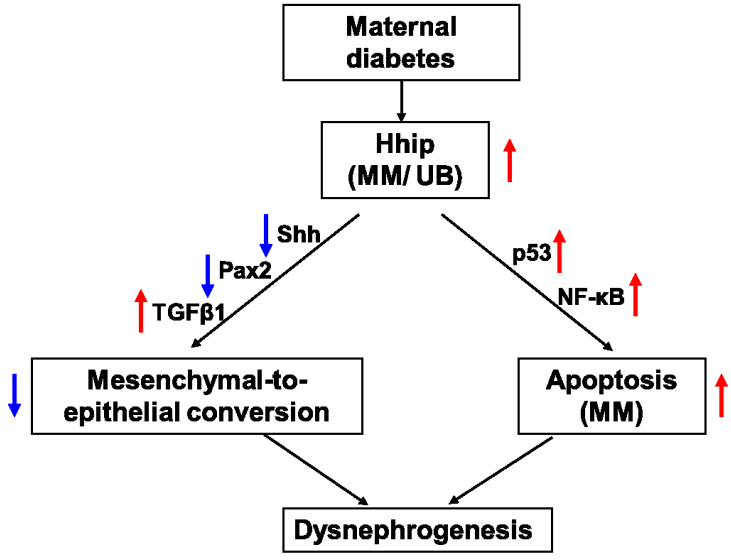

Figure 4-2 Summary of project 1.

4.2 The role of Hhip in the progression of DN

4.2.1 Hyperglycemia induces Hhip expression in mature diabetic kidneys and in vitro

The Hhip expression is barely observed after birth and in normal state, only a limited amount of Hhip is detected in mature ECs [270]. However, it is strongly expressed in GECs at 3 weeks in the kidney of Dia-offspring. Furthermore, increased Hhip expression induced by high glucose was seen in podocytes in vitro, inhibiting synaptopodin protein expression [338]. Since GECs injury is the hallmark of early renal injury in DN, we examined renal Hhip expression in several diabetic murine models (Akita, db/db, and LDSTZ-induced diabetic models). We observed that renal Hhip expression was significantly upregulated in mature diabetic kidneys. Consistent with the reported Hhip expression in endothelial cells [270], the current study showed that hyperglycemia-induced Hhip expression was predominantly expressed in GECs, suggesting that GECs might be the primary source of elevated Hhip

expression in diabetic glomeruli. The increased Hhip expression was normalized in diabetic animals that were given insulin implants. The results strengthen the conclusion that Hhip could be induced by high glucose.

Surprisingly, the Hhip expression has a quite similar pattern to the TGFβ1 expression in GECs of adult diabetic mice. It is well known that TGFβ1 plays a key role in glomerular endothelial cell damage [92, 221], the production of ECM and the development of renal interstitial fibrosis in DN [222-225]. Besides, TGFβ1 has been implicated in DN-related EndoMT transition [226, 227]. We hypothesized that elevated renal Hhip associated with TGFβ1 expression in diabetic condition might play a role in DN progression.

In the present study, high glucose could stimulate pGL4.20/mHhip promoter activity, Hhip mRNA and protein expression in a dose- and time-dependent manner in mECs in vitro. In this regard, we speculate that Hhip expression induced by high glucose may play a direct or indirect role in GECs injury during DN.

Hyperglycemia stimulates the production of AngII and develops oxidative stress in human glomerular endothelium [206]. Conversely, ROS may also work as an upstream signaling molecule of AngII [212]. AngII and ROS mutually stimulate each other in diabetic condition, playing critical roles in the pathogenesis of DN [92, 221, 325]. In the current study, AngII and H_2O_2 increase Hhip expression directly and dose-dependently, and catalase attenuates the stimulatory effect of high glucose on Hhip expression. Conversely, rHhip could promote more ROS generation as a positive feedback regulator, forming a vicious cycle.

Taken together, Hhip was significantly upregulated in the kidney of adult diabetic mice. Hhip could be induced by high glucose and AngII directly or oxidative stress triggered by hyperglycemia and AngII indirectly. Besides, Hhip has positive feedback to ROS.

4.2.2 High glucose-induced Hhip promotes caspase-3 involved apoptosis in GECs during DN

High glucose stimulated ROS overproduction was shown to play a crucial role in endothelial cell senescence [353-355], which is an early sign of vascular complications in diabetes [356]. Evidence also suggests that hyperglycemia leads to oxidative stress and this is the major trigger for tubular and glomerular cells to go into apoptosis in animal models and cell culture

systems [92, 150, 255]. In the current study, rHhip triggered ROS generation in a dose-dependent manner as revealed by DHE and Nox4 IF staining in mECs, and Nox4 inhibitor GKT137831 decreased the ROS generation induced by rHhip, indicating hyperglycemia may trigger ROS generation, probably mediated by Nox4 via upregulated Hhip expression. In contrast, H_2O_2 stimulates Hhip production, suggesting a positive feedback loop of Hhip and ROS.

Susztak et al. [258] have shown that podocyte apoptosis increased markedly with the onset of hyperglycemia in Akita mice and db/db mice, and inhibition of NADPH oxidase-induced ROS formation prevented podocyte apoptosis. Consistent with this report, in the present study, rHhip dose-dependently increased the number of apoptotic cells revealed by TUNEL assay and increased the expression of cleaved caspase-3 in mECs. This is also in keeping with our recent findings [338] where it has been observed that when Hhip expression is ectopically activated and stimulated in podocyte, Hhip could trigger caspase-3 and p53-related apoptotic processes resulting in podocyte loss.

Together, Hhip induced by hyperglycemia promotes ROS generation mediated by Nox4, and the increased ROS conversely trigger more Hhip expression, forming a vicious cycle, further to induce caspase-3 involved apoptosis in GECs during DN.

4.2.3 Hhip promotes EndoMT in DN

EndoMT has been suggested to play an important role in organ fibrosis and cancer progression [247]. Zeisberg et al. presented the first evidence of EndMT in the progress of diabetic kidney fibrosis: they found that about 40% of all fibroblast-specific protein-1-positive and 50% of the α-SMA-positive cells co-labeled with CD31 in the the STZ-induced diabetic kidney [248]. Li et al., using an endothelial-lineage traceable mouse line demonstrated that the number and percentage of endothelial-origin myofibroblasts were significantly higher in STZ-induced DN than in normal kidneys, and EndoMT occurred independently of albuminuria, suggesting that renal endothelial cells may play a role in the initiation of renal interstitial fibrosis through the process of EndoMT [249]. Based on these studies, EndoMT was considered as a potential new player in diabetic renal fibrosis. Many of the factors known to increase as part of the diabetic milieu have been implicated, such as TGFβ1, AngII [246].

TGFβ1 plays a key role in glomerular endothelial cell damage [92, 221], production of extracellular matrix and the development of renal interstitial fibrosis in DN [223-225].

In addition to upregulated Hhip expression, we observed that TGFβ1, TGFβRII, and Shh protein expression were also apparently upregulated in the renal cortex of both Akita and db/db mice. Besides, the increased renal Hhip, TGFβ1, TGFβRII and Shh protein expression in Akita mice were normalized with insulin implants. Hhip plays an essential role in cell apoptosis, angiogenesis, and tumorigenesis [270, 308, 344]. Evidence revealed several mechanisms involving cross-talk among oxidative stress, Shh signaling, and TGFβ1 signaling that have been associated with diabetic retinopathy [345], renal fibrosis [315, 343], and cancer-related epithelial to mesenchymal transition [348]. These observations made us hypothesize that Hhip might interact with ROS and TGFβ1 signaling to promote EndoMT associated with DN-fibrosis.

In the mature kidney, although Shh has been linked to the development of renal fibrosis by regulating the cell cycle progression of myofibroblast progenitors [315, 343], Hhip expression is quiescent after birth and it is unclear whether high glucose promoted Hhip gene expression could function dependently and/or independently via Shh signaling process in DN. Although our present studies revealed that Shh expression was elevated in the renal cortex of diabetic models (Akita and db/db mice), neither high glucose nor rHhip had an impact on Shh protein expression in mECs within 24 hours. However, high glucose stimulated both TGFβ1 and Hhip expression in mECs in vitro. Given that Shh expression gradationally changes from distal (high) to proximal (low) in developing kidneys and modulates tubular-interstitial fibrosis in mature kidneys [52, 55, 315], Hhip might play a role in GECs in diabetic condition independently. The Shh could be upregulated mainly in tubule part close to glomeruli rather than in the glomeruli. These data suggest the regulation of Hhip and TGFβ1 gene expression by high glucose may take place before the regulation of Shh pathway independently in GECs.

TGFβ1 has been implicated in DN-related EndoMT transition [226, 227]. Zhou et al. [278] identified Hhip targets extracellular matrix, and cell growth genes in human bronchial epithelial cells that may contribute to COPD pathogenesis and network modeling demonstrated that the extracellular matrix and cell proliferation genes influenced by Hhip

tended to be interconnected. This is consistent with our in vitro observation that rHhip triggers fibrosis by inducing Fn1, α-SMA, and p27 expression in mECs. The expression of TGFβ1 had a similar distribution to Hhip in kidneys of Akita and db/db mice, and they both co-localized with CD31 in GECs. Besides, both Hhip and TGFβ1 genes had a similar time-course responding to high glucose in mECs in vitro, and rHhip stimulated TGFβ1-Smad2/3 cascade signaling directly. These data suggested Hhip induced by hyperglycemia may be associated with the elevated TGFβ1 expression and there might be a functional interaction between them, during the progression of DN.

We further observed that rHhip triggers TGFβ1 promotor activity in a dose-dependent manner and deficiency of Hhip with a Hhip siRNA attenuated the effect of high glucose on TGFβ1 production. Blocking TGFβ1 receptors (TGFβ1RI by SB431532 or TGFβ1RII by siRNA) attenuated the action of rHhip or high glucose on TGFβ1 expression. In contrast, our data shows that rTGFβ1 can not trigger Hhip promoter and protein expression, but it directly promotes fibrotic gene expression (Shh, α-SMA, and p27) in mECs. At present, we do not have direct evidence regaing how Hhip interacts with TGFβ1. One possibility might be that Hhip acts upstream of TGFβ1 signaling, targeting TGFβ1 gene transcription and translation. Together, these data strongly support the presence of the axis of Hhip-TGFβ1 and its action on DN-related EndoMT.

It's well known that Nox4-derived ROS have a central role in TGFβ1-related EndoMT in renal fibrosis [192]. In contrast to superoxide-generating enzymes Nox1 and Nox2, Nox4 is an H_2O_2-generating enzyme and is highly expressed in murine endothelial cells [341]. We observed increased Nox4 expression in the glomeruli of both Akita and db/db mice and that the stimulatory effect of high glucose on Hhip and TGFβ1 mRNA expression in mECs could be entirely abolished by Nox4 inhibitor GKT137831, demonstrating that Nox4 is involved in the hyperglycemia induced oxidative stress. Furthermore, rHhip dose-dependently elevated ROS generation and Nox4 in mECs, suggesting Nox4-derived ROS triggered by hyperglycemia promotes Hhip expression and subsequently, TGFβ1expression.

Satoh et al. [357] provided direct evidence that AngII plays a crucial role in the development of tubulointerstitial fibrosis. We observed that AngII increased the expression of Hhip protein

and activated the TGFβ1-Smad2/3 cascade in a dose-dependent manner. To some respect, consistent with our observation, Tang et al. observed incubation of primary human aortic endothelial cells (HAECs) in high glucose resulted in the increased expression of FSP-1 and α-SMA, co-localization of CD31 and FSP-1, some spindle-shaped cells and CD31 staining loss. These changes were inhibited by irbesartan treatment, suggesting that the endothelial damage induced by high glucose was mediated via EndoMT by AngII [358]. Our data implies enhanced AngII induced by high glucose may trigger EndoMT via, at least in part, inducing Hhip expression during DN progression.

In summary, Hhip induced by high glucose and AngII directly, or Nox4-derived ROS triggered by hyperglycemia and AngII indirectly may further target TGFβ1-Smad2/3 signaling, to promote EndoMT, initiating the progression of DN.

4.2.4 Deficiency of Hhip ameliorated DN development

To further confirm the role of renal Hhip in the DN progression, we introduced adult $Hhip^{+/-}$mice to extend our investigation, because $Hhip^{-/-}$ mouse were unable to survive after birth due to lung defects. We examined the renal outcomes in male $Hhip^{+/-}$ and $Hhip^{+/+}$ mice undergoing 4 weeks of LDSTZ-induced diabetes from the age of 12 to 16 weeks old. In our study, adult non-diabetic male $Hhip^{+/-}$ mice showed normal renal morphology similar to control $Hhip^{+/+}$ mice. Diabetic $Hhip^{+/+}$ mice had a significantly increased urinary ACR in a time-dependent manner and exhibited some features such as renal hypertrophy, increased GFR, glomerulosclerosis/fibrosis, and podocyte loss, which were consistent with DN progression. In contrast, diabetic $Hhip^{+/-}$ mice had normal urinary ACR with less pronounced renal morphologic and functional changes. These data indicate that the kidney is protected from DN development with a lower level of renal Hhip expression. Evidence revealed that GECs injury might lead to podocyte damage, and that podocyte loss could further aggravate GECs injury, forming a vicious cycle ultimately leading to DN [323-325]. Consistent with these findings, our data indicate that augmented Hhip gene expression in GECs is associated with podocyte transition from a normal morphology to an apoptotic and/or fibrotic-like phenotype, which is further supported by the finding that upregulated Hhip is detected in glomerular cells of patients with focal segmental glomerulosclerosis [338]. However, these

observations are based on the systematic deficiency of Hhip murine model and so specific gain or loss-of-Hhip in GECs would be required further to demonstrate the function of Hhip in the future. Since both full-length Hhip [359-361] and the soluble form of Hhip (sHhip) [362, 363] are functional, the sHhip is potentially able to transfer to other renal cells further triggering cell injury such as apoptosis and fibrosis, aggravating the process of DN. In our study, systolic blood pressure (SBP) remained unchanged among the different groups, with or without 4-weeks of diabetes, which is consistent with other studies in an LDSTZ model [305].

Taken together, the present data suggest that Hhip plays a role in DN and further studies will be required to elucidate the mechanisms of cross-talk between GECs and/or podocyte-derived Hhip functions on EndoMT and how sHhip works between renal cells to aggravate nephropathy in diabetes.

4.2.5 Summary on the role of Hhip in the progression of DN

In summary, the present studies suggest that diabetes mellitus including T1DM and T2DM could induce ectopic Hhip expression in adult kidneys. In Akita and db/db mouse, renal Hhip expression is highly elevated in GECs compared to non-diabetic control littermates. Hyperglycemia promotes ROS generation via Nox4 activation and stimulates renal Hhip expression, causing apoptosis. The elevated renal Hhip gene expression subsequently targets the TGFβ1-Smad2/3 cascade and triggers EndoMT associated with endothelial cell fibrosis in vivo and in vitro. In addition, compared to diabetic wild type controls, LDSTZ-induced diabetic $Hhip^{+/-}$ mice displayed a normal albumin/creatinine ratio with less fibrosis, glomerular hypertrophy, hyperfiltration and fewer podocyte loss in kidneys. Therefore, hyperglycemia induced renal Hhip expression may be associated with glomerular endothelial fibrosis and apoptosis in DN.

In conclusion, Hhip plays a role in DN by promoting glomerular endothelial fibrosis and apoptosis.

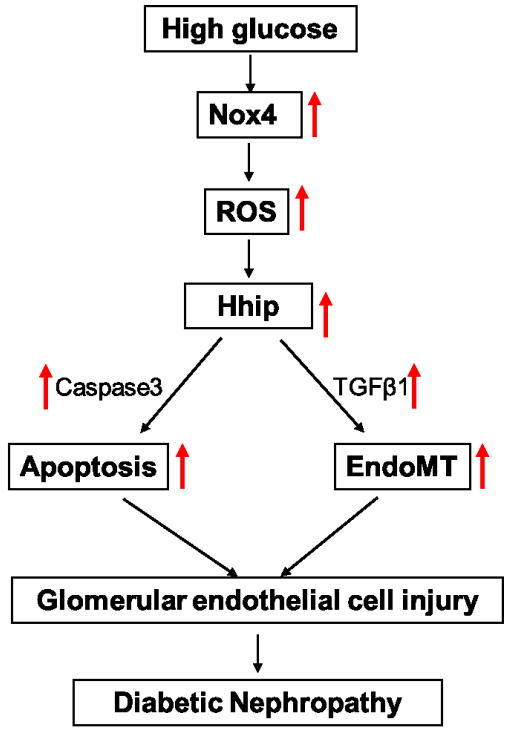

Figure 4-2 Summary of project 2.

4.3 Final conclusion

Collectively, maternal diabetes modulates nephrogenesis in young offspring via elevated Hhip expression. Increased renal Hhip expression in diabetes promotes the progression of nephropathy via mediating glomerular endothelial apoptosis and fibrosis.

Chapter 5: Unpublished Results and Perspectives of Research

In the current study, we observed that Hhip expression was significantly upregulated in the neonatal kidneys of Dia-offspring. Surprisingly, increased intracellular Hhip, as well as secreted Hhip was observed adjacent to UB tips and trunks. Hhip is a 700-residue type I transmembrane protein and both full-length Hhip [359-361], and the soluble form of Hhip (sHhip) [362, 363] can bind Hh ligands to attenuate their activities. However, the precise mechanisms of Hhip protein secretion, cleavage and sequestration are not well addressed [359-361, 363].

5.1 Expression of ADAM17 in vivo and in vitro

According to the prediction in silico tools (www.cleavpredict.sanfordburnham.org; or www.uniprot.org; or http://web.expasy.org/peptide_mass/), the ectodomain of Hhip might be cleaved by multiple enzymes including metallopeptidase and trypsin. ADAM17 belongs to the ADAM (a disintegrin and metalloprotease) family and is the enzyme responsible for cleaving type I transmembrane proteins (i.e., epidermal growth factor receptor (EGF) ligands) and shedding them as functional soluble proteins [364]. *In vivo*, glomerular ADAM17 expression (IF staining) (Figure 5-1A) and urinary ADAM17 activity/Cre ratio (Figure 5-1B) were elevated in both Akita and *db/db* mice as compared to non-diabetic littermates.

(A)

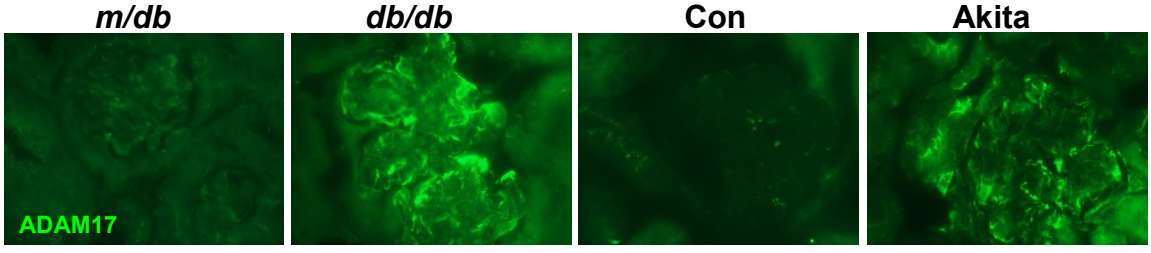

(B)

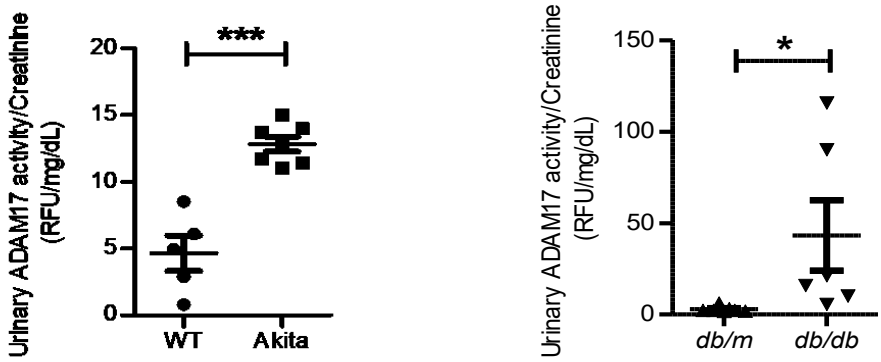

Figure 5-1 ADAM17 expression in the kidney and urinary ADAM17 activity/Cre ratio of Akita and db/db mice at the age of 20 weeks. (A) ADAM17-IF staining in the kidney of Akita and db/db mice. (B) Urinary ADAM17 activity/Cre ratio of Akita and db/db mice.

High glucose stimulated both Hhip and ADAM17 protein expression in mECs in vitro (Figure 5-2A, IF; Figure 5-2B, WB), and the expression of Hhip and ADAM17 were colocalized in mECs. Furthermore, this stimulatory effect on cellular Hhip and medium sHhip could be completely abolished by the ADAM17 inhibitor TAPI2 (Figure 5-3).

(A) **(B)**

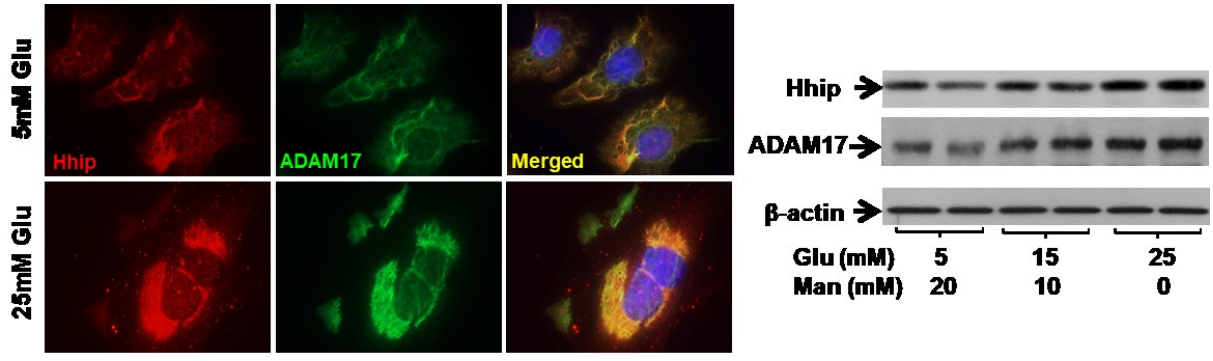

Figure 5-2 Hhip and ADAM17 expression in mECs treated with or without high glucose. (A) Hhip- and ADAM17-IF staining in mECs. (B) WB analysis in mECs.

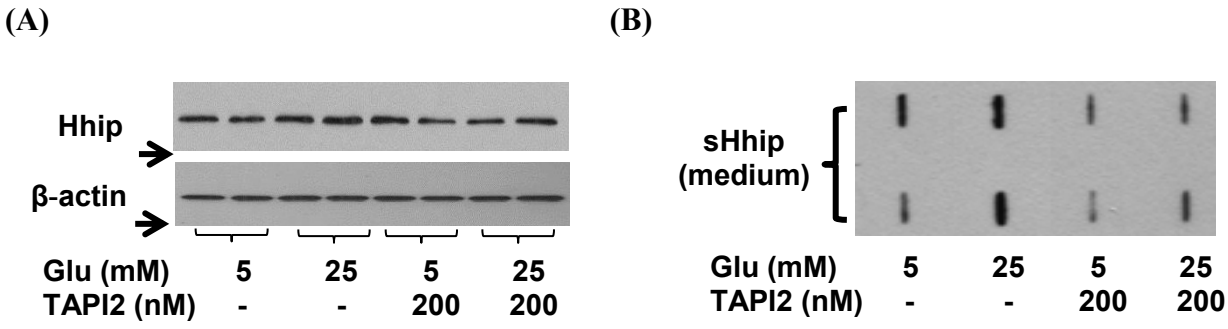

Figure 5-3 Hhip/sHhip expression in mECs with TAPI2. TAPI2 effect on (A) Hhip and (B) sHhip expression in mECs analyzed by WB and dot-blot.

5.2 Epression of soluble Hhip in the urine of diabetic murine model

We measured the urinary Hhip/Cre ratio of the diabetic mice by commercial ELISA kit, showing Hhip was significantly elevated in the urine of both Akita (Figure 5-4 A) and db/db mice (Figure 5-4 B) from the age of 12 weeks to 20 weeks. This data indicates upregulated Hhip in diabetes could be secreted into the urine and is detectable. However, what size of Hhip could be secreted out or whether the full-length Hhip could be cleaved into small pieces requires to be further addressed.

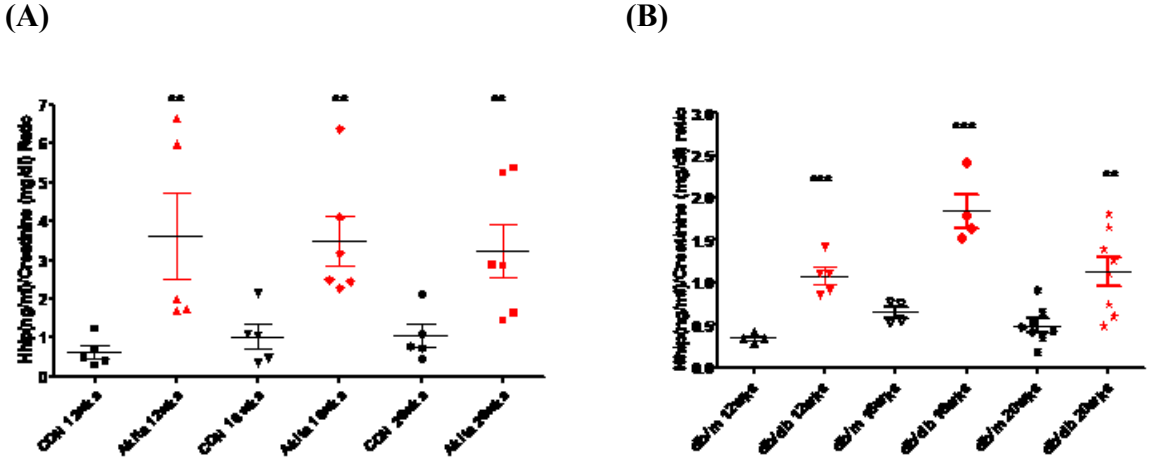

Figure 5-4 Urinary sHhip/Cre ratio in Akita and db/db mice.

Based on these analyses, we speculate that augmented Hhip induced by high glucose could be cleaved into urine by upregulated ADAM17 in diabetic condition, and urinary Hhip might be considered as a biomarker at the early stage of DN when the endothelial cells are injured. So far, we have not conclusively defined the shedding site in Hhip by ADAM17. Further studies on how ADAM17 plays a role in the cleavage of Hhip and the specific effecting site need to be investigated.

Chapter 6: References

References

1. Saxen, L. and H. Sariola, *Early organogenesis of the kidney.* Pediatr Nephrol, 1987. **1**(3): p. 385-92.

2. Boivin, F.J., et al., *The Good and Bad of beta-Catenin in Kidney Development and Renal Dysplasia.* Front Cell Dev Biol, 2015. **3**: p. 81.

3. Aufderheide, E., R. Chiquet-Ehrismann, and P. Ekblom, *Epithelial-mesenchymal interactions in the developing kidney lead to expression of tenascin in the mesenchyme.* J Cell Biol, 1987. **105**(1): p. 599-608.

4. Cebrian, C., et al., *Morphometric index of the developing murine kidney.* Dev Dyn, 2004. **231**(3): p. 601-8.

5. Song, R., S.S. El-Dahr, and I.V. Yosypiv, *Receptor tyrosine kinases in kidney development.* J Signal Transduct, 2011. **2011**: p. 869281.

6. Hughson, M., et al., *Glomerular number and size in autopsy kidneys: the relationship to birth weight.* Kidney Int, 2003. **63**(6): p. 2113-22.

7. Cain, J.E., et al., *Genetics of renal hypoplasia: insights into the mechanisms controlling nephron endowment.* Pediatr Res, 2010. **68**(2): p. 91-8.

8. Hatini, V., et al., *Essential role of stromal mesenchyme in kidney morphogenesis revealed by targeted disruption of Winged Helix transcription factor BF-2.* Genes Dev, 1996. **10**(12): p. 1467-78.

9. Cullen-McEwen, L.A., G. Caruana, and J.F. Bertram, *The where, what and why of the developing renal stroma.* Nephron Exp Nephrol, 2005. **99**(1): p. e1-8.

10. Li, W., S. Hartwig, and N.D. Rosenblum, *Developmental origins and functions of stromal cells in the normal and diseased mammalian kidney.* Dev Dyn, 2014. **243**(7): p. 853-63.

11. Das, A., et al., *Stromal-epithelial crosstalk regulates kidney progenitor cell differentiation.* Nat Cell Biol, 2013. **15**(9): p. 1035-44.

12. Hum, S., et al., *Ablation of the renal stroma defines its critical role in nephron progenitor and vasculature patterning.* PLoS One, 2014. **9**(2): p. e88400.

13. Song, R. and I.V. Yosypiv, *Genetics of congenital anomalies of the kidney and urinary tract.* Pediatr Nephrol, 2011. **26**(3): p. 353-64.

14. Eccles, M.R., et al., *PAX genes in development and disease: the role of PAX2 in urogenital tract development.* Int J Dev Biol, 2002. **46**(4): p. 535-44.

15. Porteous, S., et al., *Primary renal hypoplasia in humans and mice with PAX2 mutations: evidence of increased apoptosis in fetal kidneys of Pax2(1Neu) +/- mutant mice.* Hum Mol Genet, 2000. **9**(1): p. 1-11.

16. Dziarmaga, A., M. Eccles, and P. Goodyer, *Suppression of ureteric bud apoptosis rescues nephron endowment and adult renal function in Pax2 mutant mice.* J Am Soc Nephrol, 2006. **17**(6): p. 1568-75.

17. Torres, M., et al., *Pax-2 controls multiple steps of urogenital development.* Development, 1995. **121**(12): p. 4057-65.

18. Sanyanusin, P., et al., *Mutation of the PAX2 gene in a family with optic nerve colobomas, renal anomalies and vesicoureteral reflux.* Nat Genet, 1995. **9**(4): p. 358-64.

19. Dressler, G.R., et al., *Pax2, a new murine paired-box-containing gene and its expression in the developing excretory system.* Development, 1990. **109**(4): p. 787-95.

20. Brophy, P.D., et al., *Regulation of ureteric bud outgrowth by Pax2-dependent activation of the glial derived neurotrophic factor gene.* Development, 2001. **128**(23): p. 4747-56.

21. Hu, M.C., et al., *GLI3-dependent transcriptional repression of Gli1, Gli2 and kidney patterning genes disrupts renal morphogenesis.* Development, 2006. **133**(3): p. 569-78.

22. Dehbi, M., et al., *The paired-box transcription factor, PAX2, positively modulates expression of the Wilms' tumor suppressor gene (WT1).* Oncogene, 1996. **13**(3): p. 447-53.

23. Torban, E., et al., *PAX2 activates WNT4 expression during mammalian kidney development.* J Biol Chem, 2006. **281**(18): p. 12705-12.

24. Durbec, P., et al., *GDNF signalling through the Ret receptor tyrosine kinase.* Nature, 1996. **381**(6585): p. 789-93.

25. Schuchardt, A., et al., *Defects in the kidney and enteric nervous system of mice lacking the tyrosine kinase receptor Ret.* Nature, 1994. **367**(6461): p. 380-3.

26. Chi, X., et al., *Ret-dependent cell rearrangements in the Wolffian duct epithelium initiate ureteric bud morphogenesis.* Dev Cell, 2009. **17**(2): p. 199-209.

27. Pichel, J.G., et al., *Defects in enteric innervation and kidney development in mice lacking GDNF.* Nature, 1996. **382**(6586): p. 73-6.

28. Sanchez, M.P., et al., *Renal agenesis and the absence of enteric neurons in mice lacking GDNF.* Nature, 1996. **382**(6586): p. 70-3.

29. Skinner, M.A., et al., *Renal aplasia in humans is associated with RET mutations.* Am J Hum Genet, 2008. **82**(2): p. 344-51.

30. Pachnis, V., B. Mankoo, and F. Costantini, *Expression of the c-ret proto-oncogene during mouse embryogenesis.* Development, 1993. **119**(4): p. 1005-17.

31. Schuchardt, A., et al., *Renal agenesis and hypodysplasia in ret-k- mutant mice result from defects in ureteric bud development.* Development, 1996. **122**(6): p. 1919-29.

32. Costantini, F., *Renal branching morphogenesis: concepts, questions, and recent advances.* Differentiation, 2006. **74**(7): p. 402-21.

33. Dressler, G.R., *Advances in early kidney specification, development and patterning.* Development, 2009. **136**(23): p. 3863-74.

34. Kreidberg, J.A., et al., *WT-1 is required for early kidney development.* Cell, 1993. **74**(4): p. 679-91.

35. Moore, A.W., et al., *YAC complementation shows a requirement for Wt1 in the development of epicardium, adrenal gland and throughout nephrogenesis.* Development, 1999. **126**(9): p. 1845-57.

36. Moreau, E., et al., *Regulation of c-ret expression by retinoic acid in rat metanephros: implication in nephron mass control.* Am J Physiol, 1998. **275**(6 Pt 2): p. F938-45.

37. Basson, M.A., et al., *Branching morphogenesis of the ureteric epithelium during kidney development is coordinated by the opposing functions of GDNF and Sprouty1.* Dev Biol, 2006. **299**(2): p. 466-77.

38. Clarke, J.C., et al., *Regulation of c-Ret in the developing kidney is responsive to Pax2 gene dosage.* Hum Mol Genet, 2006. **15**(23): p. 3420-8.

39. Li, X., et al., *Eya protein phosphatase activity regulates Six1-Dach-Eya transcriptional effects in mammalian organogenesis.* Nature, 2003. **426**(6964): p. 247-54.

40. Xu, P.X., et al., *Six1 is required for the early organogenesis of mammalian kidney.* Development, 2003. **130**(14): p. 3085-94.

41. Gong, K.Q., et al., *A Hox-Eya-Pax complex regulates early kidney developmental gene expression.* Mol Cell Biol, 2007. **27**(21): p. 7661-8.

42. Ruf, R.G., et al., *SIX1 mutations cause branchio-oto-renal syndrome by disruption of EYA1-SIX1-DNA complexes.* Proc Natl Acad Sci U S A, 2004. **101**(21): p. 8090-5.

43. Chiang, C., et al., *Cyclopia and defective axial patterning in mice lacking Sonic hedgehog gene function.* Nature, 1996. **383**(6599): p. 407-13.

44. Litingtung, Y., et al., *Sonic hedgehog is essential to foregut development.* Nat Genet, 1998. **20**(1): p. 58-61.

45. Pepicelli, C.V., P.M. Lewis, and A.P. McMahon, *Sonic hedgehog regulates branching morphogenesis in the mammalian lung.* Curr Biol, 1998. **8**(19): p. 1083-6.

46. St-Jacques, B., M. Hammerschmidt, and A.P. McMahon, *Indian hedgehog signaling regulates proliferation and differentiation of chondrocytes and is essential for bone formation.* Genes Dev, 1999. **13**(16): p. 2072-86.

47. Nakano, Y., et al., *A protein with several possible membrane-spanning domains encoded by the Drosophila segment polarity gene patched.* Nature, 1989. **341**(6242): p. 508-13.

48. Hooper, J.E. and M.P. Scott, *The Drosophila patched gene encodes a putative membrane protein required for segmental patterning.* Cell, 1989. **59**(4): p. 751-65.

49. Lum, L., et al., *Hedgehog signal transduction via Smoothened association with a cytoplasmic complex scaffolded by the atypical kinesin, Costal-2.* Mol Cell, 2003. **12**(5): p. 1261-74.

50. Cain, J.E. and N.D. Rosenblum, *Control of mammalian kidney development by the Hedgehog signaling pathway.* Pediatr Nephrol, 2011. **26**(9): p. 1365-71.

51. Cain, J.E., et al., *GLI3 repressor controls nephron number via regulation of Wnt11 and Ret in ureteric tip cells.* PLoS One, 2009. **4**(10): p. e7313.

52. Yu, J., T.J. Carroll, and A.P. McMahon, *Sonic hedgehog regulates proliferation and differentiation of mesenchymal cells in the mouse metanephric kidney.* Development, 2002. **129**(22): p. 5301-12.

53. Bose, J., L. Grotewold, and U. Ruther, *Pallister-Hall syndrome phenotype in mice mutant for Gli3.* Hum Mol Genet, 2002. **11**(9): p. 1129-35.

54. Hall, J.G., et al., *Congenital hypothalamic hamartoblastoma, hypopituitarism, imperforate anus and postaxial polydactyly--a new syndrome? Part I: clinical, causal, and pathogenetic considerations.* Am J Med Genet, 1980. **7**(1): p. 47-74.

55. Ngan, E.S., K.H. Kim, and C.C. Hui, *Sonic Hedgehog Signaling and VACTERL Association.* Mol Syndromol, 2013. **4**(1-2): p. 32-45.

56. Yoo, Y.A., et al., *Sonic hedgehog signaling promotes motility and invasiveness of gastric cancer cells through TGF-beta-mediated activation of the ALK5-Smad 3 pathway.* Carcinogenesis, 2008. **29**(3): p. 480-90.

57. Javelaud, D., et al., *TGF-beta/SMAD/GLI2 signaling axis in cancer progression and metastasis.* Cancer Res, 2011. **71**(17): p. 5606-10.

58. Liu, F., J. Massague, and A. Ruiz i Altaba, *Carboxy-terminally truncated Gli3 proteins associate with Smads.* Nat Genet, 1998. **20**(4): p. 325-6.

59. Chuang, P.T. and A.P. McMahon, *Vertebrate Hedgehog signalling modulated by induction of a Hedgehog-binding protein.* Nature, 1999. **397**(6720): p. 617-21.

60. Yosypiv, I.V., *Hypothesis: a new role for the Renin-Angiotensin system in ureteric bud branching.* Organogenesis, 2004. **1**(1): p. 26-32.

61. Song, R., et al., *Angiotensin II-induced activation of c-Ret signaling is critical in ureteric bud branching morphogenesis.* Mech Dev, 2010. **127**(1-2): p. 21-7.

62. Song, R., T. Van Buren, and I.V. Yosypiv, *Histone deacetylases are critical regulators of the renin-angiotensin system during ureteric bud branching morphogenesis.* Pediatr Res, 2010. **67**(6): p. 573-8.

63. Yosypiv, I.V., *A new role for the renin-angiotensin system in the development of the ureteric bud and renal collecting system.* Keio J Med, 2008. **57**(4): p. 184-9.

64. Gribouval, O., et al., *Mutations in genes in the renin-angiotensin system are associated with autosomal recessive renal tubular dysgenesis.* Nat Genet, 2005. **37**(9): p. 964-8.

65. Niimura, F., V. Kon, and I. Ichikawa, *The renin-angiotensin system in the development of the congenital anomalies of the kidney and urinary tract.* Curr Opin Pediatr, 2006. **18**(2): p. 161-6.

66. Koseki, C., D. Herzlinger, and Q. al-Awqati, *Apoptosis in metanephric development.* J Cell Biol, 1992. **119**(5): p. 1327-33.

67. Coles, H.S., J.F. Burne, and M.C. Raff, *Large-scale normal cell death in the developing rat kidney and its reduction by epidermal growth factor.* Development, 1993. **118**(3): p. 777-84.

68. Ho, J., *The regulation of apoptosis in kidney development: implications for nephron number and pattern?* Front Pediatr, 2014. **2**: p. 128.

69. Nunez, G. and M.F. Clarke, *The Bcl-2 family of proteins: regulators of cell death and survival.* Trends Cell Biol, 1994. **4**(11): p. 399-403.

70. Ewings, K.E., C.M. Wiggins, and S.J. Cook, *Bim and the pro-survival Bcl-2 proteins: opposites attract, ERK repels.* Cell Cycle, 2007. **6**(18): p. 2236-40.

71. Plantivaux, A., et al., *Is there a role for nuclear factor kappaB in tumor necrosis factor-related apoptosis-inducing ligand resistance?* Ann N Y Acad Sci, 2009. **1171**: p. 38-49.

72. Fan, Y., et al., *Regulation of programmed cell death by NF-kappaB and its role in tumorigenesis and therapy.* Adv Exp Med Biol, 2008. **615**: p. 223-50.

73. Barnes, P.J. and M. Karin, *Nuclear factor-kappaB: a pivotal transcription factor in chronic inflammatory diseases.* N Engl J Med, 1997. **336**(15): p. 1066-71.

74. Polyak, K., et al., *Genetic determinants of p53-induced apoptosis and growth arrest.* Genes Dev, 1996. **10**(15): p. 1945-52.

75. Schmid, P., et al., *Expression of p53 during mouse embryogenesis.* Development, 1991. **113**(3): p. 857-65.

76. Carev, D., et al., *Role of mitotic, pro-apoptotic and anti-apoptotic factors in human kidney development.* Pediatr Nephrol, 2006. **21**(5): p. 627-36.

77. Donehower, L.A., et al., *Deficiency of p53 accelerates mammary tumorigenesis in Wnt-1 transgenic mice and promotes chromosomal instability.* Genes Dev, 1995. **9**(7): p. 882-95.

78. Godley, L.A., et al., *Wild-type p53 transgenic mice exhibit altered differentiation of the ureteric bud and possess small kidneys.* Genes Dev, 1996. **10**(7): p. 836-50.

79. Lichnovsky, V., et al., *Differences in p53 and Bcl-2 expression in relation to cell proliferation during the development of human embryos.* Mol Pathol, 1998. **51**(3): p. 131-7.

80. Lynch, S.A. and C. Wright, *Sirenomelia, limb reduction defects, cardiovascular malformation, renal agenesis in an infant born to a diabetic mother.* Clin Dysmorphol, 1997. **6**(1): p. 75-80.

81. Woolf, A.S., *Multiple causes of human kidney malformations.* Arch Dis Child, 1997. **77**(6): p. 471-3.

82. Schedl, A., *Renal abnormalities and their developmental origin.* Nat Rev Genet, 2007. **8**(10): p. 791-802.

83. Keller, G., et al., *Nephron number in patients with primary hypertension.* N Engl J Med, 2003. **348**(2): p. 101-8.

84. Quinlan, J., et al., *A common variant of the PAX2 gene is associated with reduced newborn kidney size.* J Am Soc Nephrol, 2007. **18**(6): p. 1915-21.

85. Amri, K., et al., *Adverse effects of hyperglycemia on kidney development in rats: in vivo and in vitro studies.* Diabetes, 1999. **48**(11): p. 2240-5.

86. Maizels, M. and S.B. Simpson, Jr., *Primitive ducts of renal dysplasia induced by culturing ureteral buds denuded of condensed renal mesenchyme.* Science, 1983. **219**(4584): p. 509-10.

87. Glassberg, K.I., *Normal and abnormal development of the kidney: a clinician's interpretation of current knowledge.* J Urol, 2002. **167**(6): p. 2339-50; discussion 2350-1.

88. Wilson, P.D., *Mouse models of polycystic kidney disease.* Curr Top Dev Biol, 2008. **84**: p. 311-50.

89. BCcampus, *ANATOMY AND PHYSIOLOGY*. Vol. chaper 24.

90. Lehninger, D.L.N.M.M.C.A.L., *Lehninger principles of biochemistry*. 2013, New York: W.H. Freeman and Company.

91. Maughan, R., *Carbohydrate metabolism.* Surgery (Oxford), 2009. **27**(1): p. 6-10.

92. Brownlee, M., *Biochemistry and molecular cell biology of diabetic complications.* Nature, 2001. **414**(6865): p. 813-20.

93. *Diagnosis and classification of diabetes mellitus.* Diabetes Care, 2013. **36 Suppl 1**: p. S67-74.

94. Metzger, B.E. and D.R. Coustan, *Summary and recommendations of the Fourth International Workshop-Conference on Gestational Diabetes Mellitus. The Organizing Committee.* Diabetes Care, 1998. **21 Suppl 2**: p. B161-7.

95. *Hyperglycemia and Adverse Pregnancy Outcome (HAPO) Study: associations with neonatal anthropometrics.* Diabetes, 2009. **58**(2): p. 453-9.

96. Chu, S.Y., et al., *Maternal obesity and risk of gestational diabetes mellitus.* Diabetes Care, 2007. **30**(8): p. 2070-6.

97. Pedersen, J., *Weight and length at birth of infants of diabetic mothers.* Acta Endocrinol (Copenh), 1954. **16**(4): p. 330-42.

98. Catalano, P.M., et al., *The hyperglycemia and adverse pregnancy outcome study: associations of GDM and obesity with pregnancy outcomes.* Diabetes Care, 2012. **35**(4): p. 780-6.

99. Catalano, P.M. and S. Hauguel-De Mouzon, *Is it time to revisit the Pedersen hypothesis in the face of the obesity epidemic?* Am J Obstet Gynecol, 2011. **204**(6): p. 479-87.

100. Radaelli, T., et al., *Differential regulation of genes for fetoplacental lipid pathways in pregnancy with gestational and type 1 diabetes mellitus.* Am J Obstet Gynecol, 2009. **201**(2): p. 209.e1-209.e10.

101. Radaelli, T., et al., *Gestational diabetes induces placental genes for chronic stress and inflammatory pathways.* Diabetes, 2003. **52**(12): p. 2951-8.

102. Vambergue, A. and I. Fajardy, *Consequences of gestational and pregestational diabetes on placental function and birth weight.* World J Diabetes, 2011. **2**(11): p. 196-203.

103. Glinianaia, S.V., et al., *HbA(1c) and birthweight in women with pre-conception type 1 and type 2 diabetes: a population-based cohort study.* Diabetologia, 2012. **55**(12): p. 3193-203.

104. Rosenn, B.M. and M. Miodovnik, *Medical complications of diabetes mellitus in pregnancy.* Clin Obstet Gynecol, 2000. **43**(1): p. 17-31.

105. Yang, J., et al., *Fetal and neonatal outcomes of diabetic pregnancies.* Obstet Gynecol, 2006. **108**(3 Pt 1): p. 644-50.

106. Gonzalez-Gonzalez, N.L., et al., *Factors influencing pregnancy outcome in women with type 2 versus type 1 diabetes mellitus.* Acta Obstet Gynecol Scand, 2008. **87**(1): p. 43-9.

107. Yogev, Y. and O. Langer, *Spontaneous preterm delivery and gestational diabetes: the impact of glycemic control.* Arch Gynecol Obstet, 2007. **276**(4): p. 361-5.

108. Hedderson, M.M., A. Ferrara, and D.A. Sacks, *Gestational diabetes mellitus and lesser degrees of pregnancy hyperglycemia: association with increased risk of spontaneous preterm birth.* Obstet Gynecol, 2003. **102**(4): p. 850-6.

109. Dudley, D.J., *Diabetic-associated stillbirth: incidence, pathophysiology, and prevention.* Obstet Gynecol Clin North Am, 2007. **34**(2): p. 293-307, ix.

110. Balsells, M., et al., *Maternal and fetal outcome in women with type 2 versus type 1 diabetes mellitus: a systematic review and metaanalysis.* J Clin Endocrinol Metab, 2009. **94**(11): p. 4284-91.

111. Cundy, T., et al., *Perinatal mortality in Type 2 diabetes mellitus.* Diabet Med, 2000. **17**(1): p. 33-9.

112. Lean, S.C., et al., *Placental Dysfunction Underlies Increased Risk of Fetal Growth Restriction and Stillbirth in Advanced Maternal Age Women.* Sci Rep, 2017. **7**(1): p. 9677.

113. Pavlinkova, G., J.M. Salbaum, and C. Kappen, *Maternal diabetes alters transcriptional programs in the developing embryo.* BMC Genomics, 2009. **10**: p. 274.

114. Chugh, S.S., E.I. Wallner, and Y.S. Kanwar, *Renal development in high-glucose ambience and diabetic embryopathy.* Semin Nephrol, 2003. **23**(6): p. 583-92.

115. Reece, E.A. and C.J. Homko, *Prepregnancy care and the prevention of fetal malformations in the pregnancy complicated by diabetes.* Clin Obstet Gynecol, 2007. **50**(4): p. 990-7.

116. Langer, O., *Ultrasound biometry evolves in the management of diabetes in pregnancy.* Ultrasound Obstet Gynecol, 2005. **26**(6): p. 585-95.

117. Balsells, M., et al., *Major congenital malformations in women with gestational diabetes mellitus: a systematic review and meta-analysis.* Diabetes Metab Res Rev, 2012. **28**(3): p. 252-7.

118. Dunne, F., et al., *Pregnancy in women with Type 2 diabetes: 12 years outcome data 1990-2002.* Diabet Med, 2003. **20**(9): p. 734-8.

119. Chang, T.I., et al., *Oxidant regulation of gene expression and neural tube development: Insights gained from diabetic pregnancy on molecular causes of neural tube defects.* Diabetologia, 2003. **46**(4): p. 538-45.

120. Zhao, Z., et al., *Caspase-8: a key role in the pathogenesis of diabetic embryopathy.* Birth Defects Res B Dev Reprod Toxicol, 2009. **86**(1): p. 72-7.

121. Simeoni, U., et al., *Adverse consequences of accelerated neonatal growth: cardiovascular and renal issues.* Pediatr Nephrol, 2011. **26**(4): p. 493-508.

122. Tran, S., et al., *Maternal diabetes modulates renal morphogenesis in offspring.* J Am Soc Nephrol, 2008. **19**(5): p. 943-52.

123. Zhang, S.L., et al., *Reactive oxygen species in the presence of high glucose alter ureteric bud morphogenesis.* J Am Soc Nephrol, 2007. **18**(7): p. 2105-15.

124. Kanwar, Y.S., et al., *Hyperglycemia: its imminent effects on mammalian nephrogenesis.* Pediatr Nephrol, 2005. **20**(7): p. 858-66.

125. Kanwar, Y.S., et al., *Renal-specific oxidoreductase biphasic expression under high glucose ambience during fetal versus neonatal development.* Kidney Int, 2005. **68**(4): p. 1670-83.

126. Chen, Y.W., et al., *High glucose promotes nascent nephron apoptosis via NF-kappaB and p53 pathways.* Am J Physiol Renal Physiol, 2011. **300**(1): p. F147-56.

127. Eriksson, U.J., J. Cederberg, and P. Wentzel, *Congenital malformations in offspring of diabetic mothers--animal and human studies.* Rev Endocr Metab Disord, 2003. **4**(1): p. 79-93.

128. New, D.A. and P.T. Coppola, *Effects of different oxygen concentrations on the development of rat embryos in culture.* J Reprod Fertil, 1970. **21**(1): p. 109-18.

129. Djurhuus, R., A.M. Svardal, and E. Thorsen, *Toxicity of hyperoxia and high pressure on C3H/10T1/2 cells and effects on cellular glutathione.* Undersea Hyperb Med, 1998. **25**(1): p. 33-41.

130. Reece, E.A., et al., *The role of free radicals and membrane lipids in diabetes-induced congenital malformations.* J Soc Gynecol Investig, 1998. **5**(4): p. 178-87.

131. Eriksson, U.J. and L.A. Borg, *Diabetes and embryonic malformations. Role of substrate-induced free-oxygen radical production for dysmorphogenesis in cultured rat embryos.* Diabetes, 1993. **42**(3): p. 411-9.

132. Trocino, R.A., et al., *Significance of glutathione depletion and oxidative stress in early embryogenesis in glucose-induced rat embryo culture.* Diabetes, 1995. **44**(8): p. 992-8.

133. Guron, G. and P. Friberg, *An intact renin-angiotensin system is a prerequisite for normal renal development.* J Hypertens, 2000. **18**(2): p. 123-37.

134. Woods, L.L. and R. Rasch, *Perinatal ANG II programs adult blood pressure, glomerular number, and renal function in rats.* Am J Physiol, 1998. **275**(5 Pt 2): p. R1593-9.

135. Konje, J.C., et al., *Human fetal kidney morphometry during gestation and the relationship between weight, kidney morphometry and plasma active renin concentration at birth.* Clin Sci (Lond), 1996. **91**(2): p. 169-75.

136. Kingdom, J.C., et al., *Intrauterine growth restriction is associated with persistent juxtamedullary expression of renin in the fetal kidney.* Kidney Int, 1999. **55**(2): p. 424-9.

137. Chen, Y.W., et al., *Reactive oxygen species and nuclear factor-kappa B pathway mediate high glucose-induced Pax-2 gene expression in mouse embryonic mesenchymal epithelial cells and kidney explants.* Kidney Int, 2006. **70**(9): p. 1607-15.

138. Zhang, S.L., et al., *Pax-2 and N-myc regulate epithelial cell proliferation and apoptosis in a positive autocrine feedback loop.* Pediatr Nephrol, 2007. **22**(6): p. 813-24.

139. Alkayyali, S. and V. Lyssenko, *Genetics of diabetes complications.* Mamm Genome, 2014. **25**(9-10): p. 384-400.

140. Caramori, M.L., P. Fioretto, and M. Mauer, *Low glomerular filtration rate in normoalbuminuric type 1 diabetic patients: an indicator of more advanced glomerular lesions.* Diabetes, 2003. **52**(4): p. 1036-40.

141. Gonzalez Suarez, M.L., et al., *Diabetic nephropathy: Is it time yet for routine kidney biopsy?* World J Diabetes, 2013. **4**(6): p. 245-55.

142. Nathan, D.M., et al., *The effect of intensive treatment of diabetes on the development and progression of long-term complications in insulin-dependent diabetes mellitus.* N Engl J Med, 1993. **329**(14): p. 977-86.

143. *United Kingdom Prospective Diabetes Study (UKPDS). 13: Relative efficacy of randomly allocated diet, sulphonylurea, insulin, or metformin in patients with newly diagnosed non-insulin dependent diabetes followed for three years.* Bmj, 1995. **310**(6972): p. 83-8.

144. Deshpande, A.D., M. Harris-Hayes, and M. Schootman, *Epidemiology of diabetes and diabetes-related complications.* Phys Ther, 2008. **88**(11): p. 1254-64.

145. Adler, A.I., et al., *Development and progression of nephropathy in type 2 diabetes: the United Kingdom Prospective Diabetes Study (UKPDS 64).* Kidney Int, 2003. **63**(1): p. 225-32.

146. Stehouwer, C.D., *Endothelial dysfunction in diabetic nephropathy: state of the art and potential significance for non-diabetic renal disease.* Nephrol Dial Transplant, 2004. **19**(4): p. 778-81.

147. Neri, S., et al., *Early endothelial alterations in non-insulin-dependent diabetes mellitus.* Int J Clin Lab Res, 1998. **28**(2): p. 100-3.

148. Calles-Escandon, J. and M. Cipolla, *Diabetes and endothelial dysfunction: a clinical perspective.* Endocr Rev, 2001. **22**(1): p. 36-52.

149. Arora, M.K. and U.K. Singh, *Molecular mechanisms in the pathogenesis of diabetic nephropathy: an update.* Vascul Pharmacol, 2013. **58**(4): p. 259-71.

150. Nishikawa, T., et al., *Normalizing mitochondrial superoxide production blocks three pathways of hyperglycaemic damage.* Nature, 2000. **404**(6779): p. 787-90.

151. Lushchak, V.I., *Free radicals, reactive oxygen species, oxidative stress and its classification.* Chem Biol Interact, 2014. **224**: p. 164-75.

152. Lushchak, V.I., *Environmentally induced oxidative stress in aquatic animals.* Aquat Toxicol, 2011. **101**(1): p. 13-30.

153. Kashihara, N., et al., *Oxidative stress in diabetic nephropathy.* Curr Med Chem, 2010. **17**(34): p. 4256-69.

154. Forbes, J.M., M.T. Coughlan, and M.E. Cooper, *Oxidative stress as a major culprit in kidney disease in diabetes.* Diabetes, 2008. **57**(6): p. 1446-54.

155. Trumpower, B.L., *The protonmotive Q cycle. Energy transduction by coupling of proton translocation to electron transfer by the cytochrome bc1 complex.* J Biol Chem, 1990. **265**(20): p. 11409-12.

156. Sahoo, S., D.N. Meijles, and P.J. Pagano, *NADPH oxidases: key modulators in aging and age-related cardiovascular diseases?* Clin Sci (Lond), 2016. **130**(5): p. 317-35.

157. Babior, B.M., *NADPH oxidase: an update.* Blood, 1999. **93**(5): p. 1464-76.

158. Etoh, T., et al., *Increased expression of NAD(P)H oxidase subunits, NOX4 and p22phox, in the kidney of streptozotocin-induced diabetic rats and its reversibity by interventive insulin treatment.* Diabetologia, 2003. **46**(10): p. 1428-37.

159. Gorin, Y., et al., *Nox4 NAD(P)H oxidase mediates hypertrophy and fibronectin expression in the diabetic kidney.* J Biol Chem, 2005. **280**(47): p. 39616-26.

160. Evans, J.L., et al., *Oxidative stress and stress-activated signaling pathways: a unifying hypothesis of type 2 diabetes.* Endocr Rev, 2002. **23**(5): p. 599-622.

161. Nam, J.S., et al., *The activation of NF-kappaB and AP-1 in peripheral blood mononuclear cells isolated from patients with diabetic nephropathy.* Diabetes Res Clin Pract, 2008. **81**(1): p. 25-32.

162. Ha, H., et al., *Activation of protein kinase c-delta and c-epsilon by oxidative stress in early diabetic rat kidney.* Am J Kidney Dis, 2001. **38**(4 Suppl 1): p. S204-7.

163. Gorin, Y. and K. Block, *Nox4 and diabetic nephropathy: with a friend like this, who needs enemies?* Free Radic Biol Med, 2013. **61**: p. 130-42.

164. Jha, J.C., et al., *Genetic targeting or pharmacologic inhibition of NADPH oxidase nox4 provides renoprotection in long-term diabetic nephropathy.* J Am Soc Nephrol, 2014. **25**(6): p. 1237-54.

165. Block, K., Y. Gorin, and H.E. Abboud, *Subcellular localization of Nox4 and regulation in diabetes.* Proc Natl Acad Sci U S A, 2009. **106**(34): p. 14385-90.

166. Shah, A., et al., *Thioredoxin-interacting protein mediates high glucose-induced reactive oxygen species generation by mitochondria and the NADPH oxidase, Nox4, in mesangial cells.* J Biol Chem, 2013. **288**(10): p. 6835-48.

167. Eid, A.A., et al., *Sestrin 2 and AMPK connect hyperglycemia to Nox4-dependent endothelial nitric oxide synthase uncoupling and matrix protein expression.* Mol Cell Biol, 2013. **33**(17): p. 3439-60.

168. Thallas-Bonke, V., et al., *Nox-4 deletion reduces oxidative stress and injury by PKC-alpha-associated mechanisms in diabetic nephropathy.* Physiol Rep, 2014. **2**(11).

169. Mariappan, M.M., et al., *High glucose, high insulin, and their combination rapidly induce laminin-beta1 synthesis by regulation of mRNA translation in renal epithelial cells.* Diabetes, 2007. **56**(2): p. 476-85.

170. Iglesias-de la Cruz, M.C., et al., *Effects of high glucose and TGF-beta1 on the expression of collagen IV and vascular endothelial growth factor in mouse podocytes.* Kidney Int, 2002. **62**(3): p. 901-13.

171. Bondi, C.D., et al., *NAD(P)H oxidase mediates TGF-beta1-induced activation of kidney myofibroblasts.* J Am Soc Nephrol, 2010. **21**(1): p. 93-102.

172. Onozato, M.L., et al., *Oxidative stress and nitric oxide synthase in rat diabetic nephropathy: effects of ACEI and ARB.* Kidney Int, 2002. **61**(1): p. 186-94.

173. Giorgi, C., et al., *Redox control of protein kinase C: cell- and disease-specific aspects.* Antioxid Redox Signal, 2010. **13**(7): p. 1051-85.

174. Koya, D., et al., *Characterization of protein kinase C beta isoform activation on the gene expression of transforming growth factor-beta, extracellular matrix components, and prostanoids in the glomeruli of diabetic rats.* J Clin Invest, 1997. **100**(1): p. 115-26.

175. Wei, X.F., et al., *Advanced oxidation protein products induce mesangial cell perturbation through PKC-dependent activation of NADPH oxidase.* Am J Physiol Renal Physiol, 2009. **296**(2): p. F427-37.

176. Satchell, S.C. and F. Braet, *Glomerular endothelial cell fenestrations: an integral component of the glomerular filtration barrier.* Am J Physiol Renal Physiol, 2009. **296**(5): p. F947-56.

177. Molema, G. and W.C. Aird, *Vascular heterogeneity in the kidney.* Semin Nephrol, 2012. **32**(2): p. 145-55.

178. Lai, W.K. and M.Y. Kan, *Homocysteine-Induced Endothelial Dysfunction.* Ann Nutr Metab, 2015. **67**(1): p. 1-12.

179. Pacher P, O.I., Mabley JG, Szabó C. , *Role of nitrosative stress and peroxynitrite in the pathogenesis of diabetic complications. Emerging new therapeutical strategies.* . Curr Med Chem, 2005. **12**(3): p. 267-75.

180. Szabo, C., et al., *Poly(ADP-Ribose) polymerase is activated in subjects at risk of developing type 2 diabetes and is associated with impaired vascular reactivity.* Circulation, 2002. **106**(21): p. 2680-6.

181. Cheng, H., et al., *Improvement of endothelial nitric oxide synthase activity retards the progression of diabetic nephropathy in db/db mice.* Kidney Int, 2012. **82**(11): p. 1176-83.

182. El-Remessy, A.B., et al., *Peroxynitrite mediates diabetes-induced endothelial dysfunction: possible role of Rho kinase activation.* Exp Diabetes Res, 2010. **2010**: p. 247861.

183. Pan, Q., X.H. Yang, and Y.X. Cheng, *Angiotensin II stimulates MCP-1 production in rat glomerular endothelial cells via NAD(P)H oxidase-dependent nuclear factor-kappa B signaling.* Braz J Med Biol Res, 2009. **42**(6): p. 531-6.

184. Jefferson, J.A., S.J. Shankland, and R.H. Pichler, *Proteinuria in diabetic kidney disease: a mechanistic viewpoint.* Kidney Int, 2008. **74**(1): p. 22-36.

185. Eid, A.A., et al., *Mechanisms of podocyte injury in diabetes: role of cytochrome P450 and NADPH oxidases.* Diabetes, 2009. **58**(5): p. 1201-11.

186. Piwkowska, A., et al., *High glucose concentration affects the oxidant-antioxidant balance in cultured mouse podocytes.* J Cell Biochem, 2011. **112**(6): p. 1661-72.

187. Das, R., et al., *Upregulation of mitochondrial Nox4 mediates TGF-beta-induced apoptosis in cultured mouse podocytes.* Am J Physiol Renal Physiol, 2014. **306**(2): p. F155-67.

188. Pagtalunan, M.E., et al., *Podocyte loss and progressive glomerular injury in type II diabetes.* J Clin Invest, 1997. **99**(2): p. 342-8.

189. Iwano, M. and E.G. Neilson, *Mechanisms of tubulointerstitial fibrosis.* Curr Opin Nephrol Hypertens, 2004. **13**(3): p. 279-84.

190. Jha, J.C., et al., *Diabetes and Kidney Disease: Role of Oxidative Stress.* Antioxid Redox Signal, 2016. **25**(12): p. 657-684.

191. Xu, Y., et al., *Role of LOX-1 in Ang II-induced oxidative functional damage in renal tubular epithelial cells.* Int J Mol Med, 2010. **26**(5): p. 679-90.

192. Barnes, J.L. and Y. Gorin, *Myofibroblast differentiation during fibrosis: role of NAD(P)H oxidases.* Kidney Int, 2011. **79**(9): p. 944-56.

193. Budanov, A.V., *Stress-responsive sestrins link p53 with redox regulation and mammalian target of rapamycin signaling.* Antioxid Redox Signal, 2011. **15**(6): p. 1679-90.

194. Chen, J., J.K. Chen, and R.C. Harris, *Angiotensin II induces epithelial-to-mesenchymal transition in renal epithelial cells through reactive oxygen species/Src/caveolin-mediated activation of an epidermal growth factor receptor-extracellular signal-regulated kinase signaling pathway.* Mol Cell Biol, 2012. **32**(5): p. 981-91.

195. Sedeek, M., et al., *Critical role of Nox4-based NADPH oxidase in glucose-induced oxidative stress in the kidney: implications in type 2 diabetic nephropathy.* Am J Physiol Renal Physiol, 2010. **299**(6): p. F1348-58.

196. Lee, D.Y., et al., *Nox4 NADPH oxidase mediates peroxynitrite-dependent uncoupling of endothelial nitric-oxide synthase and fibronectin expression in response to angiotensin II: role of mitochondrial reactive oxygen species.* J Biol Chem, 2013. **288**(40): p. 28668-86.

197. Ohshiro, Y., et al., *Reduction of diabetes-induced oxidative stress, fibrotic cytokine expression, and renal dysfunction in protein kinase Cbeta-null mice.* Diabetes, 2006. **55**(11): p. 3112-20.

198. Attisano, L. and J.L. Wrana, *Signal transduction by the TGF-beta superfamily.* Science, 2002. **296**(5573): p. 1646-7.

199. Massague, J. and R.R. Gomis, *The logic of TGFbeta signaling.* FEBS Lett, 2006. **580**(12): p. 2811-20.

200. Yue, J. and K.M. Mulder, *Requirement of Ras/MAPK pathway activation by transforming growth factor beta for transforming growth factor beta 1 production in a smad-dependent pathway.* J Biol Chem, 2000. **275**(45): p. 35656.

201. Seccia, T.M., et al., *Role of angiotensin II, endothelin-1 and L-type calcium channel in the development of glomerular, tubulointerstitial and perivascular fibrosis.* J Hypertens, 2008. **26**(10): p. 2022-9.

202. Kagami, S., et al., *Angiotensin II stimulates extracellular matrix protein synthesis through induction of transforming growth factor-beta expression in rat glomerular mesangial cells.* J Clin Invest, 1994. **93**(6): p. 2431-7.

203. Sagar, S.K., et al., *Role of expression of endothelin-1 and angiotensin-II and hypoxia-inducible factor-1alpha in the kidney tissues of patients with diabetic nephropathy.* Saudi J Kidney Dis Transpl, 2013. **24**(5): p. 959-64.

204. Liu, F., et al., *Overexpression of angiotensinogen increases tubular apoptosis in diabetes.* J Am Soc Nephrol, 2008. **19**(2): p. 269-80.

205. Pupilli, C., et al., *Angiotensin II stimulates the synthesis and secretion of vascular permeability factor/vascular endothelial growth factor in human mesangial cells.* J Am Soc Nephrol, 1999. **10**(2): p. 245-55.

206. Jaimes, E.A., et al., *Human glomerular endothelium: interplay among glucose, free fatty acids, angiotensin II, and oxidative stress.* Am J Physiol Renal Physiol, 2010. **298**(1): p. F125-32.

207. Hink, U., et al., *Mechanisms underlying endothelial dysfunction in diabetes mellitus.* Circ Res, 2001. **88**(2): p. E14-22.

208. Hsieh, T.J., et al., *High glucose stimulates angiotensinogen gene expression via reactive oxygen species generation in rat kidney proximal tubular cells.* Endocrinology, 2002. **143**(8): p. 2975-85.

209. Kobori, H., et al., *Enhancement of intrarenal angiotensinogen in Dahl salt-sensitive rats on high salt diet.* Hypertension, 2003. **41**(3): p. 592-7.

210. Grishko, V., et al., *Apoptotic cascade initiated by angiotensin II in neonatal cardiomyocytes: role of DNA damage.* Am J Physiol Heart Circ Physiol, 2003. **285**(6): p. H2364-72.

211. Qin, F., et al., *NADPH oxidase is involved in angiotensin II-induced apoptosis in H9C2 cardiac muscle cells: effects of apocynin.* Free Radic Biol Med, 2006. **40**(2): p. 236-46.

212. Xue, H., et al., *H(2)S inhibits hyperglycemia-induced intrarenal renin-angiotensin system activation via attenuation of reactive oxygen species generation.* PLoS One, 2013. **8**(9): p. e74366.

213. Millan, F.A., et al., *Embryonic gene expression patterns of TGF beta 1, beta 2 and beta 3 suggest different developmental functions in vivo.* Development, 1991. **111**(1): p. 131-43.

214. Morikawa, M., R. Derynck, and K. Miyazono, *TGF-beta and the TGF-beta Family: Context-Dependent Roles in Cell and Tissue Physiology.* Cold Spring Harb Perspect Biol, 2016. **8**(5).

215. Akhurst, R.J. and A. Hata, *Targeting the TGFbeta signalling pathway in disease.* Nat Rev Drug Discov, 2012. **11**(10): p. 790-811.

216. Shi, Y. and J. Massague, *Mechanisms of TGF-beta signaling from cell membrane to the nucleus.* Cell, 2003. **113**(6): p. 685-700.

217. Wharton, K. and R. Derynck, *TGFbeta family signaling: novel insights in development and disease.* Development, 2009. **136**(22): p. 3691-7.

218. Bush, K.T., et al., *TGF-beta superfamily members modulate growth, branching, shaping, and patterning of the ureteric bud.* Dev Biol, 2004. **266**(2): p. 285-98.

219. Rogers, S.A., et al., *Metanephric transforming growth factor-beta 1 regulates nephrogenesis in vitro.* Am J Physiol, 1993. **264**(6 Pt 2): p. F996-1002.

220. Clark, A.T., R.J. Young, and J.F. Bertram, *In vitro studies on the roles of transforming growth factor-beta 1 in rat metanephric development.* Kidney Int, 2001. **59**(5): p. 1641-53.

221. Brownlee, M., *The pathobiology of diabetic complications: a unifying mechanism.* Diabetes, 2005. **54**(6): p. 1615-1625.

222. Zimmet, P., K.G. Alberti, and J. Shaw, *Global and societal implications of the diabetes epidemic.* Nature, 2001. **414**(6865): p. 782-7.

223. Hills, C.E. and P.E. Squires, *The role of TGF-beta and epithelial-to mesenchymal transition in diabetic nephropathy.* Cytokine Growth Factor Rev, 2011. **22**(3): p. 131-9.

224. Hills, C.E., et al., *TGFbeta modulates cell-to-cell communication in early epithelial-to-mesenchymal transition.* Diabetologia, 2012. **55**(3): p. 812-24.

225. Lan, H.Y. and A.C. Chung, *TGF-beta/Smad signaling in kidney disease.* Semin Nephrol, 2012. **32**(3): p. 236-43.

226. Li, J., et al., *Blockade of endothelial-mesenchymal transition by a Smad3 inhibitor delays the early development of streptozotocin-induced diabetic nephropathy.* Diabetes, 2010. **59**(10): p. 2612-24.

227. Piera-Velazquez, S., Z. Li, and S.A. Jimenez, *Role of endothelial-mesenchymal transition (EndoMT) in the pathogenesis of fibrotic disorders.* Am J Pathol, 2011. **179**(3): p. 1074-80.

228. Leask, A. and D.J. Abraham, *TGF-beta signaling and the fibrotic response.* Faseb j, 2004. **18**(7): p. 816-27.

229. Wolf, G. and F.N. Ziyadeh, *The role of angiotensin II in diabetic nephropathy: emphasis on nonhemodynamic mechanisms.* Am J Kidney Dis, 1997. **29**(1): p. 153-63.

230. Ziyadeh, F.N., *Mediators of diabetic renal disease: the case for tgf-Beta as the major mediator.* J Am Soc Nephrol, 2004. **15 Suppl 1**: p. S55-7.

231. Ziyadeh, F.N., et al., *Glycated albumin stimulates fibronectin gene expression in glomerular mesangial cells: involvement of the transforming growth factor-beta system.* Kidney Int, 1998. **53**(3): p. 631-8.

232. Baba, M., et al., *Galectin-9 inhibits glomerular hypertrophy in db/db diabetic mice via cell-cycle-dependent mechanisms.* J Am Soc Nephrol, 2005. **16**(11): p. 3222-34.

233. Herbach, N., et al., *Diabetic kidney lesions of GIPRdn transgenic mice: podocyte hypertrophy and thickening of the GBM precede glomerular hypertrophy and glomerulosclerosis.* Am J Physiol Renal Physiol, 2009. **296**(4): p. F819-29.

234. Lee, H.S. and C.Y. Song, *Differential role of mesangial cells and podocytes in TGF-beta-induced mesangial matrix synthesis in chronic glomerular disease.* Histol Histopathol, 2009. **24**(7): p. 901-8.

235. Lee, H.S., *Mechanisms and consequences of TGF-ss overexpression by podocytes in progressive podocyte disease.* Cell Tissue Res, 2012. **347**(1): p. 129-40.

236. Lee, H.S., *Paracrine role for TGF-beta-induced CTGF and VEGF in mesangial matrix expansion in progressive glomerular disease.* Histol Histopathol, 2012. **27**(9): p. 1131-41.

237. Sharma, K. and F.N. Ziyadeh, *Biochemical events and cytokine interactions linking glucose metabolism to the development of diabetic nephropathy.* Semin Nephrol, 1997. **17**(2): p. 80-92.

238. Abbate, M., et al., *Transforming growth factor-beta1 is up-regulated by podocytes in response to excess intraglomerular passage of proteins: a central pathway in progressive glomerulosclerosis.* Am J Pathol, 2002. **161**(6): p. 2179-93.

239. Durvasula, R.V., et al., *Activation of a local tissue angiotensin system in podocytes by mechanical strain.* Kidney Int, 2004. **65**(1): p. 30-9.

240. Dessapt, C., et al., *Mechanical forces and TGFbeta1 reduce podocyte adhesion through alpha3beta1 integrin downregulation.* Nephrol Dial Transplant, 2009. **24**(9): p. 2645-55.

241. Chen, S., et al., *Angiotensin II stimulates alpha3(IV) collagen production in mouse podocytes via TGF-beta and VEGF signalling: implications for diabetic glomerulopathy.* Nephrol Dial Transplant, 2005. **20**(7): p. 1320-8.

242. Kim, J.H., et al., *Activation of the TGF-beta/Smad signaling pathway in focal segmental glomerulosclerosis.* Kidney Int, 2003. **64**(5): p. 1715-21.

243. Tojo, A., K. Asaba, and M.L. Onozato, *Suppressing renal NADPH oxidase to treat diabetic nephropathy.* Expert Opin Ther Targets, 2007. **11**(8): p. 1011-8.

244. Ziyadeh, F.N. and G. Wolf, *Pathogenesis of the podocytopathy and proteinuria in diabetic glomerulopathy.* Curr Diabetes Rev, 2008. **4**(1): p. 39-45.

245. Cheng, H. and R.C. Harris, *Renal endothelial dysfunction in diabetic nephropathy.* Cardiovasc Hematol Disord Drug Targets, 2014. **14**(1): p. 22-33.

246. He, J., et al., *Role of the endothelial-to-mesenchymal transition in renal fibrosis of chronic kidney disease.* Clin Exp Nephrol, 2013. **17**(4): p. 488-97.

247. Zeisberg, M. and E.G. Neilson, *Biomarkers for epithelial-mesenchymal transitions.* J Clin Invest, 2009. **119**(6): p. 1429-37.

248. Zeisberg, E.M., et al., *Fibroblasts in kidney fibrosis emerge via endothelial-to-mesenchymal transition.* J Am Soc Nephrol, 2008. **19**(12): p. 2282-7.

249. Li, J., X. Qu, and J.F. Bertram, *Endothelial-myofibroblast transition contributes to the early development of diabetic renal interstitial fibrosis in streptozotocin-induced diabetic mice.* Am J Pathol, 2009. **175**(4): p. 1380-8.

250. Zeisberg, M. and J.S. Duffield, *Resolved: EMT produces fibroblasts in the kidney.* J Am Soc Nephrol, 2010. **21**(8): p. 1247-53.

251. Johnson, A. and L.A. DiPietro, *Apoptosis and angiogenesis: an evolving mechanism for fibrosis.* Faseb j, 2013. **27**(10): p. 3893-901.

252. Wagener, F.A., et al., *The role of reactive oxygen species in apoptosis of the diabetic kidney.* Apoptosis, 2009. **14**(12): p. 1451-8.

253. Zou, H., et al., *Apaf-1, a human protein homologous to C. elegans CED-4, participates in cytochrome c-dependent activation of caspase-3.* Cell, 1997. **90**(3): p. 405-13.

254. Wali, J.A., S.L. Masters, and H.E. Thomas, *Linking metabolic abnormalities to apoptotic pathways in Beta cells in type 2 diabetes.* Cells, 2013. **2**(2): p. 266-83.

255. Ha, H., et al., *Role of reactive oxygen species in the pathogenesis of diabetic nephropathy.* Diabetes Res Clin Pract, 2008. **82 Suppl 1**: p. S42-5.

256. Kang, B.P., et al., *High glucose promotes mesangial cell apoptosis by oxidant-dependent mechanism.* Am J Physiol Renal Physiol, 2003. **284**(3): p. F455-66.

257. Droge, W., *Free radicals in the physiological control of cell function.* Physiol Rev, 2002. **82**(1): p. 47-95.

258. Susztak, K., et al., *Glucose-induced reactive oxygen species cause apoptosis of podocytes and podocyte depletion at the onset of diabetic nephropathy.* Diabetes, 2006. **55**(1): p. 225-33.

259. Brownlee, M., *Preventing kidney cell suicide.* Nat Med, 2007. **13**(11): p. 1284-5.

260. Isermann, B., et al., *Activated protein C protects against diabetic nephropathy by inhibiting endothelial and podocyte apoptosis.* Nat Med, 2007. **13**(11): p. 1349-58.

261. Verzola, D., et al., *Taurine prevents apoptosis induced by high ambient glucose in human tubule renal cells.* J Investig Med, 2002. **50**(6): p. 443-51.

262. Ortiz, A., F.N. Ziyadeh, and E.G. Neilson, *Expression of apoptosis-regulatory genes in renal proximal tubular epithelial cells exposed to high ambient glucose and in diabetic kidneys.* J Investig Med, 1997. **45**(2): p. 50-6.

263. Allen, D.A., et al., *High glucose-induced oxidative stress causes apoptosis in proximal tubular epithelial cells and is mediated by multiple caspases.* Faseb j, 2003. **17**(8): p. 908-10.

264. Bishop, B., et al., *Structural insights into hedgehog ligand sequestration by the human hedgehog-interacting protein HHIP.* Nat Struct Mol Biol, 2009. **16**(7): p. 698-703.

265. Bosanac, I., et al., *The structure of SHH in complex with HHIP reveals a recognition role for the Shh pseudo active site in signaling.* Nat Struct Mol Biol, 2009. **16**(7): p. 691-7.

266. Kwong, L., M.F. Bijlsma, and H. Roelink, *Shh-mediated degradation of Hhip allows cell autonomous and non-cell autonomous Shh signalling.* Nat Commun, 2014. **5**: p. 4849.

267. Lao, T., et al., *Hhip haploinsufficiency sensitizes mice to age-related emphysema.* Proc Natl Acad Sci U S A, 2016. **113**(32): p. E4681-7.

268. Kawahira, H., et al., *Combined activities of hedgehog signaling inhibitors regulate pancreas development.* Development, 2003. **130**(20): p. 4871-9.

269. Chuang, P.T., T. Kawcak, and A.P. McMahon, *Feedback control of mammalian Hedgehog signaling by the Hedgehog-binding protein, Hip1, modulates Fgf signaling during branching morphogenesis of the lung.* Genes Dev, 2003. **17**(3): p. 342-7.

270. Olsen, C.L., et al., *Hedgehog-interacting protein is highly expressed in endothelial cells but down-regulated during angiogenesis and in several human tumors.* BMC Cancer, 2004. **4**: p. 43.

271. Zhou, X., et al., *Identification of a chronic obstructive pulmonary disease genetic determinant that regulates HHIP.* Hum Mol Genet, 2012. **21**(6): p. 1325-35.

272. Wilk, J.B., et al., *A genome-wide association study of pulmonary function measures in the Framingham Heart Study.* PLoS Genet, 2009. **5**(3): p. e1000429.

273. Pillai, S.G., et al., *A genome-wide association study in chronic obstructive pulmonary disease (COPD): identification of two major susceptibility loci.* PLoS Genet, 2009. **5**(3): p. e1000421.

274. Kayed, H., et al., *Localization of the human hedgehog-interacting protein (Hip) in the normal and diseased pancreas.* Mol Carcinog, 2005. **42**(4): p. 183-92.

275. Tada, M., et al., *Down-regulation of hedgehog-interacting protein through genetic and epigenetic alterations in human hepatocellular carcinoma.* Clin Cancer Res, 2008. **14**(12): p. 3768-76.

276. Tojo, M., et al., *Expression of a sonic hedgehog signal transducer, hedgehog-interacting protein, by human basal cell carcinoma.* Br J Dermatol, 2002. **146**(1): p. 69-73.

277. Wang, B., et al., *Association of HHIP polymorphisms with COPD and COPD-related phenotypes in a Chinese Han population.* Gene, 2013. **531**(1): p. 101-5.

278. Zhou, X., et al., *Gene expression analysis uncovers novel hedgehog interacting protein (HHIP) effects in human bronchial epithelial cells.* Genomics, 2013. **101**(5): p. 263-72.

279. Shahi, M.H., et al., *Human hedgehog interacting protein expression and promoter methylation in medulloblastoma cell lines and primary tumor samples.* J Neurooncol, 2011. **103**(2): p. 287-96.

280. Katoh, Y. and M. Katoh, *Comparative genomics on HHIP family orthologs.* Int J Mol Med, 2006. **17**(2): p. 391-5.

281. Loulier, K., M. Ruat, and E. Traiffort, *Analysis of hedgehog interacting protein in the brain and its expression in nitric oxide synthase-positive cells.* Neuroreport, 2005. **16**(17): p. 1959-62.

282. Cornesse, Y., T. Pieler, and T. Hollemann, *Olfactory and lens placode formation is controlled by the hedgehog-interacting protein (Xhip) in Xenopus.* Dev Biol, 2005. **277**(2): p. 296-315.

283. Wilson, G.L. and E.H. Leiter, *Streptozotocin interactions with pancreatic beta cells and the induction of insulin-dependent diabetes.* Curr Top Microbiol Immunol, 1990. **156**: p. 27-54.

284. Bolzan, A.D. and M.S. Bianchi, *Genotoxicity of streptozotocin.* Mutat Res, 2002. **512**(2-3): p. 121-34.

285. Like, A.A., et al., *Streptozotocin-induced pancreatic insulitis in mice. Morphologic and physiologic studies.* Lab Invest, 1978. **38**(4): p. 470-86.

286. Susztak, K., et al., *Genomic strategies for diabetic nephropathy.* J Am Soc Nephrol, 2003. **14**(8 Suppl 3): p. S271-8.

287. Vuguin, P.M., *Animal models for small for gestational age and fetal programming of adult disease.* Horm Res, 2007. **68**(3): p. 113-23.

288. Caluwaerts, S., et al., *Is low-dose streptozotocin in rats an adequate model for gestational diabetes mellitus?* J Soc Gynecol Investig, 2003. **10**(4): p. 216-21.

289. Abdel-Reheim E. S., A.-E.A.A., Hosni A. A. , *Fatty-sucrosed diet/minimal dose of streptozotocin-treated rat: a novel model of gestational diabetes mellitus, metabolic and inflammatory insight.* Journal of Diabetes & Metabolism, 2014. **5**: p. 430.

290. Han, J., et al., *Rat maternal diabetes impairs pancreatic beta-cell function in the offspring.* Am J Physiol Endocrinol Metab, 2007. **293**(1): p. E228-36.

291. Wang, J., et al., *A mutation in the insulin 2 gene induces diabetes with severe pancreatic beta-cell dysfunction in the Mody mouse.* J Clin Invest, 1999. **103**(1): p. 27-37.

292. Gurley, S.B., et al., *Influence of genetic background on albuminuria and kidney injury in Ins2(+/C96Y) (Akita) mice.* Am J Physiol Renal Physiol, 2010. **298**(3): p. F788-95.

293. Yoshioka, M., et al., *A novel locus, Mody4, distal to D7Mit189 on chromosome 7 determines early-onset NIDDM in nonobese C57BL/6 (Akita) mutant mice.* Diabetes, 1997. **46**(5): p. 887-94.

294. Alpers, C.E. and K.L. Hudkins, *Mouse models of diabetic nephropathy.* Curr Opin Nephrol Hypertens, 2011. **20**(3): p. 278-84.

295. Kitada, M., Y. Ogura, and D. Koya, *Rodent models of diabetic nephropathy: their utility and limitations.* Int J Nephrol Renovasc Dis, 2016. **9**: p. 279-290.

296. Shi, Y., et al., *Angiotensin-(1-7) prevents systemic hypertension, attenuates oxidative stress and tubulointerstitial fibrosis, and normalizes renal angiotensin-converting enzyme 2 and Mas receptor expression in diabetic mice.* Clin Sci (Lond), 2015. **128**(10): p. 649-63.

297. Fang, F., et al., *Deletion of the gene for adiponectin accelerates diabetic nephropathy in the Ins2 (+/C96Y) mouse.* Diabetologia, 2015. **58**(7): p. 1668-78.

298. Fujita, H., et al., *Modulation of renal superoxide dismutase by telmisartan therapy in C57BL/6-Ins2(Akita) diabetic mice.* Hypertens Res, 2012. **35**(2): p. 213-20.

299. Lee, G.H., et al., *Abnormal splicing of the leptin receptor in diabetic mice.* Nature, 1996. **379**(6566): p. 632-5.

300. Lee, S.M. and R. Bressler, *Prevention of diabetic nephropathy by diet control in the db/db mouse.* Diabetes, 1981. **30**(2): p. 106-11.

301. Sharma, K., P. McCue, and S.R. Dunn, *Diabetic kidney disease in the db/db mouse.* Am J Physiol Renal Physiol, 2003. **284**(6): p. F1138-44.

302. Sharma, K., et al., *Adiponectin regulates albuminuria and podocyte function in mice.* J Clin Invest, 2008. **118**(5): p. 1645-56.

303. Lambin, S., et al., *Adipose tissue in offspring of Lepr(db/+) mice: early-life environment vs. genotype.* Am J Physiol Endocrinol Metab, 2007. **292**(1): p. E262-71.

304. Ishizuka, T., et al., *Effects of overexpression of human GLUT4 gene on maternal diabetes and fetal growth in spontaneous gestational diabetic C57BLKS/J Lepr(db/+) mice.* Diabetes, 1999. **48**(5): p. 1061-9.

305. Breyer, M.D., et al., *Mouse models of diabetic nephropathy.* J Am Soc Nephrol, 2005. **16**(1): p. 27-45.

306. Holemans, K., L. Aerts, and F.A. Van Assche, *Fetal growth restriction and consequences for the offspring in animal models.* J Soc Gynecol Investig, 2003. **10**(7): p. 392-9.

307. Chang, S.Y., et al., *Catalase prevents maternal diabetes-induced perinatal programming via the Nrf2-HO-1 defense system.* Diabetes, 2012. **61**(10): p. 2565-74.

308. Zeng, X., et al., *A freely diffusible form of Sonic hedgehog mediates long-range signalling.* Nature, 2001. **411**(6838): p. 716-20.

309. Yosypiv, I.V., *Renin-angiotensin system in ureteric bud branching morphogenesis: insights into the mechanisms.* Pediatr Nephrol, 2011. **26**(9): p. 1499-512.

310. Yosypiv, I.V., *Congenital anomalies of the kidney and urinary tract: a genetic disorder?* Int J Nephrol, 2012. **2012**: p. 909083.

311. Srinivas, S., et al., *Expression of green fluorescent protein in the ureteric bud of transgenic mice: a new tool for the analysis of ureteric bud morphogenesis.* Dev Genet, 1999. **24**(3-4): p. 241-51.

312. Watanabe, T. and F. Costantini, *Real-time analysis of ureteric bud branching morphogenesis in vitro.* Dev Biol, 2004. **271**(1): p. 98-108.

313. Valerius, M.T., et al., *Microarray analysis of novel cell lines representing two stages of metanephric mesenchyme differentiation.* Mech Dev, 2002. **112**(1-2): p. 219-32.

314. Barasch, J., et al., *A ureteric bud cell line induces nephrogenesis in two steps by two distinct signals.* Am J Physiol, 1996. **271**(1 Pt 2): p. F50-61.

315. Ding, H., et al., *Sonic hedgehog signaling mediates epithelial-mesenchymal communication and promotes renal fibrosis.* J Am Soc Nephrol, 2012. **23**(5): p. 801-13.

316. Katoh, Y. and M. Katoh, *Hedgehog target genes: mechanisms of carcinogenesis induced by aberrant hedgehog signaling activation.* Curr Mol Med, 2009. **9**(7): p. 873-86.

317. Bouchard, M., et al., *Nephric lineage specification by Pax2 and Pax8.* Genes Dev, 2002. **16**(22): p. 2958-70.

318. Dressler, G.R. and E.C. Douglass, *Pax-2 is a DNA-binding protein expressed in embryonic kidney and Wilms tumor.* Proc Natl Acad Sci U S A, 1992. **89**(4): p. 1179-83.

319. Dressler, G.R., *Pax-2, kidney development, and oncogenesis.* Med Pediatr Oncol, 1996. **27**(5): p. 440-4.

320. Dziarmaga, A., et al., *Ureteric bud apoptosis and renal hypoplasia in transgenic PAX2-Bax fetal mice mimics the renal-coloboma syndrome.* J Am Soc Nephrol, 2003. **14**(11): p. 2767-74.

321. Favor, J., et al., *The mouse Pax2(1Neu) mutation is identical to a human PAX2 mutation in a family with renal-coloboma syndrome and results in developmental defects of the brain, ear, eye, and kidney.* Proc Natl Acad Sci U S A, 1996. **93**(24): p. 13870-5.

322. Maeshima, A., et al., *Involvement of Pax-2 in the action of activin A on tubular cell regeneration.* J Am Soc Nephrol, 2002. **13**(12): p. 2850-9.

323. Fu, J., et al., *Glomerular endothelial cell injury and cross talk in diabetic kidney disease.* Am J Physiol Renal Physiol, 2015. **308**(4): p. F287-97.

324. Currie, G., G. McKay, and C. Delles, *Biomarkers in diabetic nephropathy: Present and future.* World J Diabetes, 2014. **5**(6): p. 763-76.

325. Reddy, M.A., E. Zhang, and R. Natarajan, *Epigenetic mechanisms in diabetic complications and metabolic memory.* Diabetologia, 2015. **58**(3): p. 443-55.

326. Shaw, J.E., R.A. Sicree, and P.Z. Zimmet, *Global estimates of the prevalence of diabetes for 2010 and 2030.* Diabetes Res Clin Pract, 2010. **87**(1): p. 4-14.

327. Coulombe, J., et al., *Hedgehog interacting protein in the mature brain: membrane-associated and soluble forms.* Mol Cell Neurosci, 2004. **25**(2): p. 323-33.

328. Holtz, A.M., et al., *Secreted HHIP1 interacts with heparan sulfate and regulates Hedgehog ligand localization and function.* J Cell Biol, 2015. **209**(5): p. 739-57.

329. Landsman, L., A. Parent, and M. Hebrok, *Elevated Hedgehog/Gli signaling causes beta-cell dedifferentiation in mice.* Proc Natl Acad Sci U S A, 2011. **108**(41): p. 17010-5.

330. Zhao, X.P., et al., *Maternal diabetes modulates kidney formation in murine progeny: the role of hedgehog interacting protein (HHIP).* Diabetologia, 2014. **57**(9): p. 1986-96.

331. Abdo, S., et al., *Catalase overexpression prevents nuclear factor erythroid 2-related factor 2 stimulation of renal angiotensinogen gene expression, hypertension, and kidney injury in diabetic mice.* Diabetes, 2014. **63**(10): p. 3483-96.

332. Lo, C.S., et al., *Dual RAS blockade normalizes angiotensin-converting enzyme-2 expression and prevents hypertension and tubular apoptosis in Akita angiotensinogen-transgenic mice.* Am J Physiol Renal Physiol, 2012. **302**(7): p. F840-52.

333. Lau, G.J., et al., *Bcl-2-modifying factor induces renal proximal tubular cell apoptosis in diabetic mice.* Diabetes, 2012. **61**(2): p. 474-84.

334. Brezniceanu, M.L., et al., *Reactive oxygen species promote caspase-12 expression and tubular apoptosis in diabetic nephropathy.* J Am Soc Nephrol, 2010. **21**(6): p. 943-54.

335. Brezniceanu, M.L., et al., *Attenuation of interstitial fibrosis and tubular apoptosis in db/db transgenic mice overexpressing catalase in renal proximal tubular cells.* Diabetes, 2008. **57**(2): p. 451-9.

336. Qi, Z., et al., *Characterization of susceptibility of inbred mouse strains to diabetic nephropathy.* Diabetes, 2005. **54**(9): p. 2628-37.

337. Aliou, Y., et al., *Post-weaning high-fat diet accelerates kidney injury, but not hypertension programmed by maternal diabetes.* Pediatr Res, 2016. **79**(3): p. 416-24.

338. Liao, M.C., et al., *AT2 R deficiency mediated podocyte loss via activation of ectopic hedgehog interacting protein (Hhip) gene expression.* J Pathol, 2017. **243**(3): p. 279-293.

339. Mundel, P., et al., *Rearrangements of the cytoskeleton and cell contacts induce process formation during differentiation of conditionally immortalized mouse podocyte cell lines.* Exp Cell Res, 1997. **236**(1): p. 248-58.

340. Shankland, S.J., et al., *Podocytes in culture: past, present, and future.* Kidney Int, 2007. **72**(1): p. 26-36.

341. Drummond, G.R. and C.G. Sobey, *Endothelial NADPH oxidases: which NOX to target in vascular disease?* Trends Endocrinol Metab, 2014. **25**(9): p. 452-63.

342. Ingham, P.W. and A.P. McMahon, *Hedgehog signaling in animal development: paradigms and principles.* Genes Dev, 2001. **15**(23): p. 3059-87.

343. Fabian, S.L., et al., *Hedgehog-Gli pathway activation during kidney fibrosis.* Am J Pathol, 2012. **180**(4): p. 1441-53.

344. Nie, D.M., et al., *Endothelial microparticles carrying hedgehog-interacting protein induce continuous endothelial damage in the pathogenesis of acute graft-versus-host disease.* Am J Physiol Cell Physiol, 2016. **310**(10): p. C821-35.

345. Zhao, X., et al., *The Effects of Sonic Hedgehog on Retinal Muller Cells Under High-Glucose Stress.* Invest Ophthalmol Vis Sci, 2015. **56**(4): p. 2773-82.

346. Dai, R.L., et al., *Sonic hedgehog protects cortical neurons against oxidative stress.* Neurochem Res, 2011. **36**(1): p. 67-75.

347. Cigna, N., et al., *The hedgehog system machinery controls transforming growth factor-beta-dependent myofibroblastic differentiation in humans: involvement in idiopathic pulmonary fibrosis.* Am J Pathol, 2012. **181**(6): p. 2126-37.

348. Javelaud, D., M.J. Pierrat, and A. Mauviel, *Crosstalk between TGF-beta and hedgehog signaling in cancer.* FEBS Lett, 2012. **586**(14): p. 2016-25.

349. Zuo, Y., et al., *Inhibition of HHIP Promoter Methylation Suppresses Human Gastric Cancer Cell Proliferation and Migration.* Cell Physiol Biochem, 2018. **45**(5): p. 1840-1850.

350. Fraser, R.B., et al., *Impact of hyperglycemia on early embryo development and embryopathy: in vitro experiments using a mouse model.* Hum Reprod, 2007. **22**(12): p. 3059-68.

351. Gareskog, M., et al., *Maternal diabetes in vivo and high glucose concentration in vitro increases apoptosis in rat embryos.* Reprod Toxicol, 2007. **23**(1): p. 63-74.

352. Ingelfinger, J.R. and L.L. Woods, *Perinatal programming, renal development, and adult renal function.* Am J Hypertens, 2002. **15**(2 Pt 2): p. 46s-49s.

353. Hayashi, T., et al., *Endothelial cellular senescence is inhibited by liver X receptor activation with an additional mechanism for its atheroprotection in diabetes.* Proc Natl Acad Sci U S A, 2014. **111**(3): p. 1168-73.

354. Hayashi, T., et al., *Endothelial cellular senescence is inhibited by nitric oxide: implications in atherosclerosis associated with menopause and diabetes.* Proc Natl Acad Sci U S A, 2006. **103**(45): p. 17018-23.

355. Matsui-Hirai, H., et al., *Dose-dependent modulatory effects of insulin on glucose-induced endothelial senescence in vitro and in vivo: a relationship between telomeres and nitric oxide.* J Pharmacol Exp Ther, 2011. **337**(3): p. 591-9.

356. Christ, M., et al., *Glucose increases endothelial-dependent superoxide formation in coronary arteries by NAD(P)H oxidase activation: attenuation by the 3-hydroxy-3-methylglutaryl coenzyme A reductase inhibitor atorvastatin.* Diabetes, 2002. **51**(8): p. 2648-52.

357. Satoh, M., et al., *Renal interstitial fibrosis is reduced in angiotensin II type 1a receptor-deficient mice.* J Am Soc Nephrol, 2001. **12**(2): p. 317-25.

358. Tang, R., et al., *Angiotensin II mediates the high-glucose-induced endothelial-to-mesenchymal transition in human aortic endothelial cells.* Cardiovasc Diabetol, 2010. **9**: p. 31.

359. Bishop, B., et al., *Structural insights into hedgehog ligand sequestration by the human hedgehog-interacting protein HHIP.* Nat. Struct. Mol. Biol, 2009. **16**(7): p. 698-703.

360. Bosanac, I., et al., *The structure of SHH in complex with HHIP reveals a recognition role for the Shh pseudo active site in signaling.* Nat. Struct. Mol. Biol, 2009. **16**(7): p. 691-697.

361. Chuang, P.T. and A.P. McMahon, *Vertebrate Hedgehog signalling modulated by induction of a Hedgehog-binding protein.* Nature, 1999. **397**(6720): p. 617-621.

362. Coulombe, J., et al., *Hedgehog interacting protein in the mature brain: membrane-associated and soluble forms.* Mol. Cell Neurosci, 2004. **25**(2): p. 323-333.

363. Kwong, L., M.F. Bijlsma, and H. Roelink, *Shh-mediated degradation of Hhip allows cell autonomous and non-cell autonomous Shh signalling.* Nat. Commun, 2014. **5**: p. 4849.

364. Rose-John, S., *ADAM17, shedding, TACE as therapeutic targets.* Pharmacol Res, 2013. **71**: p. 19-22.